White Paper on Radio Channel Modeling and Prediction to Support Future Environment-aware Wireless Communication Systems

Editors: Mate Boban and Vittorio Degli-Esposti

September 2023

COST CA20120 INTERACT
Working Group 1 (Radio Channels)

Contents

Acronyms

2D two dimensional. 45

3D three dimensional. 12, 13, 38, 43, 47, 63

3GPP 3rd generation partnership project. 37, 38, 58, 64

AI artificial intelligence. 13, 43, 44, 60–63

AP access point. 32

AS angular spread. 29, 30, 57

BS base station. 21, 41, 58, 61, 65

CNN convolutional neural networks. 43, 44, 60

CRLB Cramér-Rao Lower Bound. 46

CSI channel state information. 8, 13, 67

DKED double knife-edge diffraction. 31

DL deep learning. 3, 43, 60–62

DMC dense multipath component. 45, 46

DRT dynamic ray tracing. 39, 40

DS delay spread. 28–30, 34, 57, 60

DSS directional scanning scheme. 24–26, 30

DT decision tree. 43

EADF Effective Aperture Distribution Function. 47

ELAA extremely large antenna array. 29

EM Expectation-Maximization. 46

ESPRIT unitary Estimation of Signal Parameter via Rotational Invariance Techniques. 45

FFT fast Fourier transform. 45

GBDT gradient boosting decision tree. 43

GSCM geometry-based stochastic radio channel model. 29, 36–38, 40, 55, 56, 58

IoE Internet of Everything. 13

IoT internet of things. 8, 35

ISAC integrated sensing and communications. 3, 8, 13, 14, 27, 33, 53–58

JSAC joint sensing and communications. 54, 55

LoS line-of-sight. 14, 21, 22, 34, 38, 42, 54, 55, 60

MIMO multiple-input multiple-output. 3, 8, 13, 14, 28–30, 34, 38, 41, 47, 53, 58, 59, 64, 65, 70, 71

ML machine learning. 3, 8, 36, 41–44, 47, 60–62

MLP multi-layered perceptron. 43

mmWave millimeter-wave. 2, 3, 7, 8, 10, 14, 15, 17, 21, 23–26, 29, 30, 33, 34, 38, 41, 45–47, 56, 67, 71

MPC multipath component. 3, 24, 26, 27, 29, 32, 33, 36, 37, 41, 46–50

MUSIC MUltiple SIgnal Classification. 45

OFDM orthogonal frequency division multiplexing. 60

PDP power delay profile. 29, 33

PLE path loss exponent. 29

PN pseudo-noise. 24

PRBS pseudo-random binary sequences. 24

RIS reconfigurable intelligent surfaces. 3, 7, 10, 13, 17, 38, 40, 47, 51, 53, 67, 70

RL ray launching. 39

RL reinforcement learning. 42, 44

RMS root mean square. 28

RT ray tracing. 38–41, 43, 59, 60, 64

SAGE space-alternating generalized expectation–maximization. 30, 46, 57

SL supervised learning. 42, 43

subWG sub-working group. 2, 7, 9, 10, 26
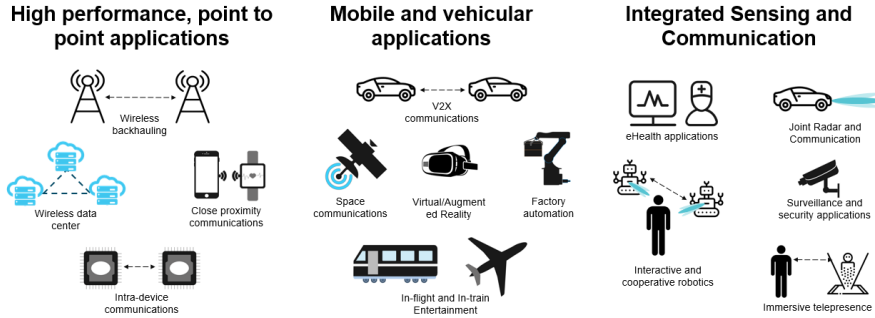
Figure 1: Selected use cases that next generation wireless communications systems aim to enable (based on [2]).

1 Introduction

by Mate Boban

COST INTERACT working group (WG)1 aims at increasing the theoretical and experimental understanding of radio propagation and channels in environments of interest and at deriving models for design, simulation, planning and operation of future wireless systems. Wide frequency ranges from sub-GHz to terahertz (THz), potentially high mobility, diverse and highly cluttered environments, dense networks, massive antenna systems, and the use of intelligent surfaces, are some of the challenges for radio channel measurements and modeling for next generation systems. As indicated in [1], with increased number of use cases (e.g., those identified by one6G [2] and shown in Fig. 1) to be supported and a larger number of frequency bands, a paradigm shift in channel measurements and modeling will be required. To address the particular challenges that come with such a paradigm shift, WG1 started the work on relevant topics, ranging from channel sounder design, metrology and measurement methodologies, measurements, modeling, and systematic dataset collection and analysis.

In addition to the core activities of WG1, based on the strong interest of the participants, two sub-working groups (subWGs) have been initiated as part of WG1: i) subWG1.1 on millimeter-wave (mmWave) and THz sounding (subWG THz) and ii) subWG1.2 on propagation aspects related to reconfigurable intelligent surfaces (RIS) (subWG RIS).

This white paper has two main goals: i) it summarizes the state-of-the-art in radio channel measurement and modeling and the key challenges that the scientific community will have to face over the next years to support the development of 6G networks, as identified by WG1 and its subWGs; and ii) it charts the main directions for the work of WG1 and subWGs for the remainder of COST INTERACT duration (i.e., until October 2025).

In this white paper, particular attention has been devoted to the concept of "environment awareness", which is defined as the ability of communications systems to sense in the broad context of object detection, positioning and ranging, and even object imaging. The repercussions of environment awareness are therefore discussed throughout the paper, ranging from the definition of use cases and their requirements (Section 2), to required frequency bands (Section 3), to the considerations on the design of channel measurements (Section 6.4 and definition of channel models (Section 7), finally to definition of new technologies such as integrated sensing and communications (ISAC) (Section 9).

1.1 Mandate of WG1

Extensive efforts are being devoted to obtaining a comprehensive understanding of radio wave propagation in several frequency bands for the development of future wireless networks. The task of WG1 is to further this understanding by providing an open and collaborative forum for the exchange of ideas, definition of key challenges, and identification of directions for research on radio channels. To that end, the efforts in WG1 relate to propagation modeling for radio systems, including the ones exploiting mmWave and higher frequency bands (sub-THz and THz), where large contiguous bandwidths are still available, and massive multiple-input multiple-output (MIMO) and beamforming techniques, which will enable spectral-efficient connectivity in densely populated areas. Understanding radio wave propagation has also been crucial to new applications, including highly dynamic scenarios, internet of things (IoT) and smart grids. Efforts on propagation modeling for these systems and applications encompassed vehicular and mmWave cellular access [3], IoT, Smart Grids [4], and energy efficient cellular radio planning. These propagation modeling studies have been carried out using various measurement setups [5] or combining measurements and theory for link- and system-level simulations [6], addressing the time, angle and polarisation characteristics of multipath channels, as well as the characterisation of material properties, outdoor-to-indoor penetration loss, and link blockage [3]. Propagation models become mature once supported by a vast amount of measured and simulated evidence of radio channels, and by our understanding about them. Ultimately, such mature propagation models may be able to perform real-time prediction of radio environments and hence provide accurate-enough channel state information (CSI) to aid radio communication systems and applications. As an example, a few studies have addressed the real-time use of deterministic propagation models to help estimate CSI [7], along with a location-aware CSI fingerprinting [8]. Their real-time use in localisation, beamforming, and resource allocation algorithms is still in its infancy.

WG1 is also committed to collecting data and sharing them to create large reference sets for model development and training of machine learning (ML) approaches, with WG1 members already contributing several datasets for this purpose (datasets available at `https://interactca20120.org/wgs/datasets-2/`).

Based on the discussion above, Figure 2 summarizes the main topics that WG1 is addressing, along with the indication of specific topics that are handled
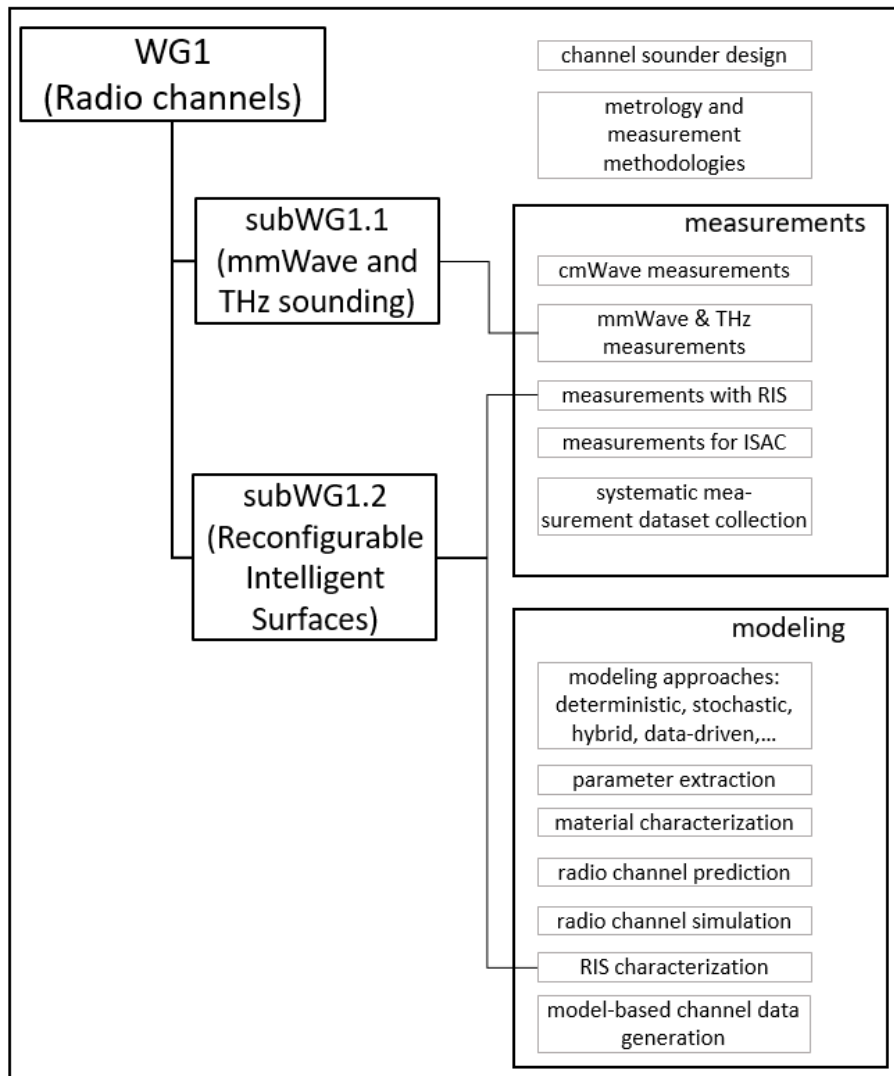
Figure 2: Topics addressed by WG1 and its subWGs.

by the subWGs. WG1 will contribute to each of these topics in order to reach its ultimate goal – definition of a comprehensive channel modeling framework that addresses new scenarios and frequency bands proposed for future wireless communications systems.

1.1.1 Mandate of subWG1.1

The goal of the subWG1.1 (mmWave and THz sounding) is to concentrate the expertise on radio channel measurements and analysis related to mm-wave frequencies and up, which represent the frontier in experimental channel characterization. Novel experimental set-ups, verification of channel sounders, radio channel measurements in different environments/for different applications are some of the key aspects to be investigated. The chain to be covered ranges from the validation of the measurement equipment to the analysis of the measurement results. The objectives of this subWG are to extend the knowledge on propagation from empirical analysis and to develop common practices, in order to create a rich pool of harmonized data from diverse sets of measurements.

1.1.2 Mandate of subWG1.2

The goal of the subWG1.2 (RIS) is the analysis and modeling of propagation in future smart radio environments empowered by controllable and smart surfaces. These surfaces enable the manipulation of propagation characteristics, including wavefront shape and polarization, and the minimization of signal losses. This is particularly of interest at mmWave and higher frequencies to extend otherwise limited communication ranges due to high path losses and the very poor signal penetration into the shadow regions of objects and obstructions. Taking the idea further, large numbers of smart surfaces would enable smart environments where it is possible to optimize the channels and to maximize the network throughput and efficiency.

In order to understand the benefits and limitations of radio channel modulation with RIS, we have to properly understand the modeling and performance of different types of RIS (e.g., reflect arrays, metasurfaces, holographic surfaces, etc.). Modeling those properly is a key to continue to the modeling and analysis of individual links, entire systems, and smart environments. Therefore, the goal of this subWG is to extend the knowledge on three fundamental aspects of RIS: 1) proper and realistic RIS models for different RIS configurations and technologies, 2) propagation models for RIS empowered links and systems, and 3) performance of smart links, systems, and environments.

1.2 White paper organization

For each subsequent section of the white paper covering technical topics, we attempted to cover the following: i) a brief description of the state of art, including key references; ii) summary of COST INTERACT WG1 contributions to the topic[1]; and iii) identification of future work needed on the topic. By implementing this approach, we hope the white paper serves as a reference for

---

[1]While COST INTERACT contributions are not made public, vast majority of contributions are published in conferences, journals, or other venues, either before or after submission to COST INTERACT. Throughout the paper, we refer to those publicly available versions of contributions.

the researchers looking to get a primer on channel measurements and modeling for future communications systems.

The rest of the white paper is structured as follows. Section 2 describes the relevant environments and channel modeling scenarios and Section 3 discusses the frequency bands of interest. Section 4 provides an introduction into the wireless channel propagation fundamentals. Relevant channel sounder designs and metrology are covered in 5. Based on the identified environments and frequency bands, Section 6 discusses the channel measurements. Channel modeling methodologies are covered in Section 7, and Section 8 discusses channel parameter estimation. Section 9 identifies new technologies and techniques related to channel modeling that need to be implemented in order to properly evaluate future communications systems. Finally, Section 10 provides an outlook on the future work and concludes the white paper.

2 Scenarios

by Vittorio Degli Esposti

Early generations of wireless networks were conceived for a limited number of propagation environments and use-cases. In terms of physical characteristics, environments were classified into rural, urban and indoor [9], which corresponded to an increasing attenuation and traffic density, and therefore to a decreasing cell radius. Further classification into suburban and dense-urban, or large-indoor, office and residential indoor is also widely used. The most important use case was that of voice services and internet access connectivity using mobile user equipment (UE) such as smart phones, tablets and laptop computers. Over the years, driven by technology advances and market demand, wireless networks have evolved into a multi-technology integrated galaxy of systems, with a large variety of connected devices, scenarios and propagation environments, as depicted in Fig. 1. Besides the traditional scenarios described above, novel scenarios will include the use of new frequencies in the THz and optical bands and of densified, cell-free networks in high-traffic areas, the realization of the "Network of Everything" with massive connectivity of objects and machines to realize "Smart Environments" and "Smart Factories", also with the use of ubiquitous Artificial Intelligence and of Reconfigurable Intelligent Surfaces, the realization of three dimensional (3D) networks including drones and UAVs as network components, and finally the implementation of automated and connected cooperative driving scenarios using dedicated or cellular-based networks and of Joint Sensing and Communication techniques .

Although the concept of "environment" or "scenario" is a vague one that encompasses physical – and therefore propagation – characteristics, frequency band, technology solutions and applications, here we provide a brief overview of the wide variety of scenarios that next-generation systems will likely have to address, with reference to the classification in Fig. 1 and with particular emphasis on COST INTERACT WG1 research.

Indoor and in-X high-performance-link scenarios. It is well known that 6G-and-beyond systems will have to raise the bar of achievable performance in term of transmission speed, throughput density, low latency and reliability. This will require the use of higher frequency bands in the mm-wave, THz and optical ranges, and of network densification [2, 10, 11]. The possibility of very high bitrates - of the order of Tbps - and very low latencies of THz links will enable new application scenarios for indoor and very short-range communications - also known as in-X communications - such as high-definition holographic infotainment and "teleportation", ultra-broadband mobile access for offices and public spaces, high-performance wireless communication links for industrial applications, data centers, in-vehicle inter-device and intra-device connections [11]. Visible Light Communications (VLC) are envisioned especially for indoor environments, where illumination LEDs, already strategically deployed across indoor premises, can be conveniently reused for communication [12].

Vehicular scenarios. Future transportation scenarios will be characterised by high mobility and will involve cars, trains and unmanned aerial vehicles flying at low altitudes. All of them will require massive use of radio applications including Vehicle to Vehicle (V2V), Vehicle to Infrastructure (V2I) and Vehicle to Everything (V2X) connections as well as radar and ISAC schemes to ensure cooperation, control and safety [13]. The dynamic nature of radio links and networks in the transportation scenarios is the key feature to be addressed in radio channel modeling research. Within the foreseen automated and connected cooperative driving application scenarios, key assets are a reliable wireless V2X connectivity and accurate localization. Most recent vehicles and last-generation wireless systems users will have such capabilities, while others will not (heterogeneous traffic). Environment-aware and cooperative solutions will have to take advantage of connectivity, localization and mapping information available to the former kind of road users or to the edge cloud, to enforce safety for the latter and the whole traffic system. Cooperative, Passive Coherent Radar solutions are being proposed where signal emitted by the fixed infrastructure and vehicles equipped with V2X can be reused as multi-static radar sources that the system can opportunistically use to determine the location of vehicles and pedestrians along streets and in proximity of road intersections [14].

ISAC and environment awareness. The CSI or at least information about multipath spatial characteristics should be known at both radio-link ends to fully exploit the potential of massive MIMO schemes as well as of highly directive mm-wave and THz links in mobile environments. The problem will therefore have to be addressed, for example through ISAC techniques, artificial intelligence (AI) techniques [15], or real time use of digital-twin schemes with embedded propagation models [16, 7]. ISAC, especially at THz frequencies, will enable high-definition environment "vision" applications, including environment mapping, medical imaging, surveillance applications, safety enhancement applications in vehicular applications, etc. All these methods, combined with the ubiquitous use of AI can be thought as enablers of the so called "Environment Awareness" and "intelligence" of future systems.

Smart and Reconfigurable Environments. AI, universal wireless connectivity (Internet of Everything (IoE)) and RIS technology will enable Smart and Reconfigurable Environments. For the first time in the history of wireless systems, RIS and the use of Unmanned Aerial Vehicles or drones (3D networks) will allow the customization of the propagation environment with the purpose of optimizing performance and enhancing the application potential [17, 18]. RIS allow the manipulation of the reflected or transmitted wavefront, enabling interesting applications such as anomalous (non-specular) reflection, focalization, signal processing. Properly placed and configured RIS can be used to enhance mm-wave and THz coverage, or to optimize channel capacity or system performance with a so-called "Scatter MIMO" approach [17, 18]. The combination of RIS and UAV is also interesting in highly cluttered mm-wave and THz scenarios

to compensate for blocked line-of-sight (LoS) communication links and create controllable and smart radio environments [18, 19].

Industrial Environment. A particular candidate to become "smart" is the Industrial Environment where advanced wireless networks will allow a variety of disruptive applications. Cable replacement with ultra reliable and high-performance wireless links is very attractive for the great flexibility and increased reliability of connections with sensors/actuators in moving parts and with robots. The use of mm-wave and sub-THz frequencies will allow ultra low-latency (below 0.1 ms) connections to avoid oscillating behaviours in control loops while enabling high-definition environment sensing through ISAC to control the production process and enforce safety [20, 21].

3 Frequency bands of interest

by Mate Boban

Spectrum is the main consideration for each generation of wireless communication technology as more spectrum is needed to support higher data rates [22]. Since mobile communication technologies evolve to new generations, the use of spectrum continues to expand to higher frequency bands. The spectrum expected to support environment-aware communications can be divided into the following frequency bands.

- **Sub-6 GHz band**: Virtually all of the spectrum up until 4G (LTE) has been allocated in the sub-6 GHz band. This band continues to play a crucial role in 5G and is expected to be vital in 6G as well. This frequency band is the most cost-effective option as a frequency range to guarantee wide coverage in mobile communication systems.

- **Mid-band**: The frequency bands between approximately 6-24 GHz are also identified as competitive candidates for supporting the continued growth of traffic and environment-aware applications, especially given the better sensing performance of larger array size per unit area. To support the continuous growth of traffic, at least 1 to 1.5 GHz of additional spectrum is needed. The 5925-7215 MHz range has been identified as a potential candidate to provide the needed spectrum. Moreover, compared to the sub-6GHz band, the propagation attenuation of these bands increase in an acceptable range while path loss will be combated by adopting advanced radio technologies, e.g., massive MIMO [23].

- **mmWave band**: The mmWave band contains a relatively large amount of available bandwidth, which is essential for ultra-high data rates and high-accuracy sensing applications. However, operation in the mmWave band is more challenging due to the unfavorable propagation characteristics compared to lower frequency bands. In the 2015 world radiocommunication conference (WRC), a variety of frequency ranges were proposed

Sub-6 GHz	Mid-band	mmWave bands	(Sub-)THz bands

0.5 GHz   6 GHz   24 GHz   100 GHz

Figure 3: Spectrum bands.

for IMT sharing study between 24 and 86 GHz and in WRC 2019; specifically a total of 17.25 GHz was identified [24]. E-bands (71-76 and 81-86 GHz) are prime candidates to support larger contiguous blocks in the future, mainly reserved for non-geostationary fixed-satellite service systems (space-to-earth and earth-to-space) [25]. The upper and lower 60 GHz, namely the 57-64 GHz and 64-71 GHz frequency ranges, further provide large contiguous chunks of bandwidth to support device-to-device communications through access and backhaul links and aeronautical and land mobile services, respectively [24]. Furthermore, technologies such as integrated access and backhaul (IAB) could make use of the available spectrum available at the mmWave band [26].

- **Sub-THz and THz bands**: Sub-THz and THz bands open new possibilities for sensing and communication [27]. A total of over 100GHz in 92-275 GHz band is *allocated*, whereas 130 GHz in 275-450 GHz band is *identified* for mobile services or land mobile services [28]. At these frequencies, there are several parts of contiguous spectrum exceeding 10 GHz, which makes it possible to support very high data rates for short- and medium-distance communication. In addition, THz bands bring enhanced sensing resolution thanks to the ultra-wide bandwidth and shorter wavelength [29]. Further up the frequency, between 450 GHz up to 10 THz there is potential for further spectrum. While there exists an unprecedented amount of spectrum in these bands, they also experience new challenges [30]: extremely high transmission losses, molecular absorption that creates non-monotonic pathloss over different frequencies, variability due to weather conditions, effect of micro-mobility, etc. These effects need to be addressed to ensure efficient use of the large spectrum. Additionally, the use of visible light spectrum [31] has gained significant momentum in recent years, given its ability to support novel communication and sensing use cases.

4 Wireless channel propagation fundamentals

by Vittorio Degli Esposti, Conor Brennan, and Katsuyuki Haneda

4.1 Basic propagation mechanisms

While an exact description of radio propagation and therefore of a radio channel might be theoretically possible via Maxwell's equations, it would be unwieldy and complex. Instead, it is possible to simplify propagation description - while retaining relevant features and characteristics - in terms of a set of basic mechanisms that will be reviewed in this section.

4.1.1 Waves in homogeneous media

The simplest case to consider is free-space, or propagation in vacuum. In this case the power density decays inversely with the square of the distance, essentially reflecting the fact that a constant amount of total source output power is being spread over a larger total surface area as the wave propagates further away from the transmitting antenna. For communication systems there is an additional loss, proportional to the square of the frequency, due to the frequency dependence of the effective aperture of a receiving antenna. At the high mm-wave and THz frequencies of interest within COST Action CA20120 this is a significant issue but can be mitigated by the use of narrowly focused beams at transmitter and receiver. However this relies on the continued existence of clear line of sight path. This is explored in [32] in which high resolution dual-polarised double directional measurements are taken in the context of industrial control communications operating at 300GHZ. Propagation and blockage spatial and temporal characteristics are obtained from the processed data indicating the presence of viable alternative communication paths.

Propagation within any other homogeneous material that can be found in a radio channel (e.g. water, air, building materials, human tissue) is broadly similar in many respects to the free space case. The precise physical effect of a particular material can be described with reference to its constitutive parameters, namely its electric permittivity, magnetic permeability and conductivity. These parameters capture the macroscopic effects of the material's atomic and molecular structure on any waves passing through them. These effects manifest in several ways including a change in the wave's phase velocity (slowing, relative to the speed in vacuum) and also a change in the characteristic impedance (the ratio of the amplitude of the electric and magnetic fields) and the wavelength (the physical distance between successive peaks or troughs along the wave). Importantly, the presence of conductivity or dielectric hysteresis in so-called lossy media manifests itself as an extra reduction in the power density as the wave propagates (in addition to the spreading discussed previously). These effects are frequency-dependent which leads to dispersion effects as the individual frequencies which comprise a pulse travel at different speeds through the material,

causing the pulse to distort.

4.1.2 Reflection, transmission, diffraction and scattering

The primary complication afflicting radio propagation is the proliferation of waves occurring at the *boundaries* between materials (such as when a wave travelling in air strikes a wall). Referring to figure (4) **reflection** and **transmission** occur when an incident electromagnetic wave strikes the face of an object which is locally smooth on a scale comparable to the wavelength. In such circumstances the incident wave produces a reflected wave travelling away from the face and a transmitted wave propagating into the object, the direction of propagation of both being governed by Snell's laws of geometric optics. The amount of power reflected from, and transmitted through, materials is frequency dependant and their specification for new communication frequencies at millimetre wave and higher is an important task being addressed in COST Action CA20120. Several contributors have conducted studies of reflection and transmission (penetration) loss for typical building materials, concentrating on their variation with angle, frequency and polarisation. [33] described the use of a wideband channel sounder to examine a variety of materials at four discrete frequencies between 28 GHz and 70 GHz and noted the increase of penetration loss with frequency. Continuous measurements of reflection and transmission losses are made in [34] and [35] for 17 common materials in the frequency range 2GHz to 170GHz. Oscillations in the reflection loss as the frequency varies are noted, due to the effect of internal reflections within the finite slab of material under test. These diminish as the frequency rises, consistent with the increased penetration loss as noted elsewhere.

Another research focus is on the development of so called reconfigurable intelligent surfaces RIS which do not obey the above laws of geometric optics but rather can reflect or transmit signals in preferred directions, thereby improving coverage or reducing interference. Within COST Action CA20120 researchers are examining ways to accurately model them using commercial Finite Element software [36]. This numerically intensive approach is shown to give good agreement with the simpler Generalised Law of Reflection approach but has the added advantage of being able to model scattering in all directions and thus can be used for interference analysis. More details on COST Action CA2 20120's work on RIS are available in section 9.1

Diffraction occurs when a wave strikes the sharp boundary between two such faces (such as at the edge of a building). In such instances the wave is scattered in a continuum of directions, as defined by the so-called Keller cone [37]. As the interface between regions becomes rougher (or equivalently the frequency becomes higher such as is the case with mmWave and THz communications) finer details at wavelength scales become important and these simple well-defined mechanisms of reflection, transmission and diffraction give way to the more general process of **diffuse scattering**, which as the name suggests results in a proliferation of waves being scattered diffusely across a wider angular range (as per figure (5). **Surface scattering**, where the inhomogeneities are assumed to
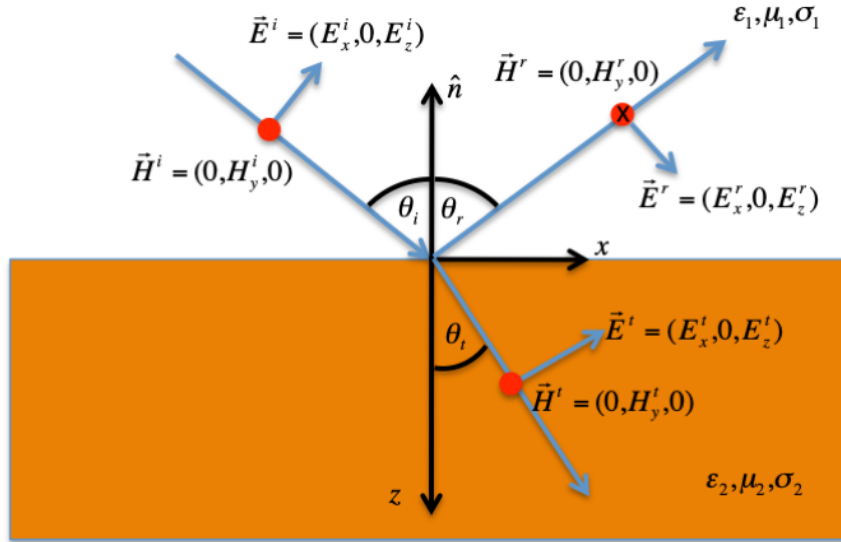
Figure 4: Plane wave reflection from smooth boundary. Incident wave $\vec{E}^i, \vec{H}^i$ produces a reflected wave $\vec{E}^r, \vec{H}^r$ and a transmitted wave $\vec{E}^t, \vec{H}^t$

lie on the material boundary, has been studied by participants in COST Action CA20120 with a variety of models proposed. [38] and [39] both use numerically precise models based on the method of moments with the former paper concentrating on efficient ways to solve the associated computationally intensive equations while the latter contribution examined depolarisation effects and the dependency on material, frequency and surface size. The accuracy of a simple directional scattering (DS) model is assessed in [40] and effective roughness and scattering coefficient are identified as key parameters. The model is extended using a t location-scale distribution in order to make it better fit electromagnetic simulation results.

Several authors have identified the process of **volume scattering**, which occurs when waves interact with fine inhomogeneities *within* a material, as being of more importance than surface scattering. The Effective Roughness model is a relatively simple tunable model and has been used to describe such scattering at mm-wave frequencies [41]. In this contribution it was noted that materials with complex internal structure (such as reinforcing mesh) can produce significant backscattering resulting in a diffuse scattering model involving two directional lobes (in the forward and backward directions). The effective roughness model

Figure 5: Laws of geometric optics gradually give way to diffuse scattering (reduced specular lobe and increased side lobes) as surface roughness increases

is heuristic but is based on a solid insight of the physical processes that take place at a material boundary. In [42] the authors enhance its scientific basis by modifying it so that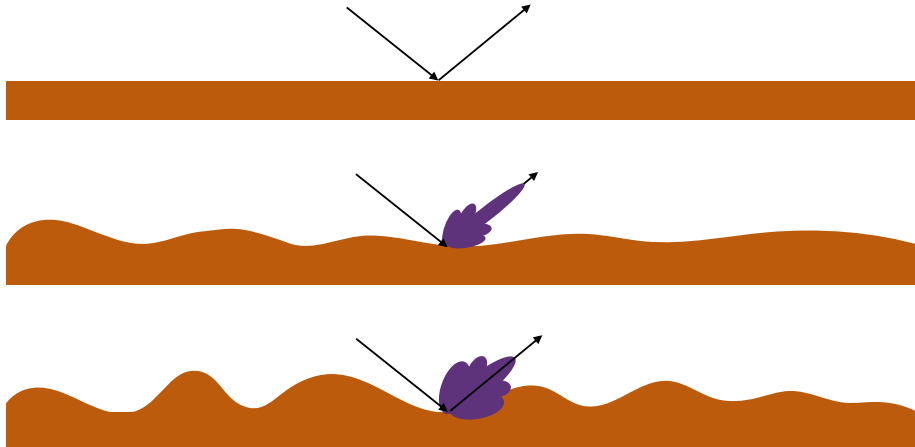 it obeys the reciprocity principle (i.e. is unchanged by an interchange of transmitter and receiver locations). As seen, diffuse scattering models are often statistical or heuristic in nature, given the uncertainty surrounding the physical form of small scale inhomogeneities that produce them. This uncertainty is caused by an unavoidable limitation in the level of detail of databases describing buildings etc. Nonetheless some COST INTERACT contributors have examined what can be achieved with an enhanced level of building geometric description. In [43] the impact of building facade detail is studied by comparing ray tracing output (see below) to measured data. It is concluded that the inclusion of enhanced information about facade features (windows, ledges etc) can result in a more discriminating identification of multipath components than would be the case with simple diffuse scattering models applied to flat facades.

4.2   Large-scale and small-scale propagation phenomena

As discussed in Section 4.1, the quality of a radio channel is ultimately determined by how electromagnetic waves interact with the materials within it. Recognising that such a full electromagnetic description is practically impossible, channel modeling has instead focused on describing the channel in terms of a number of key parameters that have the greatest effect on the performance of the digital communication scheme being enabled by the channel. The range of parameters and the accuracy with which they need to be specified have evolved in tandem with the communication schemes themselves as they grown in sophistication over the decades. Parameters are divided into large scale parameters
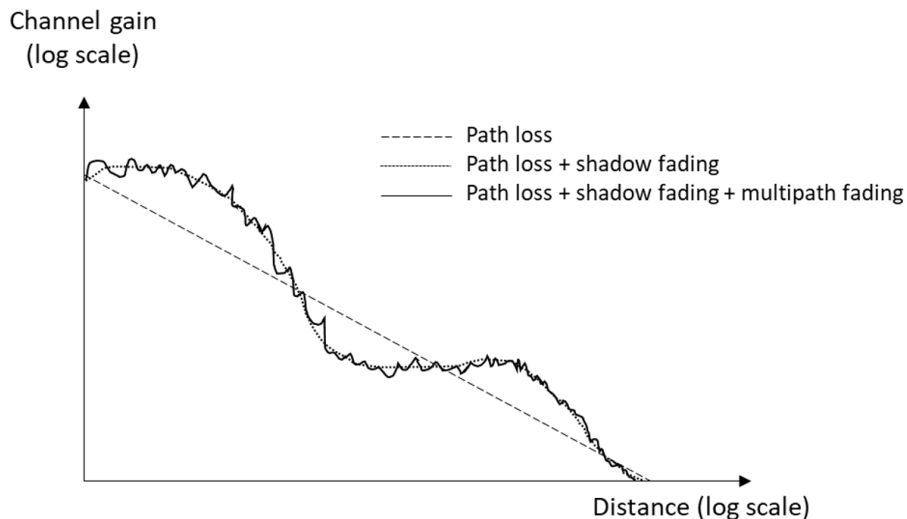
Figure 6: Path loss, shadow fading, and small scale/multipath fading.

and small scale parameters, depending on the range over which they vary significantly compared to the wavelength.

4.2.1 Large scale propagation phenomena

Path loss

Path loss describes the large-scale reduction in power density as signals move away from the transmitter. It is the most important parameter in channel modeling since it ultimately determines the possible communications range and its quality, i.e., the signal-to- noise ratio. It also determines the signal-to-interference ratios (SINR) in the case of an interference-limited environment within which frequencies are reused to ensure efficient use of spectrum. From an energy-efficient networks perspective path loss defines the minimum transmit power of base and mobile stations required to maintain a target SINR and quality of service. Consequently, path loss is the most well-studied parameter in channel modeling. Path loss is typically modeled using a power law, wherein the loss is proportional to the distance raised to the power of some specified exponent. Path loss exponents typically range from 1.5 to 4 for waveguiding to deep non-line-of-sight environments. Frequency dependency of the path loss has also been studied thoroughly, indicating good agreement with the theory, e.g., Friis' law with constant-gain antennas. Even though it is a subject that has been extensively studied, it remains a subject of research when new spectrum, use cases and scenarios emerge, e.g., rural and aircraft scenarios.

Referring to the log-log plot of Fig. 6, path loss is typically depicted as the best linear fit extracted from the measurement data.

Shadow fading

Path loss models assume a regular decay of power density with distance (e.g. linear or piecewise linear when viewed on a log scale), In practice the power density will display further random large-scale variations around this trend as some locations suffer from a greater or lesser degree of obstruction by buildings etc. This is referred to as *shadow-fading* and is typically modeled using a suitable random distribution. In legacy below-6GHz cellular radio systems, shadow fading is typically defined by fluctuation of signal strength over different sectors of base stations (BSs) at the same communication distance between base and mobile stations. A single BS site consists of multiple BS units, each covering a limited azimuth and/or elevation angular range called a sector. The level of obstruction in each sectoral direction varies, with some possibly experiencing large blockages with a consequent decrease of signal strength. The standard deviation of shadow fading is therefore not necessarily identical to the second order moment of differences between path loss and small-scale-averaged received signal strength normalized to the transmit power. Still, such a definition of shadow fading is the only one that can be used for radio communications systems and scenarios where the use of sectors would not be popular, e.g., in indoor scenarios. An open research question of shadow fading is its correlation over space and frequency [44]. Referring to Fig. 6, shadow fading adds a slowly varying process on top of the path loss.

Blockage

Blockage refers to the obstruction of the LoS path between a transmitter and a receiver by an object (e.g., building, wall, human body, etc.). It can be modeled either as part of the shadowing fading process or explicitly, where the latter is preferable in case of a known/measured additional blockage loss by a specific object [45, 46]. In case of explicit modeling, it is added as an additional loss on top of path loss and shadow fading. Below we elaborate in particular on human blockage, as it becomes increasingly relevant for handheld or on-body user devices utilizing mmWave or higher frequency spectrum.

It has been shown through experiments that losses of a LoS connectivity due to human blockage is reproduced well by modeling a human body as a set of absorbing knife edges and considering diffraction on each edge, where the LoS path is totally absorbed by the absorbing screen representing the body. The use of absorbing knife edges is advantageous to model human body in its simplicity because diffraction coefficients do not depend on polarization of an incident wave, in contrast to the case of conducting screens. As the analytical formula of diffraction coefficients assume infinitely long edges, they are better applicable to higher radio frequencies where the human body becomes electrically larger. A research question would be estimation of blockage loss when there are *multiple* objects intervening the LoS connectivity [47, 48]. The analytical treatment becomes much more complex than a single body case because diffraction coefficients of an absorbing knife edge assume incident plane wave, while an incident wave to the following edges after the first one may not be a plane wave necessarily. The same problem encounters when estimating extra losses

to free-space due to multiple diffraction over hills and buildings in long-range point-to-point links. In addition, as the cross sectional area of the Fresnel zones becomes larger as longer connection distance, estimation of the blockage losses are more challenging because only a part of the Fresnel zones may be intervened by blocking objects.

4.2.2 Small-scale propagation phenomena

Large scale effects such as path loss and shadow fading describe variation of power density that occur gradually on a scale of many wavelengths. In practice it is noted that power density varies rapidly on the scale of the wavelength also. This phenomenon, called *fast fading*,is caused by wave interference between EM waves arriving at a given location via multiple paths of differing lengths, i.e. by the propagation mechanism usually referred to as *multipath*. Given the impossibility of precisely specifying these path lengths this is an intrinsically random process and a detailed statistical modeling of such small-scale fading effects is therefore an essential part of modern radio channel models. Fast-fading signal-strength fluctuation are described using a variety of statistical distributions, Raileigh and Rice distributions being the most widely used for non-LoS and LoS channel conditions, respectively. Multiple parameters are used to model time, frequency and space dispersion effects of multipath propagation. These effects and are often represented by Fourier transform pairs, e.g., space/angle, time/Doppler and delay/frequency, the choice of which domain to use depending on the channel sounding and modeling methods.

Channel models usually prescribe the second moments of the power spectrum in the respective domains, i.e., angular, delay and Doppler spreads, or their Fourier counterparts, i.e., spatial, frequency and time correlation intervals. These parameters have been studied thoroughly through a wide range of channel sounding from a few hundreds of Megahertz to sub-THz radio frequencies across many important radio communications scenarios. However, it must be noted that the sole spread or correlation parameter values do *not* suffice to reproduce channels that resemble realistic conditions because many different shapes of power spectrum or correlation functions yield the same parameter values. Explicit knowledge, i.e., shapes of power profiles and correlation functions is therefore usually accompanied with parameter values, as discussed in the following.

Multipath dispersion and clustering
Power spectrum of multipaths over angles and delays typically does not have equal magnitude over the domain, but shows some extents of power concentration on specific angles and delays in each radio link. Such concentration of power in the spectrum is represented by *clusters* in multipath channel modeling. Each cluster can be defined by its concentration angles and delays, which are called cluster centers, along with their distributions in the respective domain. The latter is typically modeled by Laplace and exponential distributions in the angular and delay domains. Setting the right cluster centers and types

of distributions allows us to reproduce the realistic power spectrum shapes of a radio link realization while respecting their spread parameter values. The use of clusters for multi-dimensional power spectrum modeling of multipath channels is a well-established approach, as evidenced by standard channel models that rely on them. An open research question is the variation of angular and delay properties of clusters across different radio frequencies, especially at mmWaves and higher frequencies. It has been discussed among the wireless communication community that multipath channels are sparser, i.e., the number of multipaths and/or clusters is smaller, at higher radio frequencies. There are some indications from comparative channel sounding performed at various radio frequencies [49, 50, 51, 52] that support the conjecture, where the power spectrum becomes more "spiky", i.e., dominated by specular reflections while reduced scattering effects, so that clusters become more distinguishable to each other. The clearer specular reflections and reduced scattering are both explained by wave-interacting objects whose surface roughness becomes comparable to the wavelength of the radio frequency, making the wave-object interaction more angularly selective and the number of multipaths arriving at the receive side smaller becomes less. The same reports tend to show that, despite the sparsity, the spread parameter values do not necessarily change noticeably. Some other reports, on the other hand, show evidence from channel sounding at multiple frequencies that the power spectrum shapes do not change noticeably across frequencies [53, 54]. The discussion of multipath sparsity and their influence on spread parameter values is therefore not conclusive yet, requiring further evidence from multiple-band channel sounding in different scenarios. They have implications on cluster models across the radio frequencies in standard channel models. Referring to Fig. 6, multipath fading results in fast variations superposed on top of the path loss and shadow fading.

5 Channel sounder design & metrology

by Diego Dupleich and Wei Fan

5.1 Channel Sounding Design

Channel sounding consists of "sounding" the environment with a known signal and analysing the received echoes to characterize the propagation of electromagnetic waves. Since both the transmitted and the received signal are known, the time-variant channel impulse response can be extracted. The complexity of the sounding set-up depends on the propagation parameters under investigation and target channel models and systems. Nowadays, with mobile wideband MIMO systems at high frequency in sight, the ultimate goal of multidimensional channel sounding is to provide the necessary data to jointly estimate the amplitude (polarization) and different geometrical properties of the multi-path components in the channel: delay, direction of departure (DoD), direction of arrival (DoA), and Doppler. In practice, the simultaneous acquisition of these multipath component (MPC) properties is challenging and there is frequently a trade-off between resolution in the delay domain (bandwidth), angular domain (directivity), and Doppler (sampling rate).

5.1.1 Wideband Channel Sounding

Channel sounders are usually classified as frequency-domain or time-domain channel sounders.

Vector network analyser (VNA) is a widely used type of frequency-domain channel sounder, recording the frequency response between two ports of the device, as shown in Fig. 7a. They are popular due to the ease of calibration, excellent dynamic range, scalable and flexible carrier frequency and bandwidth settings. With the help of external frequency extenders, it supports channel measurements in the mmWave/(sub-)THz bands as well. However, there are some shortcomings, for example, slow measurement time (determined by the number of swept frequency points and IF settings), short measurement distance (due to high losses in the RF cable used to remote antennas), and lack of VNA ports to support multi-antenna measurements. However, different solutions have been investigated in INTERACT to work around some of these limitations. Radio-over-fiber (RoF) has been implemented to solve the problem of short measurement range for mmWave/(sub-)THz bands [55, 56]. Moreover, a phase-compensation scheme that counteracts random phase variations has been tested in [57, 58], achieving accurate and phase coherent measurements for VNA-based directional scanning schemes (DSSs) and virtual-array schemes at mmWave and (sub-)THz.

On the other hand, time-domain channel sounders utilize specially designed wideband signals. Popular signals are multi-carriers and pseudo-noise (PN) / pseudo-random binary sequencess (PRBSs) (displayed in Fig. 7b), which have special auto-correlation properties in time. In contrast to multi-carrier, PRBS
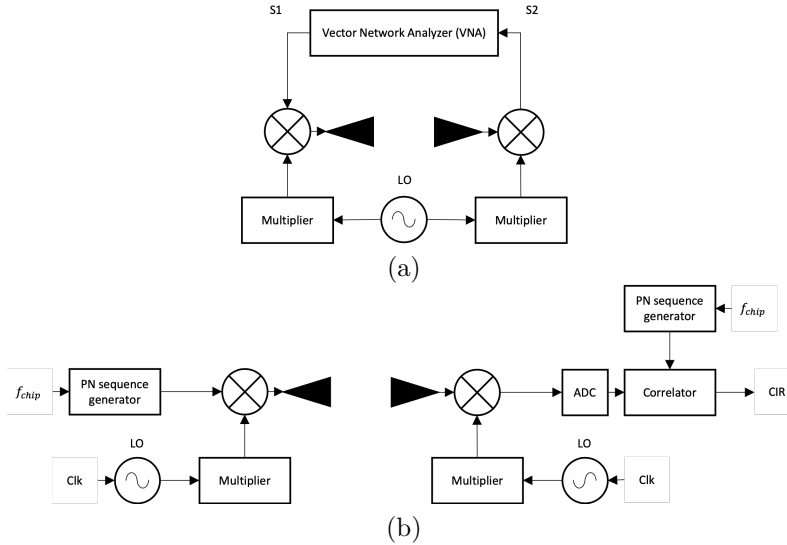
Figure 7: Wideband channel sounding architecture (a) VNA-based and (b) correlation based.

have the advantage of a low peak-to-average power ratio (PAPR), allowing the optimization of transmit power, a scarce resource at high frequencies. On the other hand, unlike with multi-carrier signals, the spectral power density of PRBS is not uniform over the measured bandwidth, which also creates difficulties on the frequency response calibration of the system. In comparison to VNAs, time-domain channel sounders allow real-time measurements. However, this requires expensive wideband digitizers that can be saved by implementing sub-sampling or the sliding correlation architecture. This also has the advantage of an increased SNR at the expense of larger measurement times.

5.1.2 Antennas and Antenna Arrays for mmWave and (sub-)THz Channel Sounding

For mmWave/(sub-)THz applications, it is of high importance to have knowledge of the spatial profile of the channel. Several strategies have been reported in the literature to capture this information, including the DSS and the utilization of virtual and physical antenna arrays. In the DSS scheme, a highly directional antenna can be centred on a turntable and rotated to record the spatial profile of the channel. The DSS scheme has been the most popular solution for mmWave and (sub-)THz bands because of its simplicity, low cost and high-gain offered by the employed antenna. However, it is slow due to the mechanical steering nature and its spatial resolution is essentially constrained by the directivity of the antenna [55, 56]. The virtual array solution is another popular scheme that employs a single antenna which is sequentially moved in pre-defined

25

spatial locations (i.e. virtual elements of the array) [57, 58]. However, the DSS and virtual array schemes can only be used for static propagation scenarios due to long measurement time. On the other hand, time-varying scenarios can be measured with physical arrays. The multiplexing antenna array scheme consists of several directional antennas pointing to different spatial directions connected to a radio frequency (RF) switch, enabling the direct recording of the spatial profile [59]. To decrease the hardware complexity and cost while maintaining the performance of the full digital structure, a switched array based channel sounder for mmWave bands was reported in [60]. By activating different antenna pairs, channels of all antenna pairs are measured at different time instants. Switched-array sounding can accomplish one MIMO channel snapshot within a very short measurement time. However, non-sequential antenna switching is needed to overcome the aliasing in the parameter estimation of Doppler frequencies and angles of MPCs [61]. With phased arrays (i.e., with an analog beam-forming structure), the process of beam-steering is much faster and it has been widely used in the mmWave bands [62]. Though highly promising, its application to large-scale configuration at mmWave/(sub-)THz bands has not been reported for channel sounding. More flexibility and capabilities compared to phased arrays can be achieved with a digital beam-forming structure, in which each antenna element has an individual RF chain [59]. However, the number of RF channels is essentially limited due to cost and complexity concerns.

5.2   Metrology of Channel Sounding

Metrological assessment of multidimensional channel sounding has gained relevance in the latest years as it can be seen from different activities around the world: the METERACOM project[1], the NextG Channel Model Alliance[2] (sponsored by NIST), and standardization activities in the IEEE P2982 group (mmWave Channel Sounder Verification), which is working towards recommendations of methods for verifying mmWave channel sounders performance. These verification methods are usually based upon comparison of processed channel measurements to either theory or to particularly designed artefacts that generate MPCs with known characteristics in the different domains [63]. These artefacts can also be measured over-the-air [64], which offers the versatility of including the measurement antennas and allowing mobility during the test, enabling the verification of angle of arrival/departure and Doppler [65].

5.3   Future Work

Within COST INTERACT WG1 and subWG1.1, we will be tackling the reduction of measurement time in virtual-arrays and DSS schemes. It is important to build statistically meaningful 6G channel models, which requires double directional channel measurements at multiple locations for many deployment scenarios. However, a key bottleneck for channel sounding at mmWave/(sub-)THz

---

[1]https://www.meteracom.de
[2]https://www.nist.gov/ctl/nextg-channel-model-alliance.

frequency bands using the DSS and virtual arrays is the long measurement time associated with the mechanical movement of the antenna. Virtual array based channel sounder for the W-band (75 GHz - 110 GHz) was designed and employed for channel measurements in [57, 58]. We will continue working on developing virtual array channel sounder for the 220 GHz to 330 GHz frequency band. A few works on channel sounder to support cell-free massive MIMO scenarios were reported within COST INTERACT [66], which we will continue to cover. The implementation of physical-arrays at (sub-)THz for dynamic measurements and joint estimation of Doppler/angle/delay of MPCs will be addressed from a metrological and practical point of view. Within the scope of ISAC, there is plenty of space for the optimization of baseband excitation signals to enhanced sounding performance, reduce uncertainties during measurements, and optimally exploit the hardware resources. Non-linearities are also challenging with the utilization of wideband multi-carrier signals and need to be addressed from a metrological and practical point of view.

6 Channel measurements

by Mate Boban, Diego Dupleich, Wei Fan, Marco Skocaj, and Wenfei Yang

6.1 sub-6 GHz Frequency Band

The first four generations of cellular systems as well as IEEE 802.11 (WiFi) standards up until a decade ago were all enabled by sub-6 GHz bands. Therefore, over the last more than 30 years, a large number of measurement campaigns have been carried out to characterize wireless propagation in sub-6 GHz bands [67].

However, these bands still garner interest, primarily due to emerging application and deployment scenarios and use of novel antenna techniques. To that end, recent studies presented at COST INTERACT meetings focused on the characterization of high mobility scenarios, such as vehicular and indoor factory environments, and considered new deployment approaches, such as cell-free and massive MIMO architectures.

In [68], authors conducted channel measurements at 3.2 and 5.81 GHz in vehicular propagation environments, including V2V, V2I, and V2P scenarios. Together with channel measurements, the authors collected LiDAR data captured by sensors installed in the connected vehicles and built a dataset with coherent perception and propagation traces. In [69], authors performed measurements in a cell-free vehicle-to-infrastructure communication scenario using a real-time channel sounder operating at 5.89 GHz and with a bandwidth of 80 MHz. At the transmitting side, they considered different setups with different number of access points and antenna elements. At the receiving side, multiple omnidirectional antennas were installed in a van and spaced more than 10 lambdas, enabling the measurement of dynamic and decorrelated channels. For each setup, the authors evaluated SNR and root mean square (RMS) delay spread (DS), and demonstrated that cell-free architecture can guarantee a better and spatially more uniform link quality.

In [70], authors performed wideband and ultra-wide band measurements and adopted a Bayesian approach to derive and empirical fading model for device-free localization purposes. They considered different setups, including outdoor measurements at 5.2 GHz and indoor measurements at 4 GHz. In [71], authors carried out a measurement campaign to characterize indoor-to-outdoor high-mobility propagation scenarios at 5.9 GHz. The transmitter antenna is installed inside a building and placed on a rotating unit that rotates with a constant velocity. The receiver is placed on the roof of another building at a distance of 140 m. The results include normalized local scattering functions for different velocities of the transmitted antenna.

In [72], authors considered a factory environment and conducted measurements at 3.7 GHz considering two different deployment options: a co-located massive MIMO antenna array and a unique randomly distributed array. Measurement results are used to quantify the channel hardening effect observed when increasing the number of antennas, and show that the usage of massive MIMO

arrays in rich scattering environment can reduce large scale power variations and help in achieving more reliable wireless channels.

6.2   Mid-band (6 GHz - 24 GHz)

As the spectrum below 6 GHz is limited, current services are already using a large proportion of the available spectrum. Therefore, resorting to higher frequency ranges becomes a necessity. Frequency bands between 6 GHz - 24 GHz are considered as a promising candidate for supporting future wireless communications systems due to the lower path loss compared to higher (mmWave and above) bands and a potential to support massive MIMO systems.

While up to now there have been limited contributions in terms of measurements in mid-bands by COST INTERACT (e.g.,[73]), channel measurements for frequency bands between 6 GHz and 24 GHz have been widely conducted in the literature, where indoor scenarios [74, 75, 76, 77, 78, 79, 80] have driven more research interest over outdoor scenarios [81, 82].

The study in [73] presented measurements for extremely large antenna array (ELAA) with a 32×32 Rx virtual planar array in 10 GHz band in two indoor environments (meeting room and classroom). Results indicate strong non-stationary effects in the spatial domain as well as significant near-field effects, both of which become non-negligible in ELAA channel modeling. As the antenna arrays become larger and since massive MIMO systems are expected to operate in mid-bands, further investigations of non-stationarity are needed with ELAA. To that end, in [78], a 20×20 virtual uniform rectangular array (URA) was used at Rx side in channel measurements at 13–17 GHz in a lecture hall environment. Channel parameters, including channel gain, K-factor, and DS were observed over the array which showed considerable variations without deterministic trends. In [79], a 64×4 virtual URA was used at Tx side in channel measurements at 11 GHz in a theater environment and channel parameters such as shadow fading, DS, and coherence bandwidth were derived over the array. Similar to [73], the spatial non-stationarity was again pronounced.

Primary channel parameters including path loss, shadowing, K-factor, DS, angular spread (AS), cross-polarization ratio (XPR), and correlation properties have been obtained in several environments. In [74], channel measurements were conducted at 11 GHz and 14 GHz in indoor environments, where the antenna elements were configured in a 7×7 square grid. The path loss exponent (PLE) and DS were derived from the averaged power delay profile (PDP) to remove the effect of small-scale fading. [75] presented a complete parametrization for a three-dimensional (3-D) geometry-based stochastic radio channel model (GSCM) at 10.1 GHz based on a measurement campaign in a lobby environment. To obtain the 3-D spatial information, a virtual conformal array consisting of four 9×9 planar arrays was used in the measurements. The estimation of signal parameters via rotation invariance techniques (e.g., ESPRIT) were employed to estimate the MPC. MPCs were first clustered by the "Power K-means" algorithm and then cluster parameters were also obtained. The study in [81] carried out similar parametrization procedure based on channel measure-

ment at 11 GHz in a micro-cell environment. A virtual uniform circular array (UCA) with 12 elements were used in measurements, hence the angular spread was only available for the azimuth plane. In [77], measurement campaigns were conducted by the DSS at 13–17 GHz in an indoor lecture hall and a laboratory environments with high gain horn antennas. The space-alternating generalized expectation–maximization (SAGE) algorithm was applied to de-embed the effect of antenna response and then the DS and AS were obtained.

The characteristics of specific propagation mechanisms, such as diffuse scattering and diffraction, have been also studied for the mid-band. [76] characterized diffuse scattering based on MIMO channel measurements at 11 GHz in indoor environments. Propagation parameters of diffuse scattering were jointly estimated by the RiMAX-based estimator, where incoherent plane waves due to diffuse scattering is modeled stochastically as dense multipath component (DMC). The measurement results showed that significant DMC exist, which affected the eigenvalue structure of the MIMO channel.

In summary, existing channel measurement campaigns in mid-band have been conducted in various indoor but few outdoor environments. The measurement results covered statistical channel parametrization, non-stationarity analysis for MIMO channels, and propagation mechanisms study.

Future measurement campaigns in mid-band are expected to cover more propagation scenarios, especially outdoors, which are necessary for defining proper channel models for outdoor scenarios in these bands. Further measurements and analysis are required to explore characteristics of massive MIMO channels, including how the propagation environment affects massive MIMO system performance in mid-band.

6.3 mmWave and (Sub-)THz band

The characterization of propagation from measurements at mmWave and the lower THz bands has gained a lot of attention in the recent years. The free blocks of spectrum available in these frequencies enable the implementation of high data rate wireless links with enhanced capacity and with an unprecedented level of resolution that makes them suitable for sensing applications.

However, there are propagation aspects related to the wavelength at mmWave and (sub-)THz differing to the well known and studied sub-6 GHz bands. As the frequency goes up, transmission loss will become high, diffraction becomes much weaker, and penetration becomes very difficult, making the propagation channel much sparse and specular. In addition, in the mmWave and (sub-)THz range, particles in the atmosphere requires further considerations for some frequency bands.

To compensate the increased isotropical path-loss, high-gain radio interfaces need to be employed. Therefore, the spatial characteristics of the channel become more relevant for channel modelling and system design, since the information on where to point the antenna beam is of special importance. Consequently, even empirical path-loss models have also been adapted from the typical isotropical characteristics of the antennas to consider the directivity [83].

Therefore, there is paradigm shifting from purely stochastic towards hybrid stochastic/deterministic models for these frequency bands with the inclusion of deterministic components. This requires a more precise characterization of the electromagnetic properties of different constructive materials and a deeper analysis on the scattering properties. The absorption coefficient and refractive index of typical building materials (glass, plaster, and wood) has shown a good agreement between the measurements and the results of the Fresnel equations, [84]. On the other hand, diffuse scattering is modelled by extending Fresnel equations for specular reflections with a Rayleigh factor obtained from the knowledge of statistics of surface roughness by Kirchhoff theory of scattering [85].

COST INTERACT contributions on the topic of material penetration and reflection losses in a wide range of frequencies covering from sub-6 GHz to the lower THz bands (up to 170 GHz) have shown a relative low dependence on frequency of the reflection coefficients for the majority of the materials under test, but an increased penetration loss above 100 GHz [86, 87]. In addition, measurement-based analysis from different typical construction materials at 27 GHz showed that the scattering from internal structures can be relevant, especially in the case of Gypsum-board dividing-walls which have a low penetration loss and relevant internal in-homogeneity [88].

Regarding weather and influence of rain in point-to-point mmWave links, the attenuation to long time exposure to rain in direct and side (NLOS) links at 25.84 GHz and 77.52 GHz have been measured and modelled in [89], showing a higher attenuation on the side links due to the scattering from the rain.

Human blockage also becomes more severe because of the directivity of the radio interfaces and the increased penetration losses with frequency. Frequently, two different approaches are used on the characterization of human blockage: an empirical, based on the analysis of fading statistics, and an analytical, based on the double knife-edge diffraction (DKED) model. The time variant human shadowing statistics at 60 GHz inside an Airbus 340 have been studied using different antenna types in [90]. Similarly, short-range measurements at 60 GHz in [91] show that the signal level attenuation follows a Gaussian distribution. In [92], 73.5 GHz measurements in pedestrian crowd scenarios have been used to derive a model based on Markov's chain, which is also considered under the stochastic modelling approach in the 3GPP TR 38.901. On the other hand, analytical models based on the knife-edge diffraction principle predicts the obstruction loss based on the Huygens' principle: the diffracted front waves interfere constructively and destructively behind the blocker. Human blockage measurements in several mmWave bands up to 60 GHz have been compared to different modelling approaches in [93, 94], where a clear frequency dependence on the losses has been observed, with maximum losses up to 25 dB at 60 GHz. Similar results at 70 GHz are presented in [95], where measurements are compared to the predictions with the DKED model considering the directivity of the antennas. COST INTERACT contributions in human blockage at (sub-)THz have been analysed from measurements in [96]. People with different complexion have been set frontally and laterally interrupting highly directional links, showing attenuation results higher than 25 dB and 30 dB, respectively. These
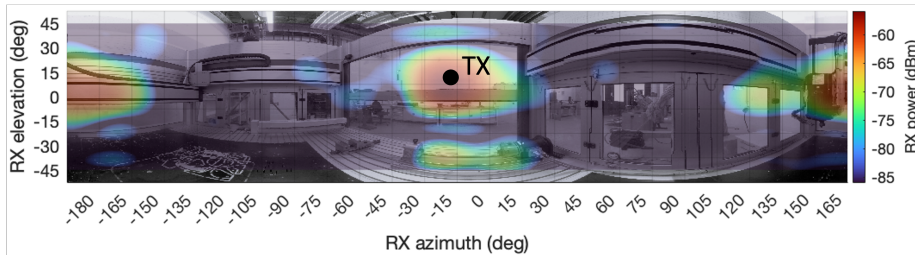
Figure 8: Power azimuth/elevation profile at RX in an external AP to inside of machine scenario at 300 GHz, [106].

results are underestimated with theoretical diffraction models as the METIS and DKED, which need to be extended including the antenna directivity, as discussed in [95].

Regarding the characterization of propagation at (sub-)THz, there are already several measurement campaigns in different scenarios, covering from very short link applications as desktop [97], rack-to-rack communications for server rooms [98]; to middle-range applications as wireless links in meeting room [99], shopping mall and airport [100], between others; and outdoor applications as parking lot [101], courtyard and crossroad [102], train stations [103], etc. The impact of polarization in the channel when considering highly directive radio-interfaces at (sub-)THz has been studied in controlled experimental set-ups and in real complex environments in [99], where the dependence of the path gain on the incident and reflected angles is observed and contrasted with Fresnel. In recent times, (sub-)THz has also been targeted to industrial applications [104], and therefore the characterization of propagation in this environments has gained a lot of relevance, [105]. COST INTERACT contributions in (sub-)THz measurements in industrial settings and machines have been presented in [106]. The temporal/spatial characteristics of the channel in an external access point (AP) to inside of machine (through penetration by protective glass) shows a channel with a rich set of multi-path components from the different metallic frames and machine components. A very precise idea of the location of the different objects in the environment can be depicted from the geometrical properties of these MPCs. This offers an immense playground for the implementation of sensing applications that can be used to control different production processes. The polarization of the MPCs also showed a behavior in concordance with the Fresnel equations. In addition, the obstruction of the LOS component by different parts of the machine or external items as a forklift truck passing by showed that there are remaining MPCs that can be used to maintain a considerable link budget for communications.

However, despite the differences in propagation between the sub-6 GHz and higher bands, simultaneous multi-band measurements at different frequencies in several environments have yielded striking results in similarities: the dominant MPCs are mostly present in the different bands [107, 108, 109, 110]. Hence,
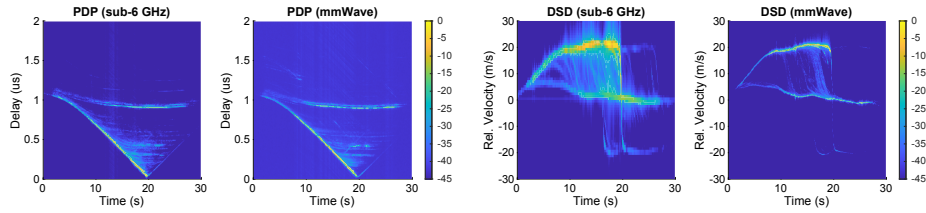
Figure 9: Power delay profiles and Doppler spectrum densities at 3.2 GHz and 34 GHz in V2V scenarios, [112].

there is a high correlation between bands, which has been further discussed and included in channel models [111].

COST INTERACT contributions in simultaneous multi-band measurements at sub-6 GHz, mmWave, and (sub-)THz in different scenarios have shown strong similarities on the multi-path components in the different bands [110, 112, 113]. The dominant paths are present with similar gain and, different with was expected, instead of an extremely sparse channel, dense-multi-path components have also been observed at mmWave frequencies in many different scenarios. The PDPs and Doppler spectral densities (DSDs) from multi-band (3.2 GHz and 34 GHz) V2V measurements in urban street scenarios showing strong similarities are displayed in Fig. 9, [112]. This similar distribution of the MPCs motivates to further explore the use of sub-6 GHz channel properties for beamforming at mmWave: the analysis of the multi-band measurements in an industrial scenario from [110] shows that this can be effectively exploited in NLOS, [114]. Similar results on the distribution of MPCs in different bands have been observed in multi-band mmWave and THz measurement in a conference room in [113], where multiple common scatterers and the presence of high order reflections at THz have been observed.

Future measurements need to be designed to cope with the requirements on channel models to cover the spectrum from sub-6 GHz to THz and consider the needs of ISAC applications. However, in case of the (sub-)THz bands, measurements are still rudimentary due to the complexity of the channel sounders and set-ups required to capture the multi-dimensional properties of the channel, making it often impossible to resolve different dimensions simultaneously. Therefore, significant work needs to be spent on the joint estimation of Doppler, angular, and delay structure of the MPCs at higher frequencies.

6.4 Measurement data collection contributed to COST INTERACT WG1

Empirical measurements are fundamental for the design, understanding and validation of radio channel models. Furthermore, the creation and sharing of standard reference datasets enables data-driven and hybrid model design approaches in an effective and reproducible way. COST INTERACT's open collaborative environment constitutes a unique opportunity to share measurements, simulation scenarios and models inside and outside the action. In this regard, the Horizontal Activity group 1 (HA1) is responsible for datasets' setup and maintenance. A total of four datasets, which are briefly reported and described in the following and made available at `https://interactca20120.org/wgs/datasets-2/`, have been collected by individual institutions and publicly shared to support the research activities and scientific collaboration within WG1. While we briefly describe the up-to-now contributed datasets below, WG1 remains open to further contributions, which will be made available at the same website.

1. **Indoor high-speed channel sounding at sub-6GHz and mmWave [115]**

   Vienna University of Technology conducted measurements to compare sub-6GHz (2.55, 5.9 GHz) and mmWave (25.5 GHz) indoor wireless channels in a high-speed scenario. For all measured scenarios, the wireless channel is measured with the same transmitter and receiver antenna positions, but with different center frequencies and velocities. This allows a direct comparison of the measured wireless channel in terms of fading environment and channel statistics. Results are provided in terms of time-variant channel transfer functions for discrete-time (snapshots) and frequency (subcarriers).

2. **UPCT Indoor 5G measurements at 1-40 GHz [116]**
   UPCT conducted indoor LoS MIMO measurements in the frequency range from 1 GHz to 40 GHz. Using a Vector Network Analyzer (VNA) setup, characteristic parameters including the relative received power, path loss, root mean square DS, and K-factor were extracted and compared with ray-tracing simulations.

3. **Measured dataset for performance analysis of wireless systems in real-world 60 GHz indoor channels [117, 118]**
   This dataset employs channel measurements of an indoor office environment at 60GHz from the measurement campaign held in Brno University of Technology (BUT), at the Department of Radio Electronics (DREL). The following measurements are employed [117] for the characterization of an indoor channel model for an IEEE 802.11ad single carrier physical layer (SC-PHY) MATLAB-based simulator, which is also provided.

4. **Transmitter Identification and Fingerprinting based on RF Imperfections [119, 120]**

These measurements are a compilation of the results [119] of experiments run on a series of datasets gathered in the Future IoT/Cognitive Radio testbed [120]. Such measurements can be employed for the detection of hardware imperfections in RF transmitters in order to identify a specific transmitter among others.

7 Modeling methodologies

by Tommaso Zugno, Enrico Vitucci, Nicola di Cicco, Diego Dupleich, Wei Fan, Ke Guan, Danping He, and Andrej Hrovat

In the following sections, we present different channel modeling methodologies that have been proposed in the literature, including stochastic, map-based, ray-based, and ML-based approaches. In each section, we describe the main concepts, overview the state of art, and summarize recent developments.

7.1 Stochastic models

The characterization of wireless channels is of paramount importance for the design and evaluation of wireless systems, however, a deterministic knowledge of the channel behavior is difficult and impractical to obtain, as it requires to perform measurement campaigns or to run complex simulations. For this reason, a common approach is to adopt models which represent wireless channels as a stochastic process whose properties resemble real propagation phenomena. In this regard, GSCM is one of the most widely adopted class of stochastic channel models. GSCMs adopt a stochastic approach to account for the presence of scatterers in the environment, and apply geometric properties to model signal propagation through multiple paths. The main advantage of this method is the possibility to easily represent different scattering environments by changing the parameters and/or probability distributions that model the physical properties of scatterers.
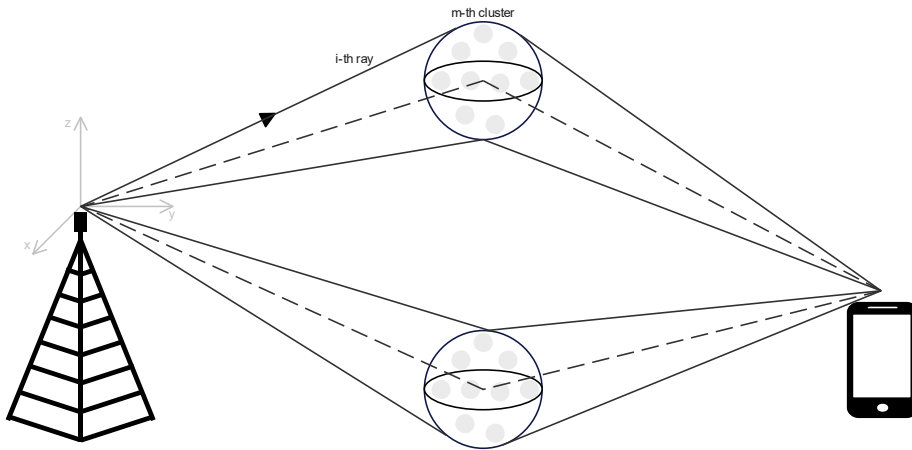

Figure 10: Geometry-based stochastic channel model.

As represented in Fig. 10, signal propagation between a transmitting and a receiving node is modeled by the superposition of multi-path components (MPCs), each representing a plane wave travelling along a different path. MPCs
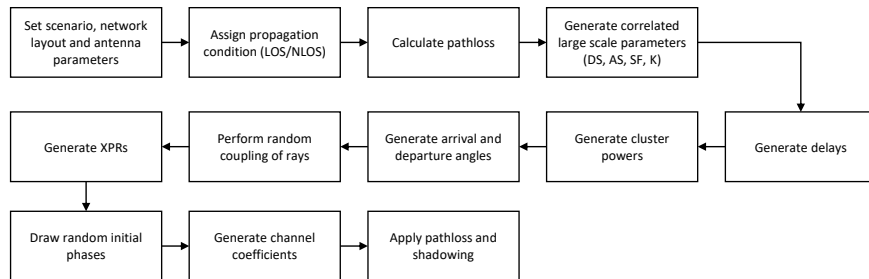
Figure 11: Block diagram of the 3GPP GSCM model, from [111].

depart from the transmitting node with different angles, and arrive at the receiving node from different directions, with different amplitudes, delays, and polarizations. Typically, MPCs that exhibit similar characteristics are grouped together into clusters. Characteristics of each cluster (e.g., power, delay, AoA/AoD, polarization, etc.) are derived from random variables whose distribution depends on the scenario under consideration.

Over the years, several works proposed GSCMs able to represent different scenarios and use cases, such as 3rd generation partnership project (3GPP) TR 38.901 [111] (depicted in Fig. 11), COST 259 [121], Winner II [122], and Quadriga [123]. In particular, 3GPP TR 38.901 was selected as the reference model for the evaluation of cellular systems by the standardization community. This models supports a wide frequency, between 0.5 and 100 GHz, and the modeling of different propagation scenarios, including urban, rural, and indoor scenarios, within the same framework. Despite offering a high scalability and good generalization properties, it presents inherent limitations related to its fully-stochastic nature. For example, it does not provide a good support for the modeling of channel dynamics and inter-link correlation, thus preventing spatially-consistent evaluations. These issues can be overcome by adopting other approaches, such as the one described in [124], albeit at the cost of increased complexity and reduced number of applicable scenarios [1].

As part of the COST INTERACT action, GSCM models have been used for the performance evaluation of emerging use cases, such as vehicular and rail communications. In [125], authors used a GSCM to build a digital twin for assessing the reliability of vehicular communications, while in [126], authors used a GSCM to perform spatially-consistent real time simulation V2X scenarios. Moreover, in [127] authors used a GSCM to train a frame error rate prediction algorithm for wireless communications among vehicles. In [128] and [129], authors designed and validated a new model for train-to-train communications.

Other works proposed new approaches to overcome the limitations of current GSCM models for the simulation of next-generation wireless systems. Indeed, the introduction of novel paradigms, such as integrated sensing and commu-

nications, reflecting intelligent surfaces, and ultra-massive MIMO, require fundamental changes in the way the channel is modeled. For example, in [130] authors extended the 3GPP TR 38.901 framework [111] for the joint modeling of communication and sensing channels. They introduce the concept of *sensing clusters* and describe the additional steps for the generation of the corresponding parameters. In addition to delays, powers, and angles, rays in sensing clusters are characterized by echo angles and radar cross section. Pathloss and shadowing are applied individually for each sensing cluster, and a multi-bounce model is applied to map scatterers to geometric positions. In [131], authors proposed a GSCM for RIS-assisted communications which accounts for movements of terminals and clusters, and the time evolution of clusters in space. The channel impulse response is expressed as a summation of the direct path between BS and UT, and the indirect path reflected by the RIS. The reflecting properties of the RIS are modeled through the Φ matrix which includes the phase responses of the reflecting elements. A birth-death process is used to simulate the evolution of clusters in the space domain. In [132], authors developed a 3D geometry-based double-spherical model for ultra-massive MIMO communications at THz frequencies which accounts for the nano-material properties of plasmonic-based arrays.

7.2   Map-based models

One of the issues regarding the GSCM approach is the modeling of spatial consistency among different links. To solve this issue, other approaches applying ray tracing (RT) principles based on simplified maps of the environment have been proposed [133].

An example of such approach is described in [134]. This model generates the channel response following the step procedure represented in Fig. 12. The first step consists of creating the map, including the definition of transmitter and receiver positions, and the placement of blockers and scatterers. Then, a simplified RT algorithm is used to compute the propagation paths and determine delays, departure and arrival angles. Finally, the channel impulse response is obtained by modeling the interaction of paths with blockers and scatterers according to the main propagation phenomena, including LoS propagation, reflection, diffraction, scattering, shadowing, and antenna patterns.

Other models based on the same principle are available, the most popular being the 3GPP map-based model [111] and the NYUSIM model [135]. More recently, the authors in [136] proposed a map-based channel model for UAV communications at mmWaves, while [137] presented a model for the evaluation of integrated sensing and communications. Moreover, a novel site-level deterministic model adopting a grid-based approach was presented as part of the COST INTERACT action [138].
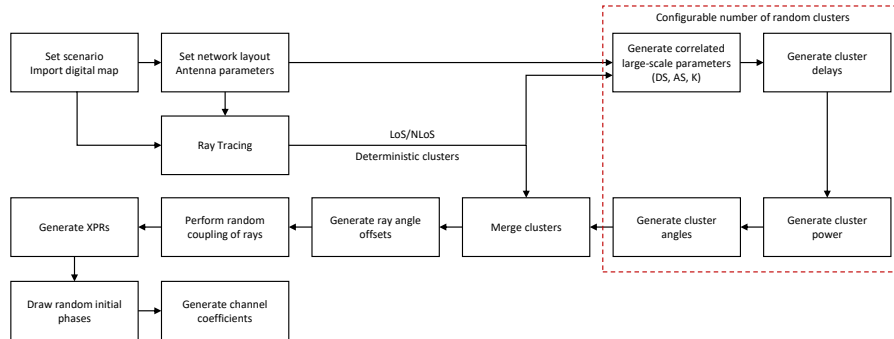
Figure 12: Block diagram of the 3GPP map-based model, from [111].

7.3 Ray-based models

Ray-based approaches relies on the high frequency approximation, where electromagnetic waves are modeled as rays, following the principles of geometric optics for reflection and transmission. Two main approaches can be identified: (i) image ray tracing (RT) and (ii) ray launching (RL). Ray tracing methods compute all rays that can reach the receiving point, e.g., by means of the Image Method represented in Fig. 13a, then apply attenuation factors to each ray to account for the propagation phenomena. The main drawback of this approach is the computation time, which increases exponentially with the number of interactions. In ray launching methods, multiple rays are launched from the transmitter into different directions according to a proper angular discretization, as depicted in Fig. 13b. As in RT, the field propagated by each ray is computed by taking into account all basic interaction mechanisms. Rays that reach the receiver contribute to the overall channel response, while those that miss the receiver or become too weak are dropped and not propagated further. In this case, the computation time increases with the number of launched rays; therefore, this parameter controls the trade-off between accuracy and computation time.

When applied to highly dynamic scenarios, both methods still suffer from the problem of high computational complexity that prevents their use in real-time. One example is the case of vehicles moving at high speed and transmitting/receiving or generating scattering in a dense urban environment. Implementations on game engines like the one proposed in [126], solved this problem by adopting GPU parallelization. Other emerging paradigms like dynamic ray tracing (DRT) can then be applied to mitigate complexity growth [139]. Since the multipath structure remains essentially the same within a given time interval T_C, it is possible to predict the multipath evolution on the base of the current multipath geometry, assuming constant speeds and/or accelerations for moving objects within T_C, and using analytical extrapolation formulas. This is done without re-running a full RT for every "snapshot" of the environment,

(a) Ray tracing.

(b) Ray launching.
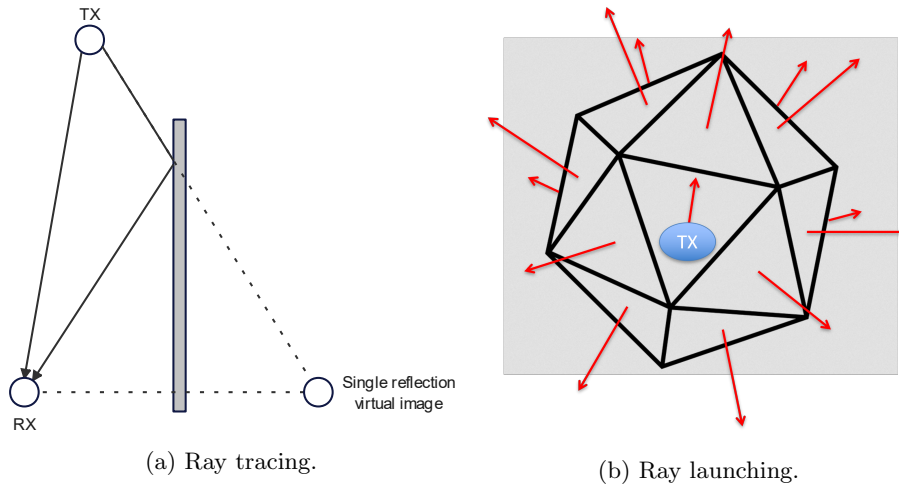
therefore providing substantial savings in terms of computation time. The DRT is then a helpful tool for decreasing computational complexity and accelerating channel calculation, but also its use in real-time becomes possible. When DRT is embedded in a mobile radio system and used in real-time, ahead-of-time (or anticipative) channel prediction is possible, thus opening the way to interesting applications. The DRT method is flexible enough to be employed either in a fully deterministic case, or when the path geometry is derived through statistical realizations of the environment, according to the GSCM approach. Therefore, a natural way of future development of highly dynamic channel modeling lies in further optimization of the execution time via merging the DRT approach with the game engine-based GSCM framework.

Another recent development is the integration of RIS models into RT/ray launching algorithms in order to carry out realistic RF-coverage evaluations in RIS-enabled communication scenarios. In [140], a previously developed RIS macroscopic model based on a "Huygens-like" approach [141] has been embedded in a RT tool, and the performance of the RIS-based solution has been analyzed in simple reference scenarios by modifying a few simple parameters of the model. The results show that a gain of about 15–20 dB can be obtained in blind-spot locations with proper RIS placement and configuration, without the use of any additional active radio head, even when using simple designs such as pre-configured lossy phase-gradient metasurfaces.

Future studies within the COST INTERACT action will deal with the development of a fully ray-based RIS model, which allows for better integration into RT algorithms and more realistic predictions involving multiple-bounce interactions where the RIS can be in any place in the interaction chain.

7.3.1 Challenges for mmWave & (sub)THz channel modeling

For any RT simulator, every object which exists within each scenario resembles kind of a Lego "building block". Once all the building blocks are realized, any communication scenario can be implemented. With the available propagation models, the full-dimensional channel information can be obtained by employing the RT methodology [142]. Nevertheless, the actual implementation of RT techniques within the THz band still faces significant challenges which need to be considered for future research [143]. Some of these challenges will be presented next as open research problems.

Ultra-massive MIMO (UM-MIMO) systems generate very narrow beams to compensate for the very high path losses encountered in the THz band. Since the RT experiments are site-specific, the correlation of all the sub-channels created by UM-MIMO antennas can be characterized by RT. However, with possibly several hundreds of antennas, the computational and storage capacities for such systems will dramatically increase [144]. One possible solution to this problem is to develop a cloud-based RT with high computation and storage capabilities.

Antenna beam management is another important challenge which needs to be carefully considered. Its main function is to steer the antenna towards the strongest ray/path and thus supporting the mobility of UE. The current assumption for 5G mmWave is that the antenna beam from the BSs sweeps all possible directions every 5 ms, while the UEs will transmit a short message as its response. However, since the THz beam will become much narrower, the time required to check all possible directions will significantly increase. With the aid of RT, firstly, the omnidirectional antenna can be used to directly identify the strongest path. Then, the BS or/and UE can select their own beam following the RT simulation results in advance.

Complex multipath is another challenge caused by the "multi-structures" configuration. One solution for identifying the characteristics of the complex multi-paths is to integrate the individual transfer functions of the propagation graph with the aid of RT. This is a new hybrid channel modeling approach which is based upon the join processing of RT and graph theory. It is our belief that such hybrid approach is a promising approach for the accurate and efficient channel modeling of such dense MPCs.

7.4 ML-based approaches

Electromagnetic propagation is a complex phenomenon, as it depends on multiple, different factors, including the properties of the propagating signal (e.g., intensity, frequency, bandwidth, polarization, etc.), the geometrical and electromagnetic characteristics of the environment, and the specific position of the transmitter and the receiver inside the environment. As ML methods are inherently fit to take care of complex problems [145], their use for wireless channel characterization has been attracting increasing attention over the last years [146], [147], [148].

If physical insight is heavily limited by the complexity of the target problem, a ML-based propagation model basically consists of a black box, that provides the existing, underlying pattern between some input data or between some output labels and the corresponding input features without any clear explanation. Conversely, ML can be aimed at improving the accuracy of some baseline propagation model through the introduction of effective correction factors [148] in case some physical/theoretical insight can be inferred.

To what extent a ML propagation tool can reliably mimic the electromagnetic propagation process depends on the accuracy of the training stage, where a large amount of propagation data are effectively fed to the tool in order to learn the way the wireless channel actually behaves. Training therefore represents a crucial task that must be carefully planned and carried out. Propagation prediction through a well trained ML tool is expected to be accurate and fast at the same time, to the extent that it can be relied on offline, i.e., for the design of wireless networks and systems, but also in real time, i.e., to assist the system (either end users or network equipment) during working operations.

We now provide a concise overview of the main learning paradigms in ML, contextualized by some illustrative applications in propagation. We then elaborate on practical guidelines for choosing the most appropriate ML algorithm for a given task, and we provide relevant pointers for future research directions of interest. The fundamental learning paradigms in ML are supervised learning (SL), unsupervised learning (UL), and reinforcement learning (RL). In SL, the task is to learn an input-output mapping given a finite dataset of input-output examples. SL problems include, but are not limited to, regression, classification, forecasting, ranking, and segmentation. Examples of SL problems in propagation are Path Loss regression [149] and LoS prediction [150]. In UL, the task consists of learning patterns and/or extracting useful information from data. UL problems may include clustering, dimensionality reduction, feature selection, density estimation, representation learning, and synthetic data generation. Finally, in RL, the task consists of learning a policy that, after repeated interactions with a dynamic system (or environment), maximizes the long-term accumulation of reward signals. RL is commonly applied to optimization and control tasks for which SL, i.e., learning to imitate an optimal control policy, is unfeasible (e.g., due to the problem of deriving an optimal policy being intractable). Relevant examples in propagation include antenna tilt control [151] and coordinated beamforming [152].

After identifying the learning paradigm that is most pertinent for a given task, the next crucial design point is the choice of the algorithm. In this regard, the "No Free Lunch" theorem states that all ML algorithms are "equally bad" if averaged over all possible optimization tasks [153]. While this result may sound discomforting, it tells us that the choice of an ML algorithm is mainly driven by the structure of the data at hand, i.e., one should choose an algorithm that can be proven (either theoretically or empirically) to be most efficient for the structure of the input data. Broadly, we can discriminate between tabular (or structured) data and unstructured data. As the name implies, tabular datasets consist of data that can be structured as a table, such that each row represents

a single observation, and each column represents a distinct feature. For SL problems, empirically, the best-performing models for tabular data are ensembles of decision trees (DTs), such as Random Forests and, more prominently, gradient boosting decision tree (GBDT) models [154]. GBDT models achieve a remarkable trade-off between ease of training, robustness to hyperparameters, model expressiveness and generalization capabilities, and are therefore advised when dealing with SL problems on tabular data. Conversely, when dealing with unstructured data (such as images, graphs, point clouds, meshes, etc.), deep learning (DL) model architectures become more prominent. Specifically, while the multi-layered perceptron (MLP) is a popular "one fits all" DL architecture, it is advised that the choice of a DL architecture is motivated by the presence of the appropriate "inductive biases" for the given data [155]. A relevant example are convolutional neural networks (CNN), which are among the state-of-the-art for Computer Vision problems [156]. By learning local filters that are convolved with spatial 2D feature maps, CNNs are able to efficiently exploit the spatial correlations in image data, i.e., the CNN architecture possesses the right inductive bias for processing image data. Similarly, Recurrent Neural Network (RNN) architectures such as Long Short Term Memory networks (LSTM) [157] and Gated Recurrent Units (GRU) [158] possess an inductive bias that makes them effective for processing sequence data. Note that an inductive bias, while desirable, is not mandatory for learning an effective model. In this regard, Transformer architectures [159] (the popular ChatGPT model [160] is one such example) have completely superseded RNNs in learning from large-scale natural language thanks to their expressiveness, scalability and ease of parallelization, albeit not possessing any particular inductive bias.

A recent family of models particularly relevant for propagation pertains to the field of Geometric Deep Learning [161]. Indeed, it can be argued that the laws of geometry are pervasive in propagation (e.g., in RT algorithms and Stochastic Geometry), such that many fundamental algorithms in propagation operate on data that displays some geometric properties. In this regard, Geometric Deep Learning aims to devise model architectures able to exploit the underlying geometrical properties of the input data. The aforementioned CNNs are a prominent example of Geometric Deep Learning applied to Euclidean domains (i.e., 2D feature maps). A generalization of CNNs to non-Euclidean domains are Graph Neural Networks (GNNs) [155, 161], which have been applied with success to physics simulation [162] and processing of 3D point cloud data [163]. As such, Geometric Deep Learning holds an untapped potential for breakthrough applications in propagation.

Finally, one major limitation of complex ML models is their lack of interpretability. Specifically, while tree-based models retain some degree of interpretability (e.g., by the means of feature importance), DL models behave fundamentally as black-boxes, which may hinder their deployment in risk-sensitive application scenarios. With the goal of opening said black boxes and deriving precious insight on the learned knowledge, several eXplainable AI (XAI) algorithms have been developed in literature. A prominent example are SHapley Additive exPlanations (SHAP) [164] which, given an arbitrary black-box

function, computes the impact of every individual input feature to the final output. XAI approaches for specific model architectures have also been developed. For instance, GradCAM [165] interprets CNNs by highlighting on the input images where the model "looks" for taking a decision. GNNExplainer [166] interprets GNNs by deriving the subgraphs of the input graph that are the most influential for the output predictions. Recent advances in ML interpretability, particularly relevant for propagation, are Symbolic Regression algorithms [167]. Briefly, the task in Symbolic Regression consists in finding the mathematical expression, modeled as a sequence of tokens (i.e., mathematical operators and physical quantities) that provides the best-fit to the data, balancing the delicate trade-off between goodness-of-fit and complexity of the derived expression. The associated optimization problem is of combinatorial nature: as such, RL can be leveraged for efficiently exploring the space of all possible symbolic expressions. Overall, model interpretability can provide precious insight on the underlying physical laws present in raw measurement data, complementing domain-specific knowledge.

8 Channel parameter estimation

by Wei Fan, Xuesong Cai, Diego Dupleich, Ruisi He, and Bo Ai

8.1 Parameter estimation techniques

Channel parameter estimation aims at extracting propagation parameters such as propagation delay, angles, polarimetric amplitudes, etc. of path components from the measurement data. COST INTERACT has contributed to the development of such algorithms. For example, the authors in [168] proposed a maximum-likelihood estimation algorithm to deal with channels that exhibit a mixture of independent dense multipath components (DMCs), which is in contrast to the commonly assumed model of single DMC mode. An auto-encoder was proposed to infer the order of DMC modes and for initializing the parameters of the DMCs. In general, channel parameter estimation techniques can be mainly classified into four categories: spectra-based techniques, subspace-based techniques, sparsity-recovery-based techniques, and maximum-likelihood-based techniques.

8.1.1 Spectra-based techniques

Bartlett beamforming is the most classical spectra-based method, aiming to find the direction(s) with dominant power(s) [169]. Its variant, a frequency-invariant beamformer for uniform circular arrays can also be found in [170]. The basic idea was to pre-compensate to frequency-dependent phase variation so that two dimensional (2D)-fast Fourier transform (FFT), i.e., beamforming, can be efficiently applied to finding the dominant paths in azimuth and delay domains jointly. For mmWave frequency bands, a widely applied spectra-based method is to obtain the joint angle-delay spectrum according to the channel measurements by rotating horn antennas to different directions [171, 172, 173, 83]. These methods are straightforward and with relatively lower complexity. However, system responses such as antenna radiation patterns are usually embedded in the resulting spectra, making it difficult to separate the propagation channels from the sounder hardware, not to mention the low resolutions.

8.1.2 Subspace-based techniques

Among the subspace-based methods, the well-known ones are MUltiple SIgnal Classification (MUSIC) [174] and unitary Estimation of Signal Parameter via Rotational Invariance Techniques (ESPRIT) [175], and their variants can be found in, e.g., [176, 177, 178, 179, 180]. In the early development of these techniques, the basic assumption is that propagation paths are uncorrelated so that the covariance matrix of the received signals can be decomposed into signal subspace and noise subspace [174]. By examining the distances (orthogonality) between steering vectors and the noise space, a spectrum can be obtained with its peaks indicating path directions. Intuitively, if a steering vector is orthogonal

to the noise space, it means that it belongs to the signal space, i.e., contributing to the received signals. Later on, these techniques were extended to dual domains such as delay vs. frequency covariance matrix. The main limitation is the deficiency in resolving a large number of paths and requiring a certain number of snapshots to obtain a sample covariance matrix.

8.1.3 Sparsity-recovery-based techniques

Sparsity recovery algorithms [181, 182] are developed based on the assumption that the channel exhibits sparsity in parameter domains, i.e., only a few paths contributing to the received signals, although the assumption is still questionable even in mmWave frequency bands [183]. By exploiting specific optimization principles, e.g., convex optimization, channel parameters can be recovered.

8.1.4 Maximum-likelihood-based techniques

Despite the high complexity of maximum-likelihood-based estimation algorithms, they can extract the propagation parameters that are properly defined in the signal model with a high resolution that approaches the theoretic lower error bound, i.e., Cramér-Rao Lower Bound (CRLB). The most widely used maximum-likelihood-based algorithm is the SAGE algorithm [184]. It is a further enhanced algorithm based on the Expectation-Maximization (EM) principle [185] that is theoretically proven to converge to a local maximum of the likelihood objective function. In SAGE, the high-dimensional estimation/optimization problem can be decomposed into several one-dimensional problems, leading to much lower complexity and faster convergence. In [186, 187, 188], variants of the SAGE algorithm can also be found for mmWave wideband large-scale arrays, where the trajectories in delay domain across the array aperture are exploited for effective initializations and interference cancellation. The SAGE algorithm usually assumes that the propagation paths are well-resolvable. However, it is possible that due to the scattering effect of rough surfaces, the resulting MPCs can be very dense in delay and angle domains that cannot be well resolved by the intrinsic ability of the sounder. In such cases, one needs to modify the signal model to consider these dense MPCs, i.e., DMCs, as colored noises (in addition to white Gaussian noises) with certain power profiles for a better estimation of other discrete MPCs, which is basically the RIMAX algorithm [189]. Although there exist not a few different parameter estimation techniques, future mmWave and THz propagation channels will pose more challenges due to much larger bandwidths, much larger array apertures, etc. Spherical-wave propagation, channel birth-death on the array, frequency-dependent responses of antennas and sounders, etc., will make the signal model much more complicated, meaning that low-complexity yet still high-resolution estimation techniques are still in need.

Another important consideration for parameter estimation is that the system response of the channel sounder must be well characterized for a realistic signal model. Otherwise, the mismatch of the signal model from reality can

result in many ghost (erroneous) paths estimated [27]. The response of cables, power amplifiers, filters, converters, etc., of the channel sounder can be easily calibrated through back-to-back measurements, i.e., directly connecting Tx and Rx without antennas. For antennas or antenna arrays, they can be placed in an anechoic chamber to measure the 3D responses of antenna elements at discrete angles. The measurement data can be later on exploited to interpolate the responses at arbitrary angles. There are different ways to do this, which include direct (linear or non-linear) interpolation, spherical harmonics, and Effective Aperture Distribution Function (EADF) [190]. Direct interpolation is straightforward but non-analytic. Alternatively, one can transform the measured pattern from the spatial domain to another domain using basis functions, either spherical harmonics or Fourier basis (EADF). Using a forward transform, the transformed spectra are obtained and then utilized to recover spatial patterns. There is also a possibility to compress the measurement data if the spectra are concentrated so that the unimportant components in the transformed domain can be removed. A practical application of EADF in dynamic mmWave channel sounding using 128×256 switched arrays can be found in [60].

8.1.5 Future challenges and directions

6G is envisioned to support applications beyond the current 5G mobile use scenarios, which will pose stringent requirement on the communication systems in terms of data-rate, latency, reliability, and so on. To meet those demanding requirements, a raft of advanced radio technologies are envisioned, e.g. utilization of higher frequency spectra (e.g. up to sub-THz frequency bands), higher system bandwidth (e.g. up to a few GHz), and larger-scale multi-antenna systems (e.g. large-scale or extremely large-scale antenna), utilization of RIS, etc. The advancement in 6G radio technologies have posed significant challenges to the channel estimation parameter. For example, the extremely large scale antenna array will bring a few new challenges for the channel parameter estimation: near-field and spatial non-stationary effects. State-of-the-art algorithms, which are developed based on plane wave model and spatial stationary channel might fail to address all the new features introduced by the massive MIMO systems. The narrow-band assumption might also be violated for 6G radio systems that potentially utilize the ultra-wide-band technology, which should be properly considered for developing channel parameter estimator. As for the sub-THz/mmWave channel measurements, the required phase accuracy might be difficult to achieve, though a few works on phase compensation concept have been reported to achieve coherent phase measurement for virtual antenna array systems. Therefore, it would be desirable to develop channel parameter estimators, which is robust to phase measurement inaccuracy.

8.2 MPC Clustering

Multipath clustering and identification have been important for channel modeling. ML naturally meets the need to group multipath components (MPCs) with

similar channel characteristics, and some well-designed clustering algorithms which naturally incorporate propagation characteristics have drawn great attention [191, 146] for cluster-based channel modeling, and many researches have been conducted in COST INTERACT. Clustering algorithms can be generally categorized into: i) Shape-based; ii) Distance-based; iii) Density-based; and iv) Computer vision-based clustering.

8.2.1 Shape-based clustering

Shape-based clustering involves revealing cluster structure of MPCs in power-delay domain. For example, MPCs belong to the same cluster are supposed to have a PDP that follows a single exponential decay, according to the Saleh-Valenzuela channel model. To recognize clusters in PDP, a fitting method is used to check if envelope shape of MPCs matches a particular distribution, as shown in Fig. 14(a). This method adjusts cluster members by seeking the best fitting result and it is able to accurately identify MPC cluster [192]. Several shape-based methods have been proposed: i) training a hidden Markov model (HMM) to learn distribution of MPCs in PDP and optimizing cluster members using the Viterbi algorithm; ii) using an observation window to separate large cluster and applying a threshold of slope to improve clustering accuracy on small clusters; iii) using kurtosis to measure peakedness of a distribution and applies region competition to divide MPCs into different clusters [193]. In summary, shape-based cluster identification has several advantages including not requiring much prior knowledge about number of clusters and having a relatively low computation complexity. However, its limitation is the lack of angle information during clustering, which can impact identification accuracy.

8.2.2 Distance-based clustering

Distance-based clustering measures similarity between different MPCs based on distance , which is defined in terms of delay, angle of arrival (AoA), and angle of departure (AoD), as shown in Fig. 14(b). Commonly used distance measures for MPC clustering include squared Euclidean distance (SED), normalized Euclidean distance (NED), and multipath components distance (MCD). SED focuses on natural difference between each parameter, while NED focuses on ratio difference. Sequential clustering-based algorithms have been proposed to identify MPC clusters using SED. However, to compare parameters in different domains, it is necessary to normalize parameters to the same scale. MCD has been proposed to address this issue by normalizing delay and angle before calculating distance, which is found to have fairly good performance [194]. Further, many distance-based clustering algorithms such as hierarchical tree clustering, K-power-means (KPM), and fuzzy-C-means (FCM) have been proposed and widely used.
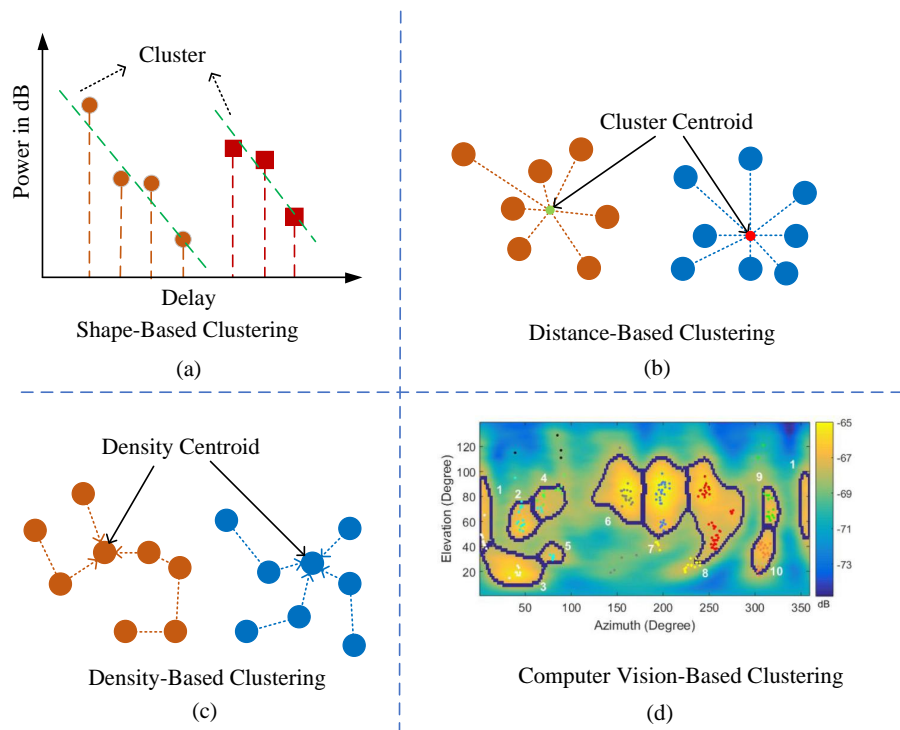
Figure 14: Illustration of different clustering algorithms.

8.2.3 Density-based clustering

In the natural propagation environment, MPC are grouped and the MPC near cluster centroid usually have higher density than those at the edge of cluster. Density-based clustering algorithms, such as DBSCAN, can identify MPC clusters based on distribution and density property, as shown in Fig. 14(c). These algorithms calculate MPC density for clustering and do not require prior knowledge such as cluster number and cluster centroids initial position. However, how to measure MPC density is important to algorithm performance. To obtain improved performance, [195] firstly proposes the perspective to consider physical propagation mechanism for clustering algorithm by designing MPC density. It proposes a novel aspect of MPC kernel-power-density to well incorporate the modeled propagation behavior of MPCs into clustering algorithm, and it obtains significant performance gain in terms of low computational complexity and high clustering accuracy.

8.2.4 Computer vision-based clustering

Computer vision-based clustering exploits image processing methods to identify MPC clusters based on visual criteria such as shape of potential cluster, distri-

bution pattern of MPC delay and angle, as shown in Fig. 14(d). One example is the Hough transform-based clustering, which uses the Hough transform to recognize trajectory of MPCs in delay domain and merges the recognized trajectory into clusters. Another example is the PAS-based clustering and tracking (PASCT) algorithm [196], which uses the maximum-between-class-variance method to separate potential cluster groups from background noise and further divides the clusters by using density-peak-search method. These methods follow an intuitive approach and provide results that conform to human observation whereas also benefit from the rapid development of computer vision.

8.2.5 Future Work

Many long-standing problems remain unsolved on this topic. For example, for time-varying non-stationary channels, the existing algorithms still need to be improved significantly. Supervised AI-based clustering and tracking methods are worth receiving more attention in the future, especially considering the phenomenal increase in both the amount of collected channel measurement data and the available computing power. Moreover, drawbacks still exist with respect to algorithm complexity, threshold choices, and assumptions about prior knowledge. Algorithms with few prior knowledge about clusters should be further developed.

9 New technologies

by **Joonas Kokkoniemi, Marco di Renzo, Narcis Cardona, Ruisi He, Bo Ai, Wei Fan, Xiping Wang, Ke Guan, Tomaz Javornik, Franco Fuschini, Yang Miao, Mi Yang, Dan Fei, Guido Valerio, and Julien Sarrazin**

9.1 Path Loss Measurements and Modeling for RIS

In recent years, RISs have been under active discussion and investigation as a promising technology to enable future 6G networks. RISs are artificial electromagnetic surfaces comprised of large numbers of sub-wavelength unit cells or antenna elements. Those are either very small elements ($\ll \lambda$) forming a larger artificial surface (a metasurface) or individually controllable antenna elements such as in reflect arrays. The RISs can flexibly control the parameters of wireless signals, such as phase, amplitude, and polarization, thus enabling the emerging concept known as "smart radio environment" [197]. The core principle of the RISs is to be able to capture a part of the radiated power with the aperture of the RIS and redirect it via reflection towards wanted direction by manipulating the phase (and amplitide) of the insident radiation. Usually the goal is to do beamsteering the amplify certain directions, but as mentioned above, it is also possible to manipulate the signal itself. Therefore, the RISs allow the manipulation of the radio channels. This is traditionally impossible and usually the only way to manipulate the signals is via antennas and arrays of those. Hence, the RISs give an interesting opportunity for added control that can be used to overcome problems, such as signal blockages and cell edge signal amplification.

Two important use cases for RISs in the literature are shoot-through RIS and reflective RIS. The former can be used for beamforming close to antenna, but the latter is more important what comes to channel modeling and especially manipulation of the channel coefficients. In this section, we talk exclusively about reflective RISs and the channel modeling related to those. So far, some of the challenges with RIS channel models is the rather limited number of physical prototypes and multitude of options and ways to manufacture RISs. Later in this section we give some examples of the channel modeling activities related RISs.

9.1.1 RIS channel modeling challenges

Generally speaking, some of the challenges in RIS channel modeling arise from the fact that the behavior of the RIS itself depends on how it's made and how it as been configured. The basic communication scenario is that we have a Tx, RIS, and an Rx. The channel between Tx and RIS and RIS and Rx are traditional channels, e.g., free space of fading channels. The phase shifts introduced by the RIS are then optimized minimize the total loss in the cascaded Tx-RIS-Rx channel. Because the RIS is an active element, often assumed to be controlled by the base station, a closed formed macroscopic channel models are hard to

derive as the RIS by definition reconfigures the channel coefficient based on the particular situation. Therefore, also the total path loss depends on the entire system setting and outcome of the optimization problem.

Whereas wireless communication engineers in the past have resorted to macroscopic channel models in system analysis and optimization, there are also other challenges what comes cascaded RIS channels. For instance, the real systems are almost never random. The network engineers design the network based on the maximization of the signal power in some local are and availability of locations for the base station and supporting hardware. In the case of RISs this can mean that the engineer may try to arrange a very good LOS channel between the base station and RIS whereas the RIS-user channel can be normal mobile fading channel, for instance. But this is just one of many options from network design point of view and the individual channels depend on the location and how the network elements can be placed. This makes the general channel modeling very challenging and the channel losses and potential gains achieved by RISs depend on the deployment environment. Especially in rural setting where distances are long, RISs are most likely not going to provide good gain as the reflected energy decreases fast with distance. However, in the case of urban and indoor scenarios where RISs are expected to be the most beneficial, there are powerful tools avaialable to test and optimize networks via simulations.

Ray tracing has become an important tool to study channel especially at high frequencies where traditional channel modeling is challenging due to difficult channel measurements. As the ray tracing relies on fixed 3D maps, they have also been used extensively in network design in order to optimize the network element placement. Ray tracing is therefore also a very good tool in studying RIS channels in various scenarios, e.g., as shown in [198] in urban environment. The downside of the ray tracing is that the simulation always require accurate 3D models of the desired environment. The upside is that testing the network elements in simulation environment is very flexible and fast. Therefore, the ray tracing is very good tool to test and evaluate the RISs as well. This is somewhat related to digital twins in which we have a replicated digital environment where we can test, e.g., RISs, but theoretically also optimize those in real time in the case of actual physical deployment.

Ray tracing is particularly powerful in system evaluations and performance testing, but can be locally used for channel modeling as well. The challenge in channel modeling tends to be that the results are representative for that particular environment, but not in general. However, it is still much faster to generate data with ray tracers that by real measurements. Therefore, an appealing option is to calibrate ray tracers with real measurement data in order to extend the measured data. In the case of RIS this still does not take away the difficulty of statistical modeling of an active reconfigurable element that can take many forms and sizes. Ray tracing can still be very efficiently used in evaluation of the RISs in the desired environment in order to deside where to place it/them and what kind of gain do those give in the scenario in hand. Whereas there are too many channel scenarios to discuss herein where RISs could be useful and what those require from the channel modeling, in below we

give some examples of the works related to RIS channel modeling.

9.1.2   RIS channel models from literature

The path loss and propagation are basic characteristics of wireless channels. The channel represents the basic relation between the wireless signal power and the transmission distance, which can provide information on how far a wireless signal can be successfully transmitted. Due to the importance of characterizing the path loss and channel reciprocity characteristics of RIS-assisted wireless communications, researchers have recently conducted related studies that are based on different analytical assumptions and approaches [199],[200].

Di Renzo et al. [201] derived asymptotic scaling laws of the path loss as a function of the transmission distances and the size of the RIS in the far-field and near-field cases. The results are obtained by leveraging the scalar Huygens-Fresnel principle in a two-dimensional space. Garcia et al. [202] calculated the radiation density of the scattered field in the near-field and far-field under the assumption of dipole antennas and discussed the scaling laws as a function of the transmission distances numerically. Ellingson [203] proposed a physical model for the path loss of an RIS-assisted wireless link under the assumption that the antenna gain of the transmitter/receiver is constant over the RIS. Najafi et al. [204] developed a physics-based RIS path loss model, in which the impact of grouped unit cells on the wireless channel is obtained by solving the integral equations for electromagnetic vector fields under the far-field assumption. Danufane et al. [205] generalized the model in [201] to a three-dimensional space by using the vector generalization of Green's theorem, and characterized the scaling laws of the path loss as a function of the transmission distances and the size of the RIS based on scattering theory. Wang et al. [206] proposed a radar cross section-based path loss model that introduces an angle-dependent reflection phase behavior of RIS unit cells. Gradoni and Di Renzo [207] developed a path loss model that is based on the theory of mutual impedances of thin dipole antennas. The end-to-end channel model resembles a MIMO communication system and considers the mutual coupling among RIS unit cells. Recently, Di Renzo et al. [208] proposed a path loss model, based on scattering theory, assuming that the incident signals are not constant over the RIS elements. A summary of the above-mentioned research works on RIS path loss modeling is available in Table I of [209].

9.2   Channel Measurements and Modeling for ISAC

In the last decade, radar has been considered in some works as the natural complement to communications, in which the radar-based sensing is a default technology. In [210] a low-complexity algorithm for joint radar and communications in automotive is developed, while in [211] the sensing from radar is used to assist the beam-steering at mmWave links. The sensing information is used to predict the communications channel in [212].Nevertheless, when we refer to ISAC inthis paper, it is done for communications-centric ISAC, meaning that

sensing is implemented using the communication signals from one or more radio access nodes. To this end, in COST INTERACT, authors in [213] are developing solutions for joint sensing and communications (JSAC), with parallel sensing and communication waveforms that share the same bandwidth.

ISAC has become a design paradigm for 6G, for which understanding and modeling the behaviour of the sensing and the communications channels simultaneously is crucial. The main ISAC applications in 6G mobile networks are vehicular communications (V2X), sensing as a service, remote sensing and environmental monitoring, while those applying to short distance wireless channels are, among others, in-cabin sensing, smart home, and human-computer interaction [21, 214, 215]. This confers different ISAC channel scenarios, which can be summarized into three types (Fig. 15): monostatic, bistatic, and distributed, depending on the deployment of the transmitter and receiver(s).

9.2.1 Sensing scenarios: monostatic, bistatic and distributed

ISAC scenarios are monostatic when sensing transmitter and receiver are at the same position; bistatic case refers to sensing transmitter and receiver being separated, while distributed scenarios account for multiple sensing paths available for the same target. In [216] a description of the monostatic, bistatic and distributed ISAC concepts, and the advantages of the centralized version of ISAC, are discussed. Figure 15 summarises the three cases.
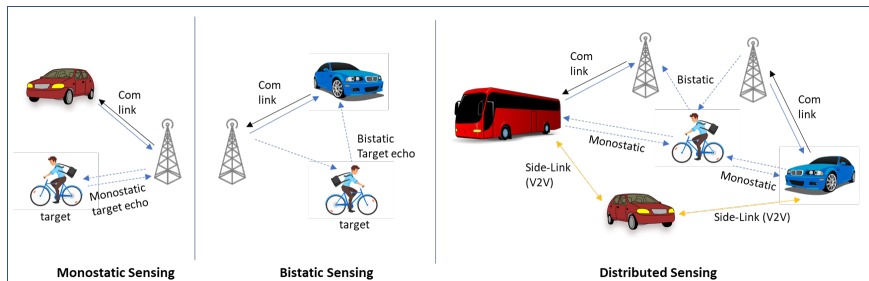
Figure 15: Monostatic, Bistatic and Distributed ISAC scenarios

For the monostatic case, many radar concepts apply, like the radar cross section (RCS) to measure the radar reflectivity of individual targets. Monostatic sensing channels can anyway be modeled from the multipath propagation, limited to the case of having the transmitter and receiver at the same position, so most of, but not all, the sensing energy coming from LoS components. To that end, [217] provides an empirical scattering model obtained from measurements of materials at 28 and 140 GHz. The implementation of monostatic ISAC sensing requires the full-duplex mode of the radio interface, which is not implemented so far in current 3GPP standards. This is the reason why some proposed systems for ISAC refer in fact to a JSAC strategy, in which a radar sensor is used to improve communication links.

The estimation of the communications channel from the sensing one is investigated in [218], where the authors consider the communication receivers to be the targets of a monostatic OTFS-based ISAC system. Thus, the two channels in this case are highly correlated.In [219] the authors use OTFS modulation for joint radar parameter estimation and communications, exploiting the channel sparsity in the Delay-Doppler domain for efficiently separate sensing (radar) parameters estimation and communications.

In the bistatic case, the transmitter sends communication and sensing signals and the receiver captures the echoes from targets and clutter together with the multipath (scattered) components that compose the communication channel. As a consequence, any model that describes simultaneously the sensing and the communications channels has to be geometrically accurate for simultaneous multiple links, and reproduce moving targets along different tracks with spatial consistency, including phase continuity [216].

9.2.2 Trends in ISAC channel modeling

The ISAC channel models are a combination of two channels in one single geometry, i.e., a common framework that develops two approaches, either simulated with more or less precision, or stochastically created. In [220], the ISAC channel is defined as a two-port system in which sensing and communication channels, as well as the common interference between them, are modeled as the reflectivity and transmission functions of such system. This scheme is adaptable to any current model in the literature, either deterministically created by precise 3D ray-tracing, stochastically from a random distribution of scatterers, targets, and clutter, or a hybrid of the two.

Stochastic models Recent approaches on ISAC stochastic channel modeling propose GSCM extensions to the 3GPP channel model [111], e.g., within COST INTERACT [221] and elsewhere [222], [223]. The stochastic channel modeling methods dominated the evaluation of wireless communications in 5G due to their low computational complexity and easy standardization, which was sufficient to evaluate the communication performance of 5G use cases. The application of GSCM models to ISAC requires adding some important elements to the model, since communication and sensing channels are somewhat different. For example, [223] includes both stochastic and deterministic approaches while accounting for spatial consistency. In [221], paths are generated by probabilistic functions derived from channel measurements made in real scenarios, thus geometrically pre-setting the distribution of effective scatterers, i.e., the objects on which the set of rays is incident. The authors in [223] propose a shared cluster-based stochastic JSAC channel model and conducts a channel measurement campaign in typical LoS and NLoS indoor scenarios at 28 GHz and obtains the power angular delay profiles (PADPs) of the communication and sensing channels. For monostatic case, the correlation between the channels may exist, but this is not so obvious correlation for bistatic and distributed cases, mainly because

sensing "targets" and communication "scatterers" are not necessary the same objects or, if they are, do not have the same reflectivity behaviour.

Deterministic models Current deterministic channel models have modeled scatterers for communications and have considered the reflection from them in the form of specular reflection or diffuse scattering. From radar/sensing perspective, any target in the scene can be modeled according to its RCS, but for ISAC, more detailed parameter are required, e.g., the bistatic target reflectivity (BTR) [216]. An example of a target is a person on a bike (Fig. 15), a moving target with local movements, causing in terms of sensing a long-term Doppler because of its displacement, and micro-Doppler originated by the person and wheels movements [216]. The same work further establishes that, for ISAC, deterministic models with more physical descriptors are needed, especially for target modeling, in contrast to the statistical approach of the GSCM models. To resolve the issue, the authors propose a propagation channel model for ISAC that is geometrically correct for multiple simultaneous sensor links and reproduce a moving target in a spatially consistent way along a track, which includes phase continuity.

Hybrid approaches Combining the stochastic and deterministic approaches has the potential to benefit from efficiency of stochastic and realism of deterministic approaches. In an ISAC context, the hybrid models would use a deterministic method to identify primary signal propagation paths and a stochastic method to generate additional objects and clusters. For example, 3GPP already includes a hybrid channel model where RT is used to find propagation paths, and stochastic clusters are generated afterward [111]. For ISAC, it is important to incorporate the object's RCS into the channel model for more realistic simulation of scattered rays, which has significant implications for applications like object recognition. Long-run simulations that maintain consistency in time and space are required for an accurate evaluation of these applications. Therefore, the GSCM needs to incorporate a spatial consistency model, as noted in [216], to meet this requirement and avoid inconsistencies and artifacts in the Doppler spectrum.

9.2.3 Characterizing ISAC channels: recent measurements and modeling at mmWave bands

Recent ISAC channel measurements at 28 GHz frequency band are carried out in Beijing Jiaotong University, China [224]. A measurement system is designed as shown in Fig. 16(a), including Tx, sensing terminal (SX) and Rx. Tx and Rx use a directional horn antenna and a 4x8 rectangular antenna array, respectively. SX also uses a 4x8 rectangular antenna array and it is located close to TX to measure sensing channel. The sounding signals have 1 GHz bandwidth and are transmitted with a maximum power of 28 dBm.

Fig. 16(b) shows ISAC channel measurement scenario on campus, and different locations for RX are considered during the measurements. The novel
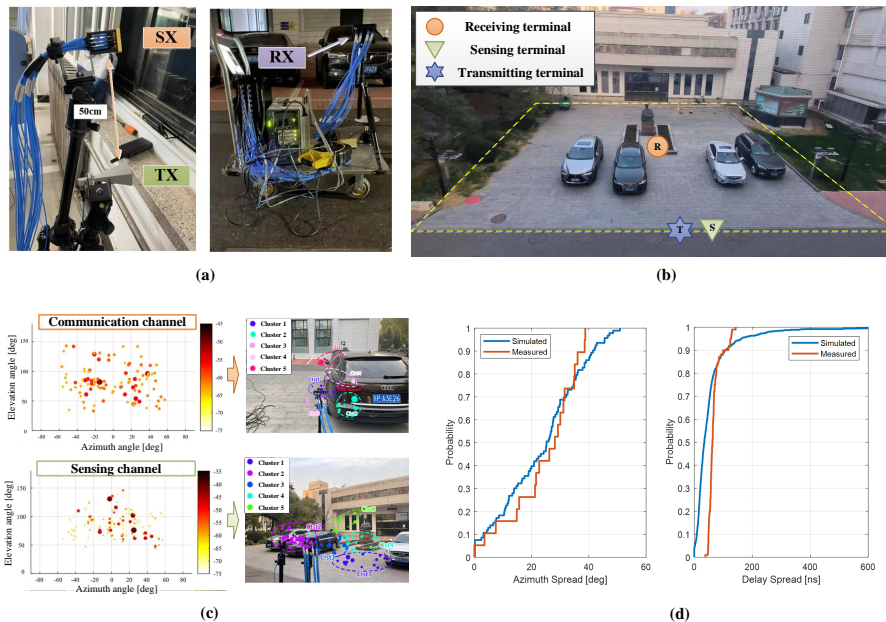
Figure 16: ISAC channel measurement and modeling in [224, 222]. (a) Photos of ISAC channel measurement systems; (b) ISAC channel measurement campaign; (c) Mapping between communication channel and sensing channel; (d) CDF comparisons of azimuth AS and DS of simulated and measured data.

idea of ISAC channel characterization and modeling in [222] is to distinguish communication channel and sensing channel from propagation perspective and characterize the both channels jointly in statistical modeling, which accurately reflects the underlying correlation between communication channel and sensing channel. According to mapping relation in environment, some communication clusters are reserved in sensing channels, which are named evolving sensing clusters. Besides, some newly generated clusters only exist in sensing channels, which are named newborn sensing clusters. ISAC channels can be modeled based on the distribution of those clusters. The ISAC channel parameters are estimated using the SAGE algorithm and channel multipaths are clustered using the K-Power-Means algorithm [146]. Based on measurements, the first five clusters with the maximum powers are mapping and matching to real physical objects in environment as shown in Fig. 16(c). According to the mapping of real physical objects, cluster transition probability from communication channels to sensing channels is firstly defined in [222] and statistically modeled. The DS and azimuth AS of simulated and measured ISAC channels are compared in Fig. 16(d) that shows fairly good agreement. This validates that the proposed ISAC channel model has fairly high accuracy.

57

9.2.4 Open challenges in ISAC channel modeling

Channel modeling scenarios for ISAC include road and air traffic, logistics, critical infrastructure protection, among others. In such scenarios, ISAC channels cannot be generalised as stationary in a wide sense. Then, models require dynamic scenarios to include moving passive objects, target track motion, pattern interpolation or model-based data compression, and Doppler effects along the track, as well as micro-Doppler, to consider local movements within the target.

ISAC targets cannot be modeled as communication scatterers, and require a model adapted to sensing channels that includes bistatic delay and Doppler, over the current RCS radar approach. Scatterers need 3D geometric modeling, including dynamic state vectors of position and orientation. Correlation between sensing and communication channels in bistatic and distributed scenarios has not been properly studied and modeled so far. On the other hand, mutual interference between the ISAC channels may also be a limiting factor for ISAC applications in some scenarios and system implementations. This knowledge will be relevant for future applications in which the estimation of the communications channel from the sensing one may help saving signalling and radio resources.

For standardisation purposes, it will be worth extending the 3GPP communication models to ISAC, either based on GSCM or hybrid approaches. Measurements can help verifying if hybrid models preserve the spatial consistency and may be useful for 6G system level evaluation.

9.3 Channel Measurements and Modeling for ultra large arrays/MIMO

MIMO technology will continue to evolve for the 6G communication system. It is expected that array with thousands of antenna elements (also refereed to as ultra-large-scale antenna systems, gigantic MIMO or extremely large-scale antenna systems) will be accommodated in 6G radios. Radio channel modeling is essential for the system design, optimization and performance evaluation of such ultra-large-scale antenna systems. In this section, state-of-art and key challenges are briefly summarized for radio channel characterization of ultra-large arrays, with a focus on channel sounder design, radio channel parameter extraction and channel modeling.

Geometry based stochastic channel models, e.g. 3GPP 25.996 [225] and 3GPP 38.901 [111] are selected as standard channel models for 4G and 5G communication systems, respectively. The UEs are small in size and far-from the scatterers and BSs. Therefore, plane wave model and stationary channel are typically adopted in the standard channel models. However, these assumptions might be violated for ultra-large-scale MIMO systems. The large array aperture would require a large far-field distance, which will be violated in practical deployment scenarios. As a result, UEs might be located in the near-field region of the BSs. Another effect introduced by the ultra-large-scale MIMO is the spatial non-stationarity. It has been generally assumed in the standard channel models

that the multipath components seen by the array elements are unchanged (i.e. spatially stationary) across array elements. However, spatial non-stationary, i.e. different channels can be observed by different array elements, might exist as the array gets larger. Channel non-stationary properties have been considered in COST 2100 channel models, where the concept of visibility region was proposed to model spatial non-stationarity over arrays. As for deterministic channel modeling approach, it is favorable for characterizing site-specific scenarios. RT simulation can in principle well capture the channel characteristics of ultra-massive MIMO systems, and it is a promising solution for such systems. However, it is computationally heavy to obtain the RT channels for all the antenna elements within the large-scale array. The problem will become much more pronounced for large-scale deployment scenario with many objects, e.g. urban environments. Several alternative approaches have been discussed to reduce the computation complexity, e.g. the database and ray interaction simplification in the METIS model.

Reliable channel sounders are essential for obtaining high-fidelity channel measurement data. As for ultra-massive MIMO antenna systems, the focus has been on measuring channel spatial profiles, since the key task of extremely large-scale antenna systems is to better exploit the spatial property of the radio channels. Typical solutions for measuring channel spatial profile reported in the literature include real antenna array (i.e. with parallel RF chains), switched antenna array (i.e. with one RF chain connected to multi-antennas with a switch), phased array, and virtual antenna array. There exists a trade-off between channel sounder capability and cost. Real antenna array based channel sounder is capable of capturing real-time channel responses, enabling measurements in highly dynamic scenarios. However, its cost and complexity is rather high, especially for ultra-massive antenna systems. Virtual array solution, which has been widely employed already for large-scale antenna based channel sounding, on the other hand, can easily achieve scalable antenna array configuration, making it highly suitable for large-scale antenna based channel measurements. However, it is limited to static scenario and it requires highly accurate positioning and phase coherent measurement system.

Generic channel parameter estimator, which can accurately extract multipath parameters with high resolution, is highly desirable. Many channel parameter estimators have been reported in the literature. Plane wave assumption is typically adopted to reduce the model complexity. However, this assumption is challenged as the antenna array size gets larger and cell size gets smaller. Narrowband is also assumed in many algorithms, to reduce complexity in multi-domain parameter estimation. However, ultra-wideband system implementation might be expected for the future radio systems, especially at the mmWave and sub-THz frequency bands. Another key general assumption in channel parameter estimation is the stationary channel for antenna array elements. This assumption is valid for small-scale arrays as well. However, as the array dimension gets large, this assumption will be eventually violated. As a result, elements across the large-scale array will experience multipath components with different parameters. These observations for ultra-massive MIMO

systems, if not properly considered, will eventually impact the channel parameter estimator performance. Oversimplification in the model will also introduce model mismatch errors for the parameter estimation.

9.4 Application of ML and DL for Propagation Classification, Clustering and Regression

An accurate wireless channel model is a necessity to support environment-aware communications. Wireless channel characteristics are vital in stochastic channel modeling (SCM), localization systems, and orthogonal frequency division multiplexing (OFDM) technology. They are also regarded as key indicators for quality of communication[226]. Wireless channel characteristics can be extracted from measurement data or simulation (such as RT). However, it is challenging to conduct measurements. Simulation is time-consuming and expensive, especially for complex environments in high-frequency band[227].

The recent surge of AI is revolutionizing almost every branch of science and technology, including wireless channel modeling[228]. Many researchers are trying to utilize DL models and ML algorithms to estimate or generate wireless channel characteristics.

In the general framework of wireless systems and communications, ML/DL can be leveraged to address three major problems:

- *classification*, e.g. for LoS/NLoS identification [150],[229]. Reliable and fast detection of LoS can be helpful to assist beamforming techniques or to deploy Fixed Wireless Access networks, as their effectiveness improves in presence of visibility between the wireless devices. Moreover, LoS/NLoS detection can be also beneficial in mobile channel modeling, as different formulas can be effectively applied depending on whether LoS or NLoS conditions occur.

- *clustering*, e.g. to identify and group multipath contributions with similar features [191, 146]. Multipath clustering is crucial to limit the complexity of channel modeling while catching the essence of the propagation process at the same time.

- *regression*, i.e. to get the cause and effect relationship between some propagation markers (like received signal strength, path loss, spread coefficients of the channel, etc.) and some input features relevant to the propagation process.

In [230], authors used linear models, artificial neural networks (ANN), and k-nearest neighbor (KNN) to estimate the power of received radio signals in urban areas. DL models are becoming increasingly popular due to their powerful ability in non-linear approximation and massive data processing. [231] introduced a deep CNN for radio map estimation. Besides channel characteristics in the power domain, many researchers also focused on the temporal domain channel characteristics such as DS [232][233]. Typically, for data (such
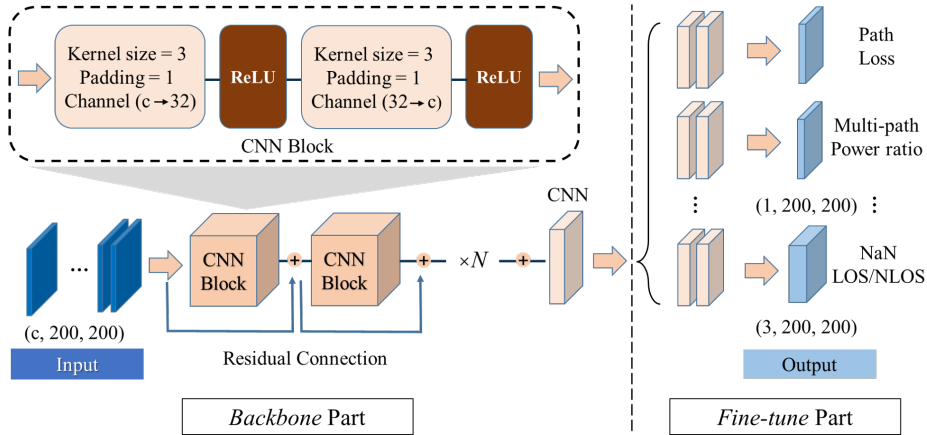
Figure 17: The MTL DL model for channel characteristics SR in [227].

as images) processed by DL models, pixels of different channels are entirely independent. However, channel characteristics (in power, temporal, and angular domain) are correlated because they originate from the same radio propagation process. Therefore, multi-task learning (MTL) can be beneficial in generating multiple channel characteristics simultaneously. [227] introduced an MTL DL model (Figure 17) for super-resolution (SR) of six kinds of channel characteristics. High-resolution channel characteristics data can be recovered by the proposed MTL DL model with low-resolution data as input. The authors also evaluated other mainstream DL models. The results indicate that without adjustment, popular DL models (such as ResNet, ViT and GAN) can not be applied for SR of wireless channel characteristics.

Certainly, AI will play an increasingly more influential role in channel modeling. Here we propose two suggestions for future research:

(1) Data is always regarded as the impetus of ML models. Measurement data and data by simulation are two primary sources of training data for ML to propagation. Novel channel measurement technologies should be studied to reduce the measurement cost and improve the precision of measurement data (such as denoising). Current simulation software should be modified to cater mainstream data formats for popular DL computing frameworks such as PyTorch and TensorFlow.

(2) Compared with typical image and voice datasets, the size of channel characteristics data is relatively small. Lightweight DL models are recommended because large DL models are inclined to overfit the small training dataset. Another advantage of the lightweight DL model is that they are easier to be computed in BSs without GPUs. Considering distributed learning and federated learning, the communication cost can be reduced due to fewer parameters being updated.

9.5 Data-Driven Radio Channel Prediction - Extrapolation in Frequency/Time-Space Domains and for Different Scenes and Systems

Channel prediction is to interpolate and extrapolate the channel responses or its properties in frequency and/or spatial-temporal domains. Environment-aware channel prediction also includes the prediction of channels in multiple scenarios/environments. Channel predictions have conventionally been dominated by model-driven approaches that reply on physics (e.g., utilizing the closed-form translation and rotation of spherical waves expanded from the received field at antennas [234]), mathematics (e.g., using Fourier transform to interpolate channel in frequency domain, using anomaly detection for blockage-aware channel prediction [235]) and statistics (e.g., scenario-based stochastic channel models with parameterization). However, with the development of 6G, it is expected to map the physical and virtual worlds and expand the boundaries of human-machine-things connectivity; thus it is expected that channel modeling/predictions could cover all spectra, different systems, and full applications in various scenarios. Model-driven prediction approaches could be enhanced with the support of the advanced data-driven methods to expand further the predictable boundaries.

The data-driven methods, or in other words, the AI or the ML/DL methods, are represented by deep neural networks and have been widely used in many fields because of the excellent nonlinear modeling ability. AI-enabled channel modeling/prediction as proposed in [15, 147, 236] is a disruptive technology, which can well improve the intelligence and accuracy of radio propagation prediction and simulation. Compared with the traditional methods, advantages of AI-enabled channel modeling/prediction are as follows:

(1) Efficient massive data mining and processing ability: With the explosive growth of available data due to the expansion of applicable bands and scenarios as well as system resolutions and capabilities, the acquisition, storage and processing of massive data have brought significant challenges to traditional channel modeling/prediction methods. Deep neural networks are good at mining complex features in highly dimensional and highly redundant data, and do not rely on additional manual feature screening.

(2) Strong modeling and adaptive ability: Deep neural network has good performance in nonlinear system modeling. Since neural network can automatically extract input features and establish mapping, it has excellent adaptability and generalization ability when input features change.

(3) Excellent learning and prediction ability: AI-driven channel model directly learns features of data sets and extracts core factors that have impacts on channels, therefore the predicted outputs can be more essentially derived from the changes of the input features, thus improving accuracy of channel prediction.
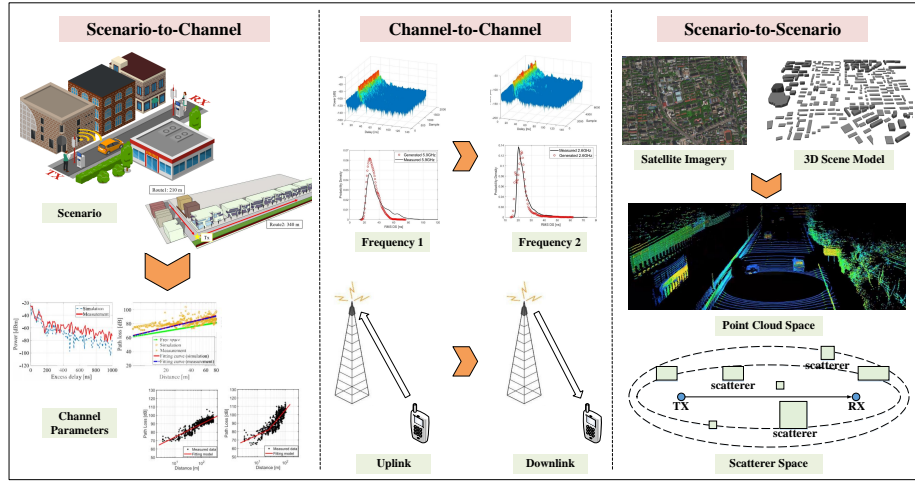
Figure 18: Implementation examples of AI for channel modeling.

The AI based data-driven methods, good at establishing the relation between massive radio channel data and complex physical propagation environment [237, 238], and have many potential applicable domains in channel prediction as shown in Fig. 18 and below.

(1) Scenario-to-Channel: Channel models based on AI take scenario features as input and then output channel parameters. The expected model is a group of trained networks by using massive channel and environment data (e.g., 3D Lidar data and 2D image data [238, 236]). The trained deep neural network is expected to well establish the mapping relationship from scenario to channel (e.g., path loss, major cluster), and the goal is to predict radio frequency channel parameters from other modalities of image or/and point clouds.

(2) Channel-to-Channel: Typical application of AI enabled channel-to-channel mapping is data enhancement and frequency migration including both interpolation and extrapolation. Neural networks can be used to learn limited channel data and quickly generate massive data with similar propagation characteristic; it is valuable for the applications requiring massive channel data, e.g., in over-the-air wireless device testing chambers [239]. Furthermore, AI models can learn frequency impacts on different channels and predict the channel for unknown frequencies. A typical case is to use uplink channels to predict downlink channels in Frequency Division Duplex systems.

(3) Scenario-to-Scenario: Mapping from physical environment to electromagnetic virtual environment is a potential field, and it's essentially to reconstruct environment from the perspective of radio wave propagation.

Scenario-to-scenario mapping aims to construct a scenario model of point cloud or scatterer space using massive data such as satellite images. The reconstructed scenario model contains rich electromagnetic environment information, and it can not only serve to predict channels but also to realize electromagnetic environment perception.

In addition to the above-mentioned deep learning based data-driven channel modeling/predictions, there are also other complexity/computation less-intensive methods that can be explored to be used for channel prediction. For instance, the evolutionary algorithms (EA) or generic algorithms (GA) [240, 241, 242]. Inspired by biological evolution, the EA algorithms encode candidate solutions using chromosomes and provides a fitness function determining their qualities; over iterations, crossover and mutation are performed to generate new chromosomes and selection is effectuated to preserve good chromosomes. EA or GA could perform channel prediction with the assistance of RT tools for fitness function and reach near-optimal solutions/predictions.

Most above mentioned methods predict channel in spatial-temporal (environment and mobility) and frequency domains. To expand the boundaries for future applications, the channel prediction needs to be performed across different systems as well. As such, the data-driven algorithms need to be trained by using data captured in different domains and systems (e.g., radar monostatic backscatterd channel data and communication signal bistatic channel data, [243, 244]). Training with data captured by different systems could make the trained AI-based algorithm robust to different system setups and non-linearities, and the goal is to obtain the domain and system invariant channel prediction algorithm.

9.6   Hardware-in-the-Loop Radio Channel Emulation

The 3GPP generally defines many standard channel models for wireless communication system simulation and evaluation. However, theoretical channel model cannot be directly used for hardware system and terminal simulation/evaluation such as air interface testing. Radio channel emulator can act as a representation of the real-world radio channel, and it enables creation of mathematical channel models representing physical radio signal transmission [245, 246]. It is still challenging for channel emulation in complex environments such as high-mobility scenario, massive MIMO scenario, etc.

Wireless channel emulator uses a down-converter to transform RF signal to baseband, and then uses high-speed digital signal processors such as FPGA to achieve digital filtering of baseband signals based on channel models, generating a signal that incorporates channel effects. Finally, RF output of the signal is achieved through an up-converter. Therefore, channel emulator can achieve equivalent substitution for field measurements in laboratory, spanning various stages of wireless communication research, core equipment development, network planning optimization, and network operation. Many researches have been conducted by COST INTERACT to improve channel emulation.
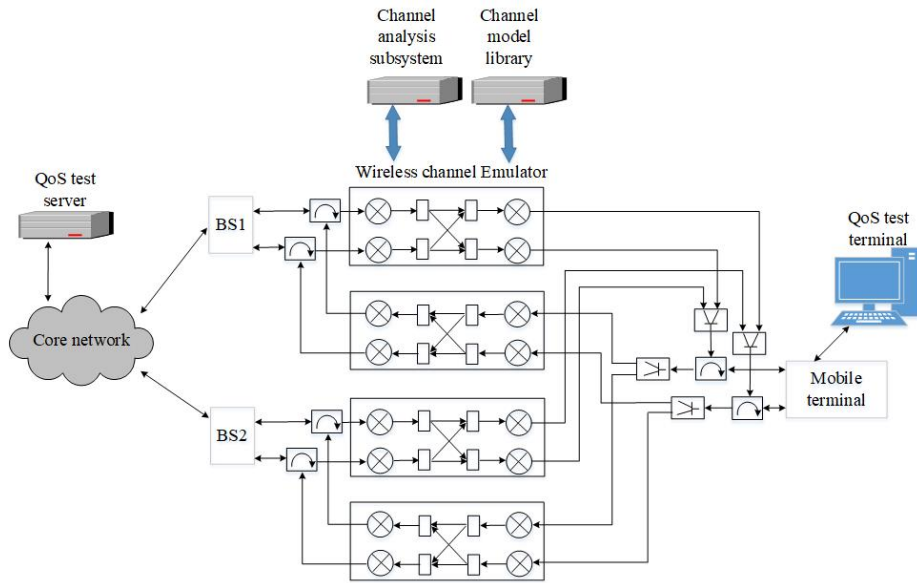
Figure 19: Hardware-in-the-loop emulation system structure for high-mobility communication.
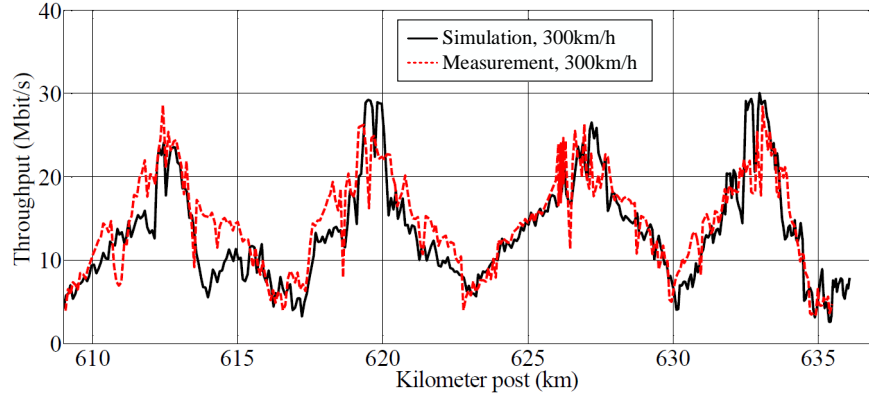
Figure 20: Example plots of instantaneous downlink throughput.

In order to further improve channel emulation especially for high-mobility scenario, a novel hardware-in-the-loop channel emulator is firstly developed by Beijing Jiaotong University so that real-world high-mobility radio environment can be accurately modeled and physically implemented [247, 248, 249], and the architecture is shown in Fig. 19. The emulation system uses two BSs and one core network, and each BS is configured as downlink 2×2 MIMO space division multiplexing mode. In order to evaluate network performance, a QoS test server
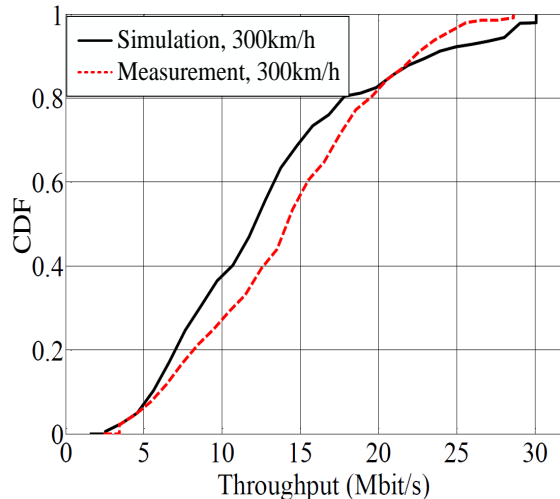
Figure 21: Example plots of downlink throughput distribution.

and test terminal are set up on core network side and mobile terminal side, respectively. In order to verify accuracy of the emulation system in high-mobility scenario, we use test instrument and network consistent with high-mobility field test to evaluate RSRP, SINR, downlink throughput by the hardware-in-the-loop channel emulator, and compare with field test results. Here, we consider high-speed railway scenario with 300 km/h moving speed. A large body of wideband channel measurements at 450 MHz, 900 MHz, 2.1 GHz bands are conducted along "Beijing-Shanghai", "Beijing-Tianjin", and "Beijing-Shenyang" high-speed railway lines, and measurement-based channel models are developed for high-mobility channel emulation [250, 251]. The instantaneous downlink throughput values and CDF curve through hardware-in-the-loop emulation and onboard measurements are compared in Fig. 20 and Fig. 21. It is found that the simulated downlink throughput by using the hardware-in-the-loop channel emulator is consistent with measurements and prediction error is less than 10% [250].

Currently, channel emulation, especially in high-mobility scenarios, mainly faces the following challenges: i) Conducting measurements in high-mobility scenario is difficult, lacking joint validation with application-level transmission performance; ii) Most channel emulators adopt an instrument-based architecture, which has limited computational and storage capabilities. This limitation hinders the generation of large-scale channel coefficient matrices in high-mobility scenario; iii) Effective emulation time is short, dynamic emulation capabilities are limited, frequency range and bandwidth are restricted, and there is also a lack of emulation capabilities for super-large-scale antenna arrays.

9.7 Channel sensing using advanced antenna concepts for mmWave and beyond

mmWave and (sub-)THz bands open unprecedented opportunities for environment-aware communications. The available spectrum in these frequency ranges enables ultra-high data rates and high-accuracy sensing applications, which are needed for the use cases considered in 6G [2, 22]. At such frequencies, highly directional beams are used to mitigate large free-space attenuation, which in turns enables better exploitation of spatial resources. Sensing the channel in its angular dimension is therefore of utmost importance but becomes challenging as carrier frequency gets higher.

Channel characterization that performs directional measurements in mmWave and (sub-)THz bands typically uses rotating horn antennas to benefit from antenna gain and thus increases measurement dynamic (see [252, 253] for indoor scenario and [254] for outdoor scenario). However, steering narrower antenna beams across azimuth and elevation at both transmitter and receiver leads to prohibitive measurement duration. To decrease it, the study in [255], conducted within the COST INTERACT action, implements a measurement based ray-launcher to estimate the double-directional path data from single-directional radio channel sounding. Other channel sounders use antenna arrays to avoid any mechanical displacement and characterize the channel faster. This includes classical phased arrays [256] or switched arrays [257] and lens-based arrays [258] to decrease cost and hardware complexity.

While these approaches are suitable for channel characterization, their high cost and complexity limit their applicability for sensing in actual communications such as for beam alignment and handover in mobile scenario or estimating CSI for RIS. These use cases require fast and energy efficient techniques to discover the angular properties of the channel.

An alternative approach is to use a dedicated peculiar antenna that estimates directions of arrival (DoA) with a single radio frequency chain. This results in a non-expensive system with real-time sensing capabilities. Such solutions leverage the frequency diversity that inherently exists in the radiation pattern of some classes of radiating structures. Those devices are purely passive and exhibit therefore low complexity and easy calibration procedure. Cavity-backed metasurfaces [259], lens-loaded cavities [260], or leaky-wave antennas (LWA) [261, 262] exhibit such properties, with the latter being a lower profile solution. LWAs also exhibit a tractable beam scanning behavior with frequency [263] which enables using standard DoA estimation techniques such as monopulse-based [264] or MUSIC algorithm [265]. While LWAs represent a cost-effective solution to estimate DoA at mmWave and (sub-)THz frequencies, they typically need to operate over a large frequency bandwidth in order to scan a large field of view (FoV), which makes them unpractical for most communication standards.

This issue has been tackled in the literature with different approaches. At mmWave, the LWA scanning velocity has been improved by loading the leaky guiding structure with a dense metasurface [266] or by adding an extra disper-

sive lens [267]. However, the required bandwidth to scan a large FoV remains larger than typical frequency channels used in telecommunications. The works in [268, 269] exploit several multiport LWAs while [270] uses reconfigurable LWAs. These approaches achieves AoA estimation over a large FoV at the expense of cost and/or complexity.

Recently, it was proposed in [265] to exploit LWAs able to radiate multiple beams at each frequency. This multibeam operation is achieved by increasing the period of the spatial modulation of periodic LWAs. This generates multiple fast spatial harmonics, each one contributing to a beam in the far-field radiation. In doing so, the FoV, at each frequency, is divided by the number of beams, which in turns greatly reduces the bandwidth required for a single beam to scan its angular sub-region. [265] shows that a subspace-based algorithm such as MUSIC can distinguish the DoAs of incoming sources among the multiple beams. Two proofs of concept have been developed within COST INTERACT in the 28 GHz band: an E-plane scanning single-port LWA [261] which needs a 2-GHz-bandwidth to scan the whole FoV (i.e., 7.4% fractional bandwidth) and an H-plane scanning dual-port LWA [262] requiring only 1-GHz-bandwidth to scan the whole FoV (i.e., 3.7% fractional bandwidth). The former was designed in a substrate-integrated waveguide technology while the latter is a fully metallic structure, which does not suffer from dielectric losses and therefore increases radiation efficiency. The H-plane scanning dual-port LWA is based on a corrugated waveguide modulated by rectangular slots. Its geometry is shown in Fig. 22 along with its radiation pattern. Up two five beams at each frequency can be observed whose directions steer with frequency. The MUSIC pseudo spectrum in Fig. 23 shows that the three DoAs considered in this example are well retrieved with no ambiguity among the multiple beams.

Currently, channel sensing using such advanced antennas concepts still faces some challenges. First, angular estimation based on frequency diversity is prone to frequency fading for spatially non-resolvable multipath components. Consequently, techniques are to be investigated to improve channel sensing robustness. Second, sensing in both elevation and azimuth planes is yet to be done. Therefore, 2D scanning with a single LWA is also an exciting perspective of research, which could lead to cost-effective solution for sensing in future mobile generations. Finally, future works should be carried out to make use of such advanced antennas in beam management to ultimately extend the time-frequency 2D resource grid used so far in 5G to a space-time-frequency 3D grid, enabling a seamless exploitation of the beam space.

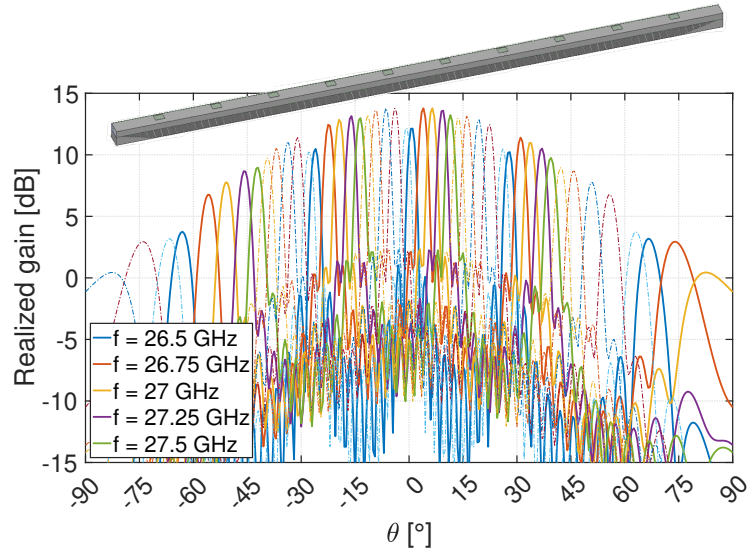Figure 22: Leaky-wave antenna radiation pattern showing the multiple-beam scanning in the 26.5-27.5 GHz band (solid lines represents the pattern generated by one LWA port and dotted lines the patter generated by the other port).
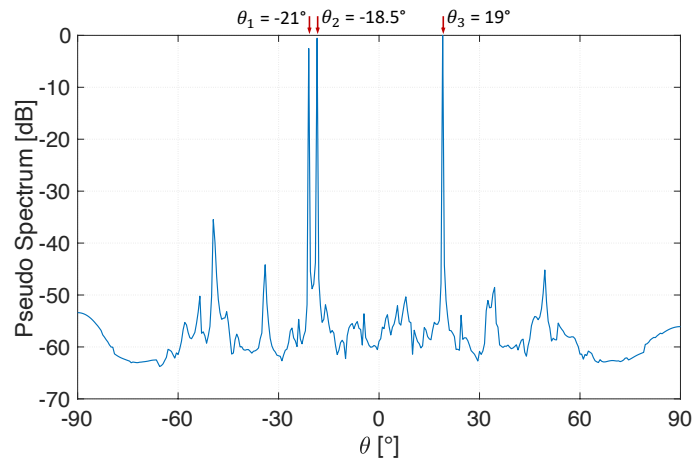

Figure 23: MUSIC pseudo spectrum obtained with the dual-port LWA (100 snapshots, SNR = 10 dB, 144 subcarriers, 3 uncorrelated sources of DoA = θ_2, θ_2, θ_3).

10 Conclusions and future outlook

by Vittorio Degli Esposti

The purpose of this paper is to summarize the key challenges in the field of radio channel measurement and modeling that need to be addressed to support the development of next generation (6G) wireless networks. Additionally, it aims at providing an overview of the main research activities undertaken by the scientific community, particularly within COST CA20120 "INTERACT", in order to achieve those goals. Next generation wireless networks will have to deal with a variety of environments and applications, with frequencies ranging from sub-6 GHz to THz, from sparse to ultra-dense networks, ultra-high performance links, and including sensing, imaging, and smart-environment applications. Therefore, a number of new studies are required to address relevant issues such as material and propagation characteristics at the new frequency bands, more sophisticated channel sounding techniques and novel modeling methodologies, including the use of machine learning techniques.

Section 4 introduces the study of propagation mechanisms and parameters that's fundamental for the definition of channel measurement and modeling techniques. Making use of proper measurement setups, several experimental studies are addressing the analysis of basic propagation mechanisms, such as the increased wall-penetration loss with frequency and blockage loss from humans and objects. Furthermore, several studies address measurement and modeling of diffuse scattering from surfaces and due to material variability, with a focus on polarization characteristics and the enforcement of reciprocity in directional scattering models. The recent advent of RIS has spurred research on the effect of such surfaces on propagation, with particular emphasis on the comparison between electromagnetic simulation and simplified scattering models, the power-decay trend of reflection from such surfaces and the development of macroscopic modeling approaches.

Other studies are addressing higher-level propagation characteristics, such as fading correlation over space and frequency. Some reports show evidence that power spectrum shapes do not change noticeably across different frequencies, while there is indication from comparative channel sounding that the channel becomes more "sparse" at higher frequencies, at least up to sub-THz frequencies, with a lower degree of multipath richness.

An important research activity within the COST INTERACT community is focused on channel sounding at both sub-6 GHz frequencies and above. Channel sounding techniques are described in Section 5 while channel measurement results are summarized in Section 6.

Measurement campaigns in sub-6 GHz bands have been conducted to characterize wireless propagation, with particular focus on vehicular scenarios. Researchers are now exploring slightly higher frequency ranges, such as those in the so-called mid-band, or FR3 range (7-24 GHz) that is under the spotlight to overcome spectrum congestion and support massive MIMO systems. Different techniques and array configurations were employed to estimate multipath

components and study non-stationarity among antenna elements.

Several other studies have addressed propagation and channel sounding techniques at mmWave and sub-THz frequencies. To compensate for the higher path-loss, high-gain antenna systems are needed, making spatial channel characteristics crucial for system design and this fact is reflected in channel sounding techniques. Since reliable massive-MIMO channel sounders are still unavailable at these frequencies, several studies resort to virtual array techniques, which require a great deal of measurement time. One crucial issue is therefore the reduction of measurement time. Another important activity within COST INTERACT is the collection of channel measurements into a unitary database that should also include detailed information on the measurement environment and technique and can be used for channel modeling and simulation purposes, as described in Section 6.4.

On the channel modeling side, a great deal of activity is being carried out, with a focus on Geometrical Stochastic Channel Models (GSCM), map-based models, Machine Learning (ML) based approaches, and advanced ray tracing techniques, as described in Section 7. GSCM models are widely used for simulation of wireless systems, considering scatterers in the environment and modeling signal propagation through multiple paths. Various works have proposed GSCM models for different use cases such as vehicular and rail communications. Map-based models use simplified maps of the environment to capture spatial consistency among different links. ML-based approaches have gained attention for wireless channel characterization, where ML algorithms can improve the accuracy of propagation models or provide a black-box representation of the channel, albeit with the drawback of a time-consuming and critical training phase. Tabular data is well-suited for ensemble models like Random Forests and gradient boosting decision tree models, while space-related, unstructured data (e.g., images) can be effectively processed using deep learning models such as convolutional neural networks and appear quite attractive for propagation modeling, given its intrinsic spatial characteristics. Ray tracing can be used as a low-cost alternative to measurements for the training phase. At the same time, advanced ray tracing techniques including parallelization techniques, dynamic ray tracing techniques and ray-based techniques for reducing the computational burden for ultra-large arrays and reconfigurable intelligent surfaces are also being developed. A range of relevant techniques that are used for parameter estimation and clustering algorithms are covered in Section 8, where it is shown there is a strong research ongoing on both the "classical" and learning-based techniques.

Finally, a look into new technologies in the field of channel measurement and modeling is given in Section 9. Among the novel channel modeling techniques that are being addressed, we can mention anticipative channel prediction for dynamic scenarios based on Artificial Intelligence (AI) techniques. AI-based methods have applications in scenario-to-channel prediction, channel-to-channel mapping for data enhancement and frequency migration, and scenario-to-scenario mapping to reconstruct the electromagnetic environment. Hardware-in-the-loop channel emulators are also being developed to accurately model

and physically implement real-world high-mobility radio environments. Finally, novel leaky-wave antennas are being proposed for channel sensing and directional channel measurements without the use of rotating directive antennas or arrays.

All considered, thanks to the foreseen new frequency bands, application scenarios and technology developments, we can conclude that research on radio channel characterization and modeling is as active as ever.

Author affiliations

Name	Affiliation	Email
Andrej Hrovat	Institut "Jozef Stefan"	andrej.hrovat@ijs.si
Bo Ai	Beijing Jiaotong University	boai@bjtu.edu.cn
Conor Brennan	Dublin City University	conor.brennan@dcu.ie
Dan Fei	Beijing Jiaotong University	dfei@bjtu.edu.cn
Danping He	Beijing Jiaotong University	hedanping@bjtu.edu.cn
Diego Andres Dupleich	TU Ilmenau	Diego.Dupleich@tu-ilmenau.de
Enrico Maria Vitucci	University of Bologna	enricomaria.vitucci@unibo.it
Franco Fuschini	University of Bologna	franco.fuschini@unibo.it
Guido Valerio	Sorbonne University	guido.valerio@sorbonne-universite.fr
Joonas Kokkoniemi	Oulu University	joonas.kokkoniemi@oulu.fi
Julien Sarrazin	Sorbonne University	julien.sarrazin@sorbonne-universite.fr
Katsuyuki Haneda	Aalto University	katsuyuki.haneda@aalto.fi
Ke Guan	Beijing Jiaotong University	ke.guan.bjtu@qq.com
Marco Di Renzo	Centrale Supelec	marco.direnzo@l2s.centralesupelec.fr
Marco Skocaj	University of Bologna	marco.skocaj@unibo.it
Mate Boban	Huawei, Munich Research Center	mate.boban@huawei.com
Mi Yang	Beijing Jiaotong University	myang@bjtu.edu.cn
Narcís Cardona	Valencia Polytechnic University	ncardona@iteam.upv.es
Nicola Di Cicco	Politecnico di Milano	nicola.dicicco@polimi.it
Ruisi He	Beijing Jiaotong University	he.ruisi.china@gmail.com
Tomaz Javornik	Institut "Jozef Stefan"	tomaz.javornik@ijs.si
Tommaso Zugno	Huawei, Munich Research Center	tommaso.zugno@huawei.com
Vittorio Degli Esposti	University of Bologna	v.degliesposti@unibo.it
Wei Fan	Aalborg University	wfa@es.aau.dk
Wenfei Yang	Huawei Technologies Co., Ltd	yangwenfei4@huawei.com
Xiping Wang	Beijing Jiaotong University	wangxiping@bjtu.edu.cn
Xuesong Cai	Lund University	xuesong.cai@eit.lth.se
Yang Miao	University of Twente	y.miao@utwente.nl

References

[1] S. Salous, K. Haneda, and V. Degli-Esposti, "5G to 6G: A paradigm shift in radio channel modeling," *Radio Science*, vol. 57, no. 7, 2022.

[2] "one6G Whitepaper: 6G Technology Overview," June 2022.

[3] S. Salous, V. Degli Esposti, F. Fuschini, R. S. Thomae, R. Mueller, D. Dupleich, K. Haneda, J.-M. M. Garcia-Pardo, J. P. Garcia, D. P. Gaillot *et al.*, "Millimeter-wave propagation: Characterization and modeling toward fifth-generation systems.[wireless corner]," *IEEE Antennas and Propagation Magazine*, vol. 58, no. 6, pp. 115–127, 2016.

[4] R. M. Sandoval, A.-J. Garcia-Sanchez, and J. Garcia-Haro, "Improving rssi-based path-loss models accuracy for critical infrastructures: A smart grid substation case-study," *IEEE Transactions on Industrial Informatics*, vol. 14, no. 5, pp. 2230–2240, 2017.

[5] N. Cardona, *Cooperative radio communications for green smart environments*. River Publishers, 2016.

[6] S. Wu, C.-X. Wang, M. M. Alwakeel, X. You *et al.*, "A general 3-d non-stationary 5g wireless channel model," *IEEE Transactions on Communications*, vol. 66, no. 7, pp. 3065–3078, 2017.

[7] F. Fuschini, M. Zoli, E. M. Vitucci, M. Barbiroli, and V. Degli-Esposti, "A study on millimeter-wave multiuser directional beamforming based on measurements and ray tracing simulations," *IEEE Transactions on Antennas and Propagation*, vol. 67, no. 4, pp. 2633–2644, 2019.

[8] R. Di Taranto, S. Muppirisetty, R. Raulefs, D. Slock, T. Svensson, and H. Wymeersch, "Location-aware communications for 5g networks: How location information can improve scalability, latency, and robustness of 5g," *IEEE Signal Processing Magazine*, vol. 31, no. 6, pp. 102–112, 2014.

[9] 3GPP, "Universal Mobile Telecommunications System (UMTS); Deployment aspects (Release 4)," TR 25.943, 2001.

[10] M. Giordani, M. Polese, M. Mezzavilla, S. Rangan, and M. Zorzi, "Toward 6g networks: Use cases and technologies," *IEEE Communications Magazine*, vol. 58, no. 3, pp. 55–61, 2020.

[11] H. Elayan, O. Amin, B. Shihada, R. M. Shubair, and M.-S. Alouini, "Terahertz band: The last piece of rf spectrum puzzle for communication systems," *IEEE Open Journal of the Communications Society*, vol. 1, pp. 1–32, 2020.

[12] N. Chi, Y. Zhou, Y. Wei, and F. Hu, "Visible light communication in 6g: Advances, challenges, and prospects," *IEEE Vehicular Technology Magazine*, vol. 15, no. 4, pp. 93–102, 2020.

[13] M. Boban, A. Kousaridas, K. Manolakis, J. Eichinger, and W. Xu, "Connected roads of the future: Use cases, requirements, and design considerations for vehicle-to-everything communications," *IEEE Vehicular Technology Magazine*, vol. 13, no. 3, pp. 110–123, 2018.

[14] R. S. Thoma, C. Andrich, G. D. Galdo, M. Dobereiner, M. A. Hein, M. Kaske, G. Schafer, S. Schieler, C. Schneider, A. Schwind, and P. Wendland, "Cooperative passive coherent location: A promising 5g service to support road safety," *IEEE Communications Magazine*, vol. 57, no. 9, pp. 86–92, 2019.

[15] M. Yang, R. He, B. Ai, C. Huang, C. Wang, Y. Zhang, and Z. Zhong, "AI-enabled data-driven channel modeling for future communications," *IEEE Communications Magazine, to be published*, 2023.

[16] L. U. Khan, W. Saad, D. Niyato, Z. Han, and C. S. Hong, "Digital-twin-enabled 6g: Vision, architectural trends, and future directions," *IEEE Communications Magazine*, vol. 60, no. 1, pp. 74–80, 2022.

[17] M. Di Renzo, A. Zappone, M. Debbah, M.-S. Alouini, C. Yuen, J. de Rosny, and S. Tretyakov, "Smart radio environments empowered by reconfigurable intelligent surfaces: How it works, state of research, and the road ahead," *IEEE Journal on Selected Areas in Communications*, vol. 38, no. 11, pp. 2450–2525, 2020.

[18] X. Zhang, J. Wang, and H. V. Poor, "Joint optimization of irs and uav-trajectory: For supporting statistical delay and error-rate bounded qos over murllc-driven 6g mobile wireless networks using fbc," *IEEE Vehicular Technology Magazine*, vol. 17, no. 2, pp. 55–63, 2022.

[19] Y. Pan, K. Wang, C. Pan, H. Zhu, and J. Wang, "Uav-assisted and intelligent reflecting surfaces-supported terahertz communications," *IEEE Wireless Communications Letters*, vol. 10, no. 6, pp. 1256–1260, 2021.

[20] H. Tataria, M. Shafi, A. F. Molisch, M. Dohler, H. Sjöland, and F. Tufvesson, "6g wireless systems: Vision, requirements, challenges, insights, and opportunities," *Proceedings of the IEEE*, vol. 109, no. 7, pp. 1166–1199, 2021.

[21] D. K. P. Tan, J. He, Y. Li, A. Bayesteh, Y. Chen, P. Zhu, and W. Tong, "Integrated sensing and communication in 6g: Motivations, use cases, requirements, challenges and future directions," in *2021 1st IEEE International Online Symposium on Joint Communications & Sensing (JC&S)*. IEEE, 2021, pp. 1–6.

[22] W. Tong and P. Zhu, "6g: The next horizon. from connected people and things to connected intelligence," in *6G Mobile Wireless Networks*. Cambridge University Press, 2021.

[23] V. Kristem, C. U. Bas, R. Wang, and A. F. Molisch, "Outdoor wideband channel measurements and modeling in the 3–18 ghz band," *IEEE Transactions on Wireless Communications*, vol. 17, no. 7, pp. 4620–4633, 2018.

[24] S. Tripathi, N. V. Sabu, A. K. Gupta, and H. S. Dhillon, "Millimeter-wave and terahertz spectrum for 6g wireless," in *6G Mobile Wireless Networks*. Springer, 2021, pp. 83–121.

[25] "World Radiocommunication Conference 2019 (WRC-19): Final Acts," in *ITU Publications*, 2012, p. 32.

[26] M. Polese, M. Giordani, T. Zugno, A. Roy, S. Goyal, D. Castor, and M. Zorzi, "Integrated access and backhaul in 5g mmwave networks: Potential and challenges," *IEEE Communications Magazine*, vol. 58, no. 3, pp. 62–68, 2020.

[27] X. Cai, X. Cheng, and F. Tufvesson, "Toward 6G with terahertz communications: Understanding the propagation channels," *IEEE Communications Magazine*, 2023.

[28] "WRC-19 Agenda Item 1.15: Studies towards an identification for use by administrations for land mobile and fixed services applications operating in the frequency range 275-450 GHz," 2019.

[29] D. K. Pin Tan, J. He, Y. Li, A. Bayesteh, Y. Chen, P. Zhu, and W. Tong, "Integrated sensing and communication in 6g: Motivations, use cases, requirements, challenges and future directions," in *2021 1st IEEE International Online Symposium on Joint Communications Sensing (JCS)*, 2021, pp. 1–6.

[30] T. Kürner, D. M. Mittleman, and T. Nagatsuma, Eds., *THz Communications*. Springer Nature, 2021.

[31] P. H. Pathak, X. Feng, P. Hu, and P. Mohapatra, "Visible light communication, networking, and sensing: A survey, potential and challenges," *IEEE communications surveys & tutorials*, vol. 17, no. 4, pp. 2047–2077, 2015.

[32] D. Dupleich, A. Ebert, Y. Völker-Schöneberg, L. Löser, M. Boban, and R. Thomä, "Spatial/temporal characterization of propagation and blockage from measurements at sub-thz in industrial machines," in *2023 17th European Conference on Antennas and Propagation (EuCAP)*, 2023.

[33] S. El-Faitori and S. Salous, "Reflection and penetration loss wideband measurements of building materials at 28 ghz and 39 ghz," in *16th European Conference on Antennas and Propagation, EuCAP Madrid, Spain, March 2022*, 2022.

[34] M. Aliouane, J.-M. Conrat, J.-C. Cousin, and X. Begaud, "Indoor material transmission measurements between 2 ghz and 170 ghz for 6g wireless communication systems," in *16th European Conference on Antennas and Propagation, EuCAP Madrid, Spain, March 2022*, 2022.

[35] ——, "Material reflection measurements in centimeter and millimeter wave ranges for 6g wireless communications," in *2022 Joint European Conference on Networks and Communications 6G summit, Grenoble, France, June 2022*, 2022.

[36] B. T. Csathó and B. P. Horváth, "Finite element method-based analysis of controlled reflections from ris," in *2022 Sixteenth International Congress on Artificial Materials for Novel Wave Phenomena (Metamaterials)*, 2022.

[37] C. Balanis, *Advanced Engineering Electromagnetics.* Wiley.

[38] C. Brennan, I. Islam, J. Basquill, and K. M. Soodhalter, "Computation of scattering from rough surfaces using successive symmetric over relaxation and eigenvalue deflation," in *16th European Conference on Antennas and Propagation, EuCAP Madrid, Spain, March 2022*, 2022.

[39] P. Xie, K. Guan, D. He, H. Yi, J. Dou, and Z. Zhong, "Terahertz wave propagation characteristics on rough surfaces based on full-wave simulations," in *Radio Science*, vol. 57, no. 6, 2022.

[40] K. Guan, P. Xie, D. He, Z. Zhong, J. Dou, and F. Zhu, "On the modeling of scattering mechanisms of rough surfaces at the terahertz band (invited paper)," in *the 6th ACM Workshop on Millimeter-Wave and Terahertz Networks and Sensing Systems (mmNets 2022)*, 2022.

[41] E. M. Vitucci, M. Buccioli, and V. Degli Esposti, "Analysis of mm-wave scattering from construction materials," in *Proceedings of the XXXIVth URSI General Assembly and Scientific Symposium (URSI GASS 2021)*, 2021.

[42] E. M. Vitucci, N. Cenni, F. Fuschini, and V. Degli-Esposti, "A reciprocal heuristic model for diffuse scattering from walls and surfaces," *IEEE Transactions Antennas and Propagation (Early Access)*.

[43] M. Kleijer, G. Steinböck, B.-E. Olsson, M. Johansson, and B. Smolders, "Impact of facade details on radio propagation at 28 ghz," in *17th European Conference on Antennas and Propagation (EuCAP)*, 2023.

[44] D. Burghal, S. L. H. Nguyen, K. Haneda, and A. F. Molisch, "Dual frequency bands shadowing correlation model in a micro-cellular environment," in *2019 IEEE Global Communications Conference (GLOBECOM)*, 2019, pp. 1–6.

[45] J. Du, D. Chizhik, R. Feick, G. Castro, M. Rodríguez, and R. A. Valenzuela, "Suburban residential building penetration loss at 28 ghz for fixed wireless access," *IEEE Wireless Communications Letters*, vol. 7, no. 6, pp. 890–893, 2018.

[46] U. T. Virk and K. Haneda, "Modeling human blockage at 5g millimeter-wave frequencies," *IEEE Transactions on Antennas and Propagation*, vol. 68, no. 3, pp. 2256–2266, 2019.

[47] G. L. Ramos, P. Kyösti, V. Hovinen, and M. Latva-aho, "Multiple-screen diffraction measurement at 10–18 ghz," *IEEE Antennas and Wireless Propagation Letters*, vol. 16, pp. 2002–2005, 2017.

[48] D. Prado-Alvarez, S. Inca, D. Martín-Sacristán, and J. F. Monserrat, "Millimeter-wave human blockage model enhancements for directional antennas and multiple blockers," *IEEE Communications Letters*, vol. 25, no. 9, pp. 2776–2780, 2021.

[49] U. T. Virk, S. L. H. Nguyen, and K. Haneda, "Multi-frequency power angular spectrum comparison for an indoor environment," in *2017 11th European Conference on Antennas and Propagation (EUCAP)*, 2017, pp. 3389–3393.

[50] S. L. H. Nguyen, J. Järveläinen, A. Karttunen, K. Haneda, and J. Putkonen, "Comparing radio propagation channels between 28 and 140 GHz bands in a shopping mall," in *Proc. 12th European Conf. Ant. Prop. (EuCAP 2018)*, London, UK, 2018, pp. 1–5.

[51] D. Dupleich, R. Müller, S. Skoblikov, C. Schneider, J. Luo, G. Del Galdo, and R. Thomä, "Multi-band indoor propagation characterization by measurements from 6 to 60 ghz," in *2019 13th European Conference on Antennas and Propagation (EuCAP)*, 2019, pp. 1–5.

[52] D. Dupleich, R. Müller, M. Landmann, E.-A. Shinwasusin, K. Saito, J.-I. Takada, J. Luo, R. Thomä, and G. Del Galdo, "Multi-band propagation and radio channel characterization in street canyon scenarios for 5g and beyond," *IEEE Access*, vol. 7, pp. 160 385–160 396, 2019.

[53] J. Vehmas, J. Jarvelainen, S. L. H. Nguyen, R. Naderpour, and K. Haneda, "Millimeter-wave channel characterization at helsinki airport in the 15, 28, and 60 ghz bands," in *2016 IEEE 84th Vehicular Technology Conference (VTC-Fall)*, 2016, pp. 1–5.

[54] M. Boban, D. Dupleich, N. Iqbal, J. Luo, C. Schneider, R. Müller, Z. Yu, D. Steer, T. Jämsä, J. Li, and R. S. Thomä, "Multi-band vehicle-to-vehicle channel characterization in the presence of vehicle blockage," *IEEE Access*, vol. 7, pp. 9724–9735, 2019.

[55] Y. Lyu, Z. Yuan, H. Gao, Q. Zhu, X. Zhang, and W. Fan, "Measurement-based channel characterization in a large hall scenario at 300 ghz," *China Communications*, vol. 20, no. 4, pp. 118–131, 2023.

[56] M. Bengtson, Y. Lyu, and W. Fan, "Long-range vna-based channel sounder: Design and measurement validation at mmwave and sub-thz frequency bands," *China Communications*, vol. 19, no. 11, pp. 47–59, 2022.

[57] Y. Lyu, A. W. Mbugua, K. Olesen, P. Kyösti, and W. Fan, "Design and validation of the phase-compensated long-range sub-thz vna-based channel sounder," *IEEE Antennas and Wireless Propagation Letters*, vol. 20, no. 12, pp. 2461–2465, 2021.

[58] Y. Lyu, Z. Yuan, M. Li, A. W. Mbugua, P. Kyösti, and W. Fan, "Enabling long-range large-scale channel sounding at sub-thz bands: Virtual array and radio-over-fiber concepts," *IEEE Communications Magazine*, 2023.

[59] J. O. Nielsen, W. Fan, P. C. F. Eggers, and G. F. Pedersen, "A channel sounder for massive mimo and mmwave channels," *IEEE Communications Magazine*, vol. 56, no. 12, pp. 67–73, 2018.

[60] X. Cai, E. Bengtsson, O. Edfors, and F. Tufvesson, "A switched array sounder for dynamic millimeter-wave channel characterization: Design, implementation and measurements," *IEEE Transactions on Antennas and Propagation (submitted)*, 2023.

[61] A. Al-Ameri, J. Park, J. Sanchez, X. Cai, and F. Tufvesson, "A hybrid antenna switching scheme for dynamic channel sounding," in *IEEE 97th Vehicular Technology Conference*, 2023, pp. 1–6.

[62] D. Caudill, J. Chuang, S. Y. Jun, C. Gentile, and N. Golmie, "Real-time mmwave channel sounding through switched beamforming with 3-d dual-polarized phased-array antennas," *IEEE Transactions on Microwave Theory and Techniques*, vol. 69, no. 11, pp. 5021–5032, 2021.

[63] J. N. H. Dortmans, J. T. Quimby, K. A. Remley, D. F. Williams, J. Senic, and R. Sun, "Design of a portable verification artifact for millimeter-wave-frequency channel sounders," *IEEE Transactions on Antennas and Propagation*, vol. 67, no. 9, pp. 6149–6158, 2019.

[64] D. Dupleich, S. Semper, M. D. Al-Dabbagh, A. Ebert, T. Kleine-Ostmann, and R. Thomä, "Verification of thz channel sounder and delay estimation with over-the-air multipath artifact," in *2022 16th European Conference on Antennas and Propagation (EuCAP)*, 2022, pp. 1–5.

[65] M. Döbereiner, M. Käske, A. Schwind, C. Andrich, M. A. Hein, R. S. Thomä, and G. D. Galdo, "Joint high-resolution delay-doppler estimation for bi-static radar measurements," in *2019 16th European Radar Conference (EuRAD)*, 2019, pp. 145–148.

[66] P. Laly, D. Gaillot, G. Delbarre, M. V. d. Bossche, G. Vermeeren, F. Challita, E. Tanghe, E. Simon, W. Joseph, L. Martens, and M. Liénard, "Massive radio channel sounder architecture for 5g mobility scenarios: Mamimosa," in *2020 14th European Conference on Antennas and Propagation (EuCAP)*, 2020, pp. 1–5.

[67] A. F. Molisch, "Ultrawideband propagation channels-theory, measurement, and modeling," *IEEE transactions on vehicular technology*, vol. 54, no. 5, pp. 1528–1545, 2005.

[68] B. Rainer, S. Zelenbaba, A. Dakić, M. Hofer, D. Löschenbrand, T. Zemen, X. Ye, G. Nan, S. Teschl, and P. Priller, "Wili - vehicular wireless channel dataset enriched with lidar and radar data," in *GLOBECOM 2022 - 2022 IEEE Global Communications Conference*, 2022, pp. 4770–4775.

[69] E. P. Simon, P. Laly, J. Farah, E. Tanghe, W. Joseph, and D. Gaillot, "Measurement of the V2I Channel in Cell-free Vehicular Networks with the Distributed MaMIMOSA Channel Sounder," in *17th European Conference on Antennas and Propagation (EUCAP 2023)*, Florence, Italy, Mar. 2023, best Measurement Paper Award. [Online]. Available: https://hal.science/hal-03952309

[70] M. Schmidhammer, B. Siebler, C. Gentner, S. Sand, and U.-C. Fiebig, "Bayesian multipath-enhanced device-free localisation: Simulation- and measurement-based evaluation," *IET Microwaves, Antennas & Propagation*, vol. 16, no. 6, pp. 327–337, 2022. [Online]. Available: https://ietresearch.onlinelibrary.wiley.com/doi/abs/10.1049/mia2.12244

[71] F. Pasic, S. Pratschner, R. Langwieser, and C. F. Mecklenbräuker, "High-mobility wireless channel measurements at 5.9 ghz in an urban environment," in *2022 International Balkan Conference on Communications and Networking (BalkanCom)*, 2022, pp. 100–104.

[72] S. Willhammar, L. V. der Perre, and F. Tufvesson, "Fading in reflective and heavily shadowed industrial environments with large arrays," 2022.

[73] G. Jing, J. Hong, X. Yin, J. Rodríguez-Piñeiro, and Z. Yu, "Measurement-based 3d channel modeling with cluster-of-scatterers estimated under spherical-wave assumption," *IEEE Transactions on Wireless Communications*, pp. 1–1, 2023.

[74] Z. Z. B. X. H. R. S. R. G. K. Zhou, X. and K. Liu, "Indoor wideband channel measurements and analysis at 11 and 14 ghz," *IET Microw. Antennas Propag.*, vol. 11, pp. 1393–1400, 2017.

[75] A. Roivainen, C. Ferreira Dias, N. Tervo, V. Hovinen, M. Sonkki, and M. Latva-aho, "Geometry-based stochastic channel model for two-story lobby environment at 10 ghz," *IEEE Transactions on Antennas and Propagation*, vol. 64, no. 9, pp. 3990–4003, 2016.

[76] K. Saito, J.-I. Takada, and M. Kim, "Dense multipath component characteristics in 11-ghz-band indoor environments," *IEEE Transactions on Antennas and Propagation*, vol. 65, no. 9, pp. 4780–4789, 2017.

[77] C. Ling, X. Yin, H. Wang, and R. S. Thomä, "Experimental characterization and multipath cluster modeling for 13–17 ghz indoor propagation channels," *IEEE Transactions on Antennas and Propagation*, vol. 65, no. 12, pp. 6549–6561, 2017.

[78] J. Chen, X. Yin, and S. Wang, "Measurement-based massive mimo channel modeling in 13–17 ghz for indoor hall scenarios," in *2016 IEEE International Conference on Communications (ICC)*, 2016, pp. 1–5.

[79] J. Li, B. Ai, R. He, M. Yang, Y. Zhang, X. Liu, and Z. Zhong, "Characterization of indoor massive mimo channel at 11 ghz," in *2017 XXXIInd General Assembly and Scientific Symposium of the International Union of Radio Science (URSI GASS)*, 2017, pp. 1–4.

[80] G. Jing, J. Hong, X. Yin, J. Rodríguez-Piñeiro, and Z. Yu, "Measurement-based 3d channel modeling with cluster-of-scatterers estimated under spherical-wave assumption," *IEEE Transactions on Wireless Communications*, pp. 1–1, 2023.

[81] M. KIM, J. ichi TAKADA, and K. SAITO, "Multi-dimensional radio channel measurement, analysis and modeling for high frequency bands," *IEICE Transactions on Communications*, vol. advpub, p. 2017ISI0003, 2017.

[82] N. Tervo, C. F. Dias, V. Hovinen, M. Sonkki, A. Roivainen, J. Meinilä, and M. Latva-aho, "Diffraction measurements around a building corner at 10 ghz," in *1st International Conference on 5G for Ubiquitous Connectivity*, 2014, pp. 187–191.

[83] T. S. Rappaport, G. R. MacCartney, M. K. Samimi, and S. Sun, "Wideband millimeter-wave propagation measurements and channel models for future wireless communication system design," *IEEE Transactions on Communications*, vol. 63, no. 9, pp. 3029–3056, Sept 2015.

[84] T. Kleine-Ostmann, R. Piesiewicz, N. Krumbholz, D. Mittleman, T. Kurner, and M. Koch, "Characterization of building materials for the modeling of pico-cellular thz communication systems," in *2005 Joint 30th International Conference on Infrared and Millimeter Waves and 13th International Conference on Terahertz Electronics*, vol. 2, 2005, pp. 592–593 vol. 2.

[85] R. Piesiewicz, C. Jansen, D. Mittleman, T. Kleine-Ostmann, M. Koch, and T. Kurner, "Scattering analysis for the modeling of thz communication systems," *IEEE Transactions on Antennas and Propagation*, vol. 55, no. 11, pp. 3002–3009, 2007.

[86] M. A. Aliouane, J.-M. Conrat, J.-C. Cousin, and X. Begaud, "Indoor material transmission measurements between 2 ghz and 170 ghz for 6g wireless communication systems," in *2022 16th European Conference on Antennas and Propagation (EuCAP)*, 2022, pp. 1–5.

[87] ——, "Material reflection measurements in centimeter and millimeter wave ranges for 6g wireless communications," in *2022 Joint European Conference on Networks and Communications 6G Summit (EuCNC/6G Summit)*, 2022, pp. 43–48.

[88] M. Buccioli, E. M. Vitucci, and V. Degli-Esposti, "Analysis of mm-wave scattering from construction materials," in *2021 URSI GASS*, 2021.

[89] O. Zahid, J. Huang, and S. Salous, "Long term rain attenuation measurements at millimeter wave bands for direct and side short-range fixed links," in *2020 XXXIIIrd General Assembly and Scientific Symposium of the International Union of Radio Science*, 2020, pp. 1–4.

[90] A. P. Garcia, W. Kotterman, U. Trautwein, D. Brückner, J. Kunisch, and R. S. Thomä, "60 ghz time-variant shadowing characterization within an airbus 340," in *Proceedings of the Fourth European Conference on Antennas and Propagation*, 2010, pp. 1–5.

[91] P. Karadimas, B. Allen, and P. Smith, "Human body shadowing characterization for 60-ghz indoor short-range wireless links," *IEEE Antennas and Wireless Propagation Letters*, vol. 12, pp. 1650–1653, 2013.

[92] G. R. MacCartney, T. S. Rappaport, and S. Rangan, "Rapid fading due to human blockage in pedestrian crowds at 5g millimeter-wave frequencies," in *GLOBECOM 2017 - 2017 IEEE Global Communications Conference*, 2017, pp. 1–7.

[93] W. Qi, J. Huang, J. Sun, Y. Tan, C.-X. Wang, and X. Ge, "Measurements and modeling of human blockage effects for multiple millimeter wave bands," in *2017 13th International Wireless Communications and Mobile Computing Conference (IWCMC)*, 2017, pp. 1604–1609.

[94] U. T. Virk and K. Haneda, "Modeling human blockage at 5g millimeter-wave frequencies," *IEEE Transactions on Antennas and Propagation*, vol. 68, no. 3, pp. 2256–2266, 2020.

[95] G. R. MacCartney, S. Deng, S. Sun, and T. S. Rappaport, "Millimeter-wave human blockage at 73 ghz with a simple double knife-edge diffraction model and extension for directional antennas," in *2016 IEEE 84th Vehicular Technology Conference (VTC-Fall)*, 2016, pp. 1–6.

[96] P. Zhang, P. Kyösti, M. Bengtson, V. Hovinen, K. Nevala, J. Kokkoniemi, and A. Pärssinen, "Measurement-based characterization of d-band human body shadowing," in *2023 17th European Conference on Antennas and Propagation (EuCAP)*, 2023.

[97] S. Kim and A. G. Zajić, "Statistical characterization of 300-ghz propagation on a desktop," *IEEE Transactions on Vehicular Technology*, vol. 64, no. 8, pp. 3330–3338, 2015.

[98] C.-L. Cheng and A. Zajić, "Characterization of propagation phenomena relevant for 300 ghz wireless data center links," *IEEE Transactions on Antennas and Propagation*, vol. 68, no. 2, pp. 1074–1087, 2020.

[99] D. Dupleich, R. Müller, S. Skoblikov, M. Landmann, G. D. Galdo, and R. Thomä, "Characterization of the propagation channel in conference room scenario at 190 ghz," in *2020 14th European Conference on Antennas and Propagation (EuCAP)*, 2020, pp. 1–5.

[100] S. L. H. Nguyen, K. Haneda, J. Järveläinen, A. Karttunen, and J. Putkonen, "Large-scale parameters of spatio-temporal short-range indoor backhaul channels at 140 ghz," in *2021 IEEE 93rd Vehicular Technology Conference (VTC2021-Spring)*, 2021, pp. 1–6.

[101] F. Undi, A. Schultze, W. Keusgen, M. Peter, and T. Eichler, "Angle-resolved thz channel measurements at 300 ghz in an outdoor environment," in *2021 IEEE International Conference on Communications Workshops (ICC Workshops)*, 2021, pp. 1–7.

[102] N. A. Abbasi, J. L. Gomez, R. Kondaveti, S. M. Shaikbepari, S. Rao, S. Abu-Surra, G. Xu, J. Zhang, and A. F. Molisch, "Thz band channel measurements and statistical modeling for urban d2d environments," *IEEE Transactions on Wireless Communications*, vol. 22, no. 3, pp. 1466–1479, 2023.

[103] K. Guan, B. Peng, D. He, J. M. Eckhardt, S. Rey, B. Ai, Z. Zhong, and T. Kürner, "Measurement, simulation, and characterization of train-to-infrastructure inside-station channel at the terahertz band," *IEEE Transactions on Terahertz Science and Technology*, vol. 9, no. 3, pp. 291–306, 2019.

[104] T. Kürner, "Isg thz activity report 2022," https://www.etsi.org/committee-activity/activity-report-thz, accessed: 2023-06-04.

[105] S. Ju, Y. Xing, O. Kanhere, and T. S. Rappaport, "Sub-terahertz channel measurements and characterization in a factory building," in *ICC 2022 - IEEE International Conference on Communications*, 2022, pp. 2882–2887.

[106] D. Dupleich, A. Ebert, Y. Völker-Schöneberg, L. Löser, M. Boban, and R. Thomä, "Spatial/temporal characterization of propagation and blockage from measurements at sub-thz in industrial machines," in *2023 17th European Conference on Antennas and Propagation (EuCAP)*, 2023.

[107] D. Dupleich, R. Müller, S. Skoblikov, C. Schneider, J. Luo, G. Del Galdo, and R. Thomä, "Multi-band indoor propagation characterization by measurements from 6 to 60 ghz," in *2019 13th European Conference on Antennas and Propagation (EuCAP)*, 2019, pp. 1–5.

[108] D. Dupleich, R. Muller, C. Schneider, S. Skoblikov, J. Luo, M. Boban, G. Del Galdo, and R. Thoma, "Multi-band vehicle to vehicle channel measurements from 6 ghz to 60 ghz at "t" intersection," in *2019 IEEE 2nd Connected and Automated Vehicles Symposium (CAVS)*, 2019, pp. 1–5.

[109] D. Dupleich, R. Müller, M. Landmann, J. Luo, G. D. Galdo, and R. S. Thomä, "Multi-band characterization of propagation in industry scenarios," in *2020 14th European Conference on Antennas and Propagation (EuCAP)*, 2020, pp. 1–5.

[110] D. Dupleich, N. Han, A. Ebert, R. Müller, S. Ludwig, A. Artemenko, J. Eichinger, T. Geiss, G. Del Galdo, and R. Thomä, "From sub-6 ghz to mm-wave: Simultaneous multi-band characterization of propagation from measurements in industry scenarios," in *2022 16th European Conference on Antennas and Propagation (EuCAP)*, 2022, pp. 1–5.

[111] 3GPP, "Study on channel model for frequencies from 0.5 to 100 GHz," TR 38.901, 2018.

[112] M. Hofer, D. Lóschenbrand, S. Zelenbaba, A. Dakić, B. Rainer, and T. Zemen, "Wireless 3ghz and 30 ghz vehicle-to-vehicle measurements in an urban street scenario," in *2022 IEEE 96th Vehicular Technology Conference (VTC2022-Fall)*, 2022, pp. 1–5.

[113] R. Takahashi, K. Shibata, A. Ghosh, and M. Kim, "Validation of 300 ghz channel sounder through indoor multipath measurements," *IEICE Communications Express*, vol. advpub, p. 2023SPL0013, 2023.

[114] D. Dupleich, A. Ebert, and R. Thomä, "Measurement-based analysis of multi-band assisted beam-forming at mmwave in industrial scenarios," in *2023 17th European Conference on Antennas and Propagation (EuCAP)*, 2023.

[115] F. Pasic, D. Schützenhöfer, E. Jirousek, R. Langwieser, H. Groll, S. Pratschner, S. Caban, S. Schwarz, and M. Rupp, "Comparison of Sub 6 GHz and mmWave Wireless Channel Measurements at High Speeds," in *16th European Conference on Antennas and Propagation (EuCAP 2022)*, 2022, pp. 1–5.

[116] J. Pascual-García, M.-T. Martinez-Ingles, D. P. Gaillot, L. Juan-Llácer, and J.-M. Molina-Garcia-Pardo, "Los theoretical and experimental mimo study from 1–40 ghz in indoor environments," *Electronics*, vol. 9, no. 10, 2020. [Online]. Available: https://www.mdpi.com/2079-9292/9/10/1688

[117] J. Blumenstein, J. Milos, L. Polak, and C. Mecklenbräuker, "Ieee 802.11ad sc-phy layer simulator: Performance in real-world 60 ghz indoor channels," in *2019 IEEE Nordic Circuits and Systems Conference (NORCAS): NORCHIP and International Symposium of System-on-Chip (SoC)*, 2019, pp. 1–4.

[118] P. Liu, J. Blumenstein, N. S. Perović, M. Di Renzo, and A. Springer, "Performance of generalized spatial modulation mimo over measured 60ghz indoor channels," *IEEE Transactions on Communications*, vol. 66, no. 1, pp. 133–148, 2018.

[119] C. Morin, L. S. Cardoso, J. Hoydis, J.-M. Gorce, and T. Vial, "Transmitter classification with supervised deep learning," in *Cognitive Radio-Oriented Wireless Networks: 14th EAI International Conference, CrownCom 2019, Poznan, Poland, June 11–12, 2019, Proceedings 14*. Springer, 2019, pp. 73–86.

[120] A. Massouri, L. Cardoso, B. Guillon, F. Hutu, G. Villemaud, T. Risset, and J.-M. Gorce, "Cortexlab: An open fpga-based facility for testing sdr cognitive radio networks in a reproducible environment," in *2014 IEEE Conference on Computer Communications Workshops (INFOCOM WK-SHPS)*, 2014, pp. 103–104.

[121] A. F. Molisch, H. Asplund, R. Heddergott, M. Steinbauer, and T. Zwick, "The cost259 directional channel model-part i: Overview and methodology," *IEEE Transactions on Wireless Communications*, vol. 5, no. 12, pp. 3421–3433, 2006.

[122] P. Kyösti, J. Meinilä, L. Hentila, X. Zhao, T. Jämsä, C. Schneider, M. Narandzic, M. Milojević, A. Hong, J. Ylitalo, V.-M. Holappa, M. Alatossava, R. Bultitude, Y. Jong, and T. Rautiainen, "Winner ii channel models," *IST-4-027756 WINNER II D1.1.2 V1.2*, 02 2008.

[123] S. Jaeckel, L. Raschkowski, K. Börner, and L. Thiele, "Quadriga: A 3-d multi-cell channel model with time evolution for enabling virtual field trials," *IEEE Transactions on Antennas and Propagation*, vol. 62, no. 6, pp. 3242–3256, 2014.

[124] L. Liu, C. Oestges, J. Poutanen, K. Haneda, P. Vainikainen, F. Quitin, F. Tufvesson, and P. D. Doncker, "The cost 2100 mimo channel model," *IEEE Wireless Communications*, vol. 19, no. 6, pp. 92–99, 2012.

[125] S. Zelenbaba, B. Rainer, M. Hofer, and T. Zemen, "Wireless digital twin for assessing the reliability of vehicular communication links," in *2022 IEEE Globecom Workshops (GC Wkshps)*, 2022, pp. 1034–1039.

[126] A. Fedorov, N. Lyamin, and F. Tufvesson, "Implementation of spatially consistent channel models for real-time full stack c-its v2x simulations," in *2021 55th Asilomar Conference on Signals, Systems, and Computers*, 2021, pp. 67–71.

[127] A. Dakić, M. Hofer, B. Rainer, S. Zelenbaba, L. Bernadó, and T. Zemen, "Real-time vehicular wireless system-level simulation," *IEEE Access*, vol. 9, pp. 23 202–23 217, 2021.

[128] P. Unterhuber, M. Walter, and T. Kürner, "Geometry-based stochastic channel model for train-to-train communication in open field environment," in *2022 16th European Conference on Antennas and Propagation (EuCAP)*, 2022, pp. 1–5.

[129] P. Unterhuber, M. Walter, and T. Kürner, "Parametrization and validation of the geometry-based stochastic channel model for train-to-train communication," in *17th European Conference on Antennas and Propagation*, July 2023. [Online]. Available: https://elib.dlr.de/192826/

[130] Z. Zhang, R. He, B. Ai, M. Yang, C. Li, H. Mi, and Z. Zhang, "A general channel model for integrated sensing and communication scenarios," *IEEE Communications Magazine*, pp. 1–7, 2022.

[131] G. Sun, R. He, Z. Ma, B. Ai, and Z. Zhong, "A 3d geometry-based non-stationary mimo channel model for ris-assisted communications," in *2021 IEEE 94th Vehicular Technology Conference (VTC2021-Fall)*, 2021, pp. 1–5.

[132] Y. Yuan, R. He, B. Ai, Z. Ma, Y. Miao, Y. Niu, J. Zhang, R. Chen, and Z. Zhong, "A 3d geometry-based thz channel model for 6g ultra massive mimo systems," *IEEE Transactions on Vehicular Technology*, vol. 71, no. 3, pp. 2251–2266, 2022.

[133] I. Carton, W. Fan, P. Kyösti, and G. F. Pedersen, "Validation of 5g metis map-based channel model at mmwave bands in indoor scenarios," in *2016 10th European Conference on Antennas and Propagation (EuCAP)*, 2016, pp. 1–5.

[134] V. Nurmela, A. Karttunen, A. Roivainen, L. Raschkowski, V. Hovinen, J. Y. EB, N. Omaki, K. Kusume, A. Hekkala, R. Weiler *et al.*, "Deliverable d1. 4 metis channel models," *Proc. Mobile Wireless Commun. Enablers Inf. Soc.(METIS)*, vol. 1, 2015.

[135] M. K. Samimi and T. S. Rappaport, "3-d millimeter-wave statistical channel model for 5g wireless system design," *IEEE Transactions on Microwave Theory and Techniques*, vol. 64, no. 7, pp. 2207–2225, 2016.

[136] Q. Zhu, K. Mao, M. Song, X. Chen, B. Hua, W. Zhong, and X. Ye, "Map-based channel modeling and generation for u2v mmwave communication," *IEEE Transactions on Vehicular Technology*, vol. 71, no. 8, pp. 8004–8015, 2022.

[137] J. Deng, "A hybrid millimeter-wave channel simulator for joint communication and localization," *arXiv preprint arXiv:2210.11422*, 2022.

[138] N. Keerativoranan and J.-i. Takada, "Site-level deterministic channel emulator: Grid-based architecture and continuous channel emulation technique," in *2022 16th European Conference on Antennas and Propagation (EuCAP)*, 2022, pp. 1–5.

[139] D. Bilibashi, E. M. Vitucci, and V. Degli-Esposti, "On dynamic ray tracing and anticipative channel prediction for dynamic environments," *IEEE Transactions on Antennas and Propagation*, Early Access, 2023. [Online]. Available: https://ieeexplore.ieee.org/document/10089404

[140] E. M. Vitucci, M. Fabiani, and V. Degli-Esposti, "Use of a realistic ray-based model for the evaluation of indoor rf coverage solutions using reconfigurable intelligent surfaces," *Electronics*, vol. 12, no. 5, 2023. [Online]. Available: https://www.mdpi.com/2079-9292/12/5/1173

[141] V. Degli-Esposti, E. M. Vitucci, M. D. Renzo, and S. A. Tretyakov, "Reradiation and scattering from a reconfigurable intelligent surface: A general macroscopic model," *IEEE Transactions on Antennas and Propagation*, vol. 70, no. 10, pp. 8691–8706, 2022.

[142] D. He, B. Ai, K. Guan, L. Wang, Z. Zhong, and T. Kürner, "The design and applications of high-performance ray-tracing simulation platform for 5g and beyond wireless communications: A tutorial," *IEEE communications surveys & tutorials*, vol. 21, no. 1, pp. 10–27, 2018.

[143] H. Yi, D. He, P. T. Mathiopoulos, B. Ai, J. M. Garcia-Loygorri, J. Dou, and Z. Zhong, "Ray tracing meets terahertz: Challenges and opportunities," *IEEE Communications Magazine*, 2022.

[144] Z. Yuan, J. Zhang, Y. Ji, G. F. Pedersen, and W. Fan, "Spatial non-stationary near-field channel modeling and validation for massive mimo systems," *IEEE Transactions on Antennas and Propagation*, vol. 71, no. 1, pp. 921–933, 2023.

[145] S. Israel and P. Sallee, "Applied machine learning strategies," *IEEE Potentials*, vol. 39, no. 3, pp. 38–42, 2020.

[146] C. Huang, R. He, B. Ai, A. F. Molisch, B. K. Lau, K. Haneda, B. Liu, C.-X. Wang, M. Yang, C. Oestges *et al.*, "Artificial intelligence enabled radio propagation for communications—part I: Channel characterization and antenna-channel optimization," *IEEE Transactions on Antennas and Propagation*, vol. 70, no. 6, pp. 3939–3954, 2022.

[147] ——, "Artificial intelligence enabled radio propagation for communications—part II: Scenario identification and channel modeling," *IEEE Transactions on Antennas and Propagation*, vol. 70, no. 6, pp. 3955–3969, 2022.

[148] A. Seretis and C. Sarris, "An overview of machine learning techniques for radiowave propagation modeling," *IEEE trans. on Ant. and Propagat.*, vol. 70, no. 6, pp. 3970–3885, 2022.

[149] J. Thrane, D. Zibar, and H. L. Christiansen, "Model-aided deep learning method for path loss prediction in mobile communication systems at 2.6 ghz," *IEEE Access*, vol. 8, pp. 7925–7936, 2020.

[150] N. Di Cicco, S. Del Prete, S. Kodra, M. Barbiroli, F. Fuschini, E. M. Vitucci, and M. Tornatore, "Machine learning-based line-of-sight prediction in urban manhattan-like environments," in *17th European Conference on Antennas and Propagation (EuCAP 2023)*, 2023.

[151] F. Vannella, A. Proutiere, Y. Jedra, and J. Jeong, "Learning optimal antenna tilt control policies: A contextual linear bandit approach," in *IEEE INFOCOM 2022 - IEEE Conference on Computer Communications*, 2022, pp. 740–749.

[152] M. Fozi, A. R. Sharafat, and M. Bennis, "Fast mimo beamforming via deep reinforcement learning for high mobility mmwave connectivity," *IEEE Journal on Selected Areas in Communications*, vol. 40, no. 1, pp. 127–142, 2022.

[153] D. Wolpert and W. Macready, "No free lunch theorems for optimization," *IEEE Transactions on Evolutionary Computation*, vol. 1, no. 1, pp. 67–82, 1997.

[154] R. Shwartz-Ziv and A. Armon, "Tabular data: Deep learning is not all you need," *Information Fusion*, vol. 81, pp. 84–90, 2022. [Online]. Available: https://www.sciencedirect.com/science/article/pii/S1566253521002360

[155] P. W. Battaglia, J. B. Hamrick, V. Bapst, A. Sanchez-Gonzalez, V. Zambaldi, M. Malinowski, A. Tacchetti, D. Raposo, A. Santoro, R. Faulkner, C. Gulcehre, F. Song, A. Ballard, J. Gilmer, G. Dahl, A. Vaswani, K. Allen, C. Nash, V. Langston, C. Dyer, N. Heess, D. Wierstra, P. Kohli, M. Botvinick, O. Vinyals, Y. Li, and R. Pascanu, "Relational inductive biases, deep learning, and graph networks," 2018. [Online]. Available: https://arxiv.org/abs/1806.01261

[156] Z. Liu, H. Mao, C.-Y. Wu, C. Feichtenhofer, T. Darrell, and S. Xie, "A convnet for the 2020s," in *Proceedings of the IEEE/CVF Conference on Computer Vision and Pattern Recognition (CVPR)*, June 2022, pp. 11 976–11 986.

[157] S. Hochreiter and J. Schmidhuber, "Long short-term memory," *Neural computation*, vol. 9, pp. 1735–80, 12 1997.

[158] J. Chung, C. Gulcehre, K. Cho, and Y. Bengio, "Empirical evaluation of gated recurrent neural networks on sequence modeling," 2014. [Online]. Available: https://arxiv.org/abs/1412.3555

[159] A. Vaswani, N. Shazeer, N. Parmar, J. Uszkoreit, L. Jones, A. N. Gomez, L. u. Kaiser, and I. Polosukhin, "Attention is all you need," in *Advances in Neural Information Processing Systems*, I. Guyon, U. V. Luxburg, S. Bengio, H. Wallach, R. Fergus, S. Vishwanathan, and R. Garnett, Eds., vol. 30. Curran Associates, Inc., 2017. [Online]. Available: https://proceedings.neurips.cc/paper/2017/file/3f5ee243547dee91fbd053c1c4a845aa-Paper.pdf

[160] T. Brown *et al.*, "Language models are few-shot learners," in *Advances in Neural Information Processing Systems*, H. Larochelle, M. Ranzato, R. Hadsell, M. Balcan, and H. Lin, Eds., vol. 33. Curran Associates, Inc., 2020, pp. 1877–1901. [Online]. Available: https://proceedings.neurips.cc/paper/2020/file/1457c0d6bfcb4967418bfb8ac142f64a-Paper.pdf

[161] M. M. Bronstein, J. Bruna, T. Cohen, and P. Veličković, "Geometric deep learning: Grids, groups, graphs, geodesics, and gauges," 2021. [Online]. Available: https://arxiv.org/abs/2104.13478

[162] A. Sanchez-Gonzalez, J. Godwin, T. Pfaff, R. Ying, J. Leskovec, and P. Battaglia, "Learning to simulate complex physics with graph networks," in *Proceedings of the 37th International Conference on Machine Learning*, ser. Proceedings of Machine Learning Research, H. D. III and A. Singh, Eds., vol. 119. PMLR, 13–18 Jul 2020, pp. 8459–8468. [Online]. Available: https://proceedings.mlr.press/v119/sanchez-gonzalez20a.html

[163] C. R. Qi, H. Su, K. Mo, and L. J. Guibas, "Pointnet: Deep learning on point sets for 3d classification and segmentation," in *Proceedings of the IEEE Conference on Computer Vision and Pattern Recognition (CVPR)*, July 2017.

[164] S. M. Lundberg and S.-I. Lee, "A unified approach to interpreting model predictions," in *Proceedings of the 31st International Conference on Neural Information Processing Systems*, ser. NIPS'17. Red Hook, NY, USA: Curran Associates Inc., 2017, p. 4768–4777.

[165] R. R. Selvaraju, M. Cogswell, A. Das, R. Vedantam, D. Parikh, and D. Batra, "Grad-cam: Visual explanations from deep networks via gradient-based localization," in *2017 IEEE International Conference on Computer Vision (ICCV)*, 2017, pp. 618–626.

[166] R. Ying, D. Bourgeois, J. You, M. Zitnik, and J. Leskovec, *GNNExplainer: Generating Explanations for Graph Neural Networks*. Red Hook, NY, USA: Curran Associates Inc., 2019.

[167] W. Tenachi, R. Ibata, and F. I. Diakogiannis, "Deep symbolic regression for physics guided by units constraints: toward the automated discovery of physical laws," 2023. [Online]. Available: https://arxiv.org/abs/2303.03192

[168] S. Schieler, M. Döbereiner, S. Semper, and M. Landmann, "Estimating multi-modal dense multipath components using auto-encoders," in *2022 30th European Signal Processing Conference (EUSIPCO)*, 2022, pp. 1716–1720.

[169] H. Krim and M. Viberg, "Two decades of array signal processing research: the parametric approach," *IEEE Signal Processing Magazine*, vol. 13, no. 4, pp. 67–94, 1996.

[170] F. Zhang, W. Fan, and G. F. Pedersen, "Frequency-invariant uniform circular array for wideband mm-wave channel characterization," *IEEE Antennas and Wireless Propagation Letters*, vol. 16, pp. 641–644, 2017.

[171] C. Ling, X. Yin, R. Müller, S. Häfner, D. Dupleich, C. Schneider, J. Luo, H. Yan, and R. Thomä, "Double-directional dual-polarimetric cluster-based characterization of 70-77 GHz indoor channels," *IEEE Transactions on Antennas and Propagation*, vol. 66, no. 2, pp. 857–870, Feb 2018.

[172] C. Ling, X. Yin, H. Wang, and R. S. Thomä, "Experimental characterization and multipath cluster modeling for 13-17 GHz indoor propagation channels," *IEEE Transactions on Antennas and Propagation*, vol. 65, no. 12, pp. 6549–6561, Dec 2017.

[173] S. Hur, S. Baek, B. Kim, Y. Chang, A. F. Molisch, T. S. Rappaport, K. Haneda, and J. Park, "Proposal on millimeter-wave channel modeling for 5G cellular system," *IEEE Journal of Selected Topics in Signal Processing*, vol. 10, no. 3, pp. 454–469, April 2016.

[174] R. Schmidt, "Multiple emitter location and signal parameter estimation," *IEEE Transactions on Antennas and Propagation*, vol. 34, no. 3, pp. 276–280, 1986.

[175] A. Paulraj, R. Roy, and T. Kailath, "A subspace rotation approach to signal parameter estimation," *Proceedings of the IEEE*, vol. 74, no. 7, pp. 1044–1046, 1986.

[176] A. Liao, Z. Gao, Y. Wu, H. Wang, and M. Alouini, "2D unitary ESPRIT based super-resolution channel estimation for millimeter-wave massive MIMO with hybrid precoding," *IEEE Access*, vol. 5, pp. 24 747–24 757, 2017.

[177] F. Gao and A. B. Gershman, "A generalized ESPRIT approach to direction-of-arrival estimation," *IEEE Signal Processing Letters*, vol. 12, no. 3, pp. 254–257, March 2005.

[178] A. . van der Veen, M. C. Vanderveen, and A. J. Paulraj, "Joint angle and delay estimation using shift-invariance properties," *IEEE Signal Processing Letters*, vol. 4, no. 5, pp. 142–145, May 1997.

[179] C. Tsai, Y. Liu, and A. Wu, "Efficient compressive channel estimation for millimeter-wave large-scale antenna systems," *IEEE Transactions on Signal Processing*, vol. 66, no. 9, pp. 2414–2428, May 2018.

[180] M. C. Vanderveen, C. B. Papadias, and A. Paulraj, "Joint angle and delay estimation (jade) for multipath signals arriving at an antenna array," *IEEE Communications Letters*, vol. 1, no. 1, pp. 12–14, Jan 1997.

[181] Z. Marzi, D. Ramasamy, and U. Madhow, "Compressive channel estimation and tracking for large arrays in mm-wave picocells," *IEEE Journal of Selected Topics in Signal Processing*, vol. 10, no. 3, pp. 514–527, April 2016.

[182] X. Li, J. Fang, H. Li, and P. Wang, "Millimeter wave channel estimation via exploiting joint sparse and low-rank structures," *IEEE Transactions on Wireless Communications*, vol. 17, no. 2, pp. 1123–1133, Feb 2018.

[183] S. Sun, T. S. Rappaport, M. Shafi, P. Tang, J. Zhang, and P. J. Smith, "Propagation models and performance evaluation for 5g millimeter-wave bands," *IEEE Transactions on Vehicular Technology*, vol. 67, no. 9, pp. 8422–8439, Sept 2018.

[184] B. H. Fleury, M. Tschudin, R. Heddergott, D. Dahlhaus, and K. I. Pedersen, "Channel parameter estimation in mobile radio environments using the SAGE algorithm," *IEEE Journal on Selected Areas in Communications*, vol. 17, no. 3, pp. 434–450, Mar 1999.

[185] T. Moon, "The expectation-maximization algorithm," *IEEE Signal Processing Magazine*, vol. 13, no. 6, pp. 47–60, 1996.

[186] X. Cai and W. Fan, "A complexity-efficient high resolution propagation parameter estimation algorithm for ultra-wideband large-scale uniform circular array," *IEEE Transactions on Communications*, vol. 67, no. 8, pp. 5862–5874, 2019.

[187] X. Cai, W. Fan, X. Yin, and G. F. Pedersen, "Trajectory-aided maximum-likelihood algorithm for channel parameter estimation in ultrawideband large-scale arrays," *IEEE Transactions on Antennas and Propagation*, vol. 68, no. 10, pp. 7131–7143, 2020.

[188] X. Cai, G. Zhang, C. Zhang, W. Fan, J. Li, and G. F. Pedersen, "Dynamic channel modeling for indoor millimeter-wave propagation channels based on measurements," *IEEE Transactions on Communications*, vol. 68, no. 9, pp. 5878–5891, 2020.

[189] A. Richter, "Estimation of radio channel parameters: Models and algorithms," Ph.D. dissertation, Technische Universität Ilmenau, Germany, 2005.

[190] X. Cai, M. Zhu, A. Fedorov, and F. Tufvesson, "Enhanced effective aperture distribution function for characterizing large-scale antenna arrays," *IEEE Transactions on Antennas and Propagation*, vol. 71, no. 8, pp. 6869–6877, 2023.

[191] R. He, B. Ai, A. F. Molisch, G. L. Stuber, Q. Li, Z. Zhong, and J. Yu, "Clustering enabled wireless channel modeling using big data algorithms," *IEEE Communications Magazine*, vol. 56, no. 5, pp. 177–183, 2018.

[192] R. He, W. Chen, B. Ai, A. F. Molisch, W. Wang, Z. Zhong, J. Yu, and S. Sangodoyin, "On the clustering of radio channel impulse responses using sparsity-based methods," *IEEE Transactions on Antennas and Propagation*, vol. 64, no. 6, pp. 2465–2474, 2016.

[193] C. Gentile, "Using the kurtosis measure to identify clusters in wireless channel impulse responses," *IEEE Transactions on Antennas and Propagation*, vol. 61, no. 6, pp. 3392–3395, 2013.

[194] M. Steinbauer, H. Ozcelik, H. Hofstetter, C. F. Mecklenbrauker, and E. Bonek, "How to quantify multipath separation," *IEICE Transactions on Electronics*, vol. 85, no. 3, pp. 552–557, 2002.

[195] R. He, Q. Li, B. Ai, Y. L.-A. Geng, A. F. Molisch, V. Kristem, Z. Zhong, and J. Yu, "A kernel-power-density-based algorithm for channel multi-path components clustering," *IEEE Transactions on Wireless Communications*, vol. 16, no. 11, pp. 7138–7151, 2017.

[196] C. Huang, R. He, Z. Zhong, B. Ai, Y.-A. Geng, Z. Zhong, Q. Li, K. Haneda, and C. Oestges, "A power-angle-spectrum based clustering and tracking algorithm for time-varying radio channels," *IEEE Transactions on Vehicular Technology*, vol. 68, no. 1, pp. 291–305, 2018.

[197] M. Di Renzo, A. Zappone, M. Debbah, M.-S. Alouini, C. Yuen, J. de Rosny, and S. Tretyakov, "Smart radio environments empowered by reconfigurable intelligent surfaces: How it works, state of research, and the road ahead," *IEEE Journal on Selected Areas in Communications*, vol. 38, no. 11, pp. 2450–2525, 2020.

[198] J. Pyhtilae, J. Kokkoniemi, P. Sangi, N. Vaara, and M. Juntti, "Ray tracing based radio channel modelling applied to ris," in *WSA SCC 2023; 26th International ITG Workshop on Smart Antennas and 13th Conference on Systems, Communications, and Coding*, 2023, pp. 1–6.

[199] W. Tang, M. Z. Chen, X. Chen, J. Y. Dai, Y. Han, M. Di Renzo, Y. Zeng, S. Jin, Q. Cheng, and T. J. Cui, "Wireless communications with reconfigurable intelligent surface: Path loss modeling and experimental measurement," *IEEE Transactions on Wireless Communications*, vol. 20, no. 1, pp. 421–439, 2021.

[200] W. Tang, X. Chen, M. Z. Chen, J. Y. Dai, Y. Han, M. D. Renzo, S. Jin, Q. Cheng, and T. J. Cui, "Path loss modeling and measurements for reconfigurable intelligent surfaces in the millimeter-wave frequency band," *IEEE Transactions on Communications*, vol. 70, no. 9, pp. 6259–6276, 2022.

[201] M. Di Renzo, F. Habibi Danufane, X. Xi, J. de Rosny, and S. Tretyakov, "Analytical modeling of the path-loss for reconfigurable intelligent surfaces – anomalous mirror or scatterer ?" in *2020 IEEE 21st International*

Workshop on Signal Processing Advances in Wireless Communications (SPAWC), 2020, pp. 1–5.

[202] J. C. B. Garcia, A. Sibille, and M. Kamoun, "Reconfigurable intelligent surfaces: Bridging the gap between scattering and reflection," *IEEE Journal on Selected Areas in Communications*, vol. 38, no. 11, pp. 2538–2547, 2020.

[203] S. W. Ellingson, "Path loss in reconfigurable intelligent surface-enabled channels," in *2021 IEEE 32nd Annual International Symposium on Personal, Indoor and Mobile Radio Communications (PIMRC)*, 2021, pp. 829–835.

[204] M. Najafi, V. Jamali, R. Schober, and H. V. Poor, "Physics-based modeling and scalable optimization of large intelligent reflecting surfaces," *IEEE Transactions on Communications*, vol. 69, no. 4, pp. 2673–2691, 2021.

[205] F. H. Danufane, M. D. Renzo, J. de Rosny, and S. Tretyakov, "On the path-loss of reconfigurable intelligent surfaces: An approach based on green's theorem applied to vector fields," *IEEE Transactions on Communications*, vol. 69, no. 8, pp. 5573–5592, 2021.

[206] Z. Wang, L. Tan, H. Yin, K. Wang, X. Pei, and D. Gesbert, "A received power model for reconfigurable intelligent surface and measurement-based validations," in *2021 IEEE 22nd International Workshop on Signal Processing Advances in Wireless Communications (SPAWC)*, 2021, pp. 561–565.

[207] G. Gradoni and M. Di Renzo, "End-to-end mutual coupling aware communication model for reconfigurable intelligent surfaces: An electromagnetic-compliant approach based on mutual impedances," *IEEE Wireless Communications Letters*, vol. 10, no. 5, pp. 938–942, 2021.

[208] M. D. Renzo, A. Ahmed, A. Zappone, V. Galdi, G. Gradoni, M. Moccia, and G. Castaldi, "Digital reconfigurable intelligent surfaces: On the impact of realistic reradiation models," *arXiv preprint arXiv:2205.09799*, 2022.

[209] V. Degli-Esposti, E. M. Vitucci, M. D. Renzo, and S. A. Tretyakov, "Reradiation and scattering from a reconfigurable intelligent surface: A general macroscopic model," *IEEE Transactions on Antennas and Propagation*, vol. 70, no. 10, pp. 8691–8706, 2022.

[210] S. H. Dokhanchi, B. S. Mysore, K. V. Mishra, and B. Ottersten, "A mmwave automotive joint radar-communications system," *IEEE Transactions on Aerospace and Electronic Systems*, vol. 55, no. 3, pp. 1241–1260, 2019.

[211] P. Kumari, J. Choi, N. González-Prelcic, and R. W. Heath, "Ieee 802.11 ad-based radar: An approach to joint vehicular communication-radar system," *IEEE Transactions on Vehicular Technology*, vol. 67, no. 4, pp. 3012–3027, 2017.

[212] Z. Ni, J. A. Zhang, X. Huang, K. Yang, and J. Yuan, "Uplink sensing in perceptive mobile networks with asynchronous transceivers," *IEEE Transactions on Signal Processing*, vol. 69, pp. 1287–1300, 2021.

[213] L. Rinaldi, D. Tagliaferri, F. Linsalata, M. Mizmizi, M. Magarini, and U. Spagnolini, "Dual domain waveform design for joint communication and sensing systems," *arXiv preprint arXiv:2111.12339*, 2021.

[214] C. Han, Y. Wu, Z. Chen, Y. Chen, and G. Wang, "Thz isac: A physical-layer perspective of terahertz integrated sensing and communication," *arXiv preprint arXiv:2209.03145*, 2022.

[215] Y. Cui, F. Liu, X. Jing, and J. Mu, "Integrating sensing and communications for ubiquitous iot: Applications, trends, and challenges," *IEEE Network*, vol. 35, no. 5, pp. 158–167, 2021.

[216] R. S. Thomä, C. Andrich, S. J. Myint, C. Schneider, and G. Sommerkorn, "Characterization of multi-link propagation and bistatic target reflectivity for distributed isac," *arXiv preprint arXiv:2210.11840*, 2022.

[217] X. Li, J. He, Z. Yu, Y. Chen, W. Yang, and G. Wang, "Rough-surface scattering theory and modeling for 6g isac," in *2022 IEEE Globecom Workshops (GC Wkshps)*. IEEE, 2022, pp. 1310–1316.

[218] S. Li, W. Yuan, C. Liu, Z. Wei, J. Yuan, B. Bai, and D. W. K. Ng, "A novel isac transmission framework based on spatially-spread orthogonal time frequency space modulation," *IEEE Journal on Selected Areas in Communications*, vol. 40, no. 6, pp. 1854–1872, 2022.

[219] L. Gaudio, M. Kobayashi, G. Caire, and G. Colavolpe, "On the effectiveness of otfs for joint radar parameter estimation and communication," *IEEE Transactions on Wireless Communications*, vol. 19, no. 9, pp. 5951–5965, 2020.

[220] N. Cardona, J. S. Romero, W. Yang, and J. Li, "Integrating the sensing and radio communications channel modelling from radar mutual interference," in *ICASSP 2023-2023 IEEE International Conference on Acoustics, Speech and Signal Processing (ICASSP)*. IEEE, 2023, pp. 1–5.

[221] A. López-Reche, D. Prado-Alvarez, A. Ramos, S. Inca, J. F. Monserrat, Y. Zhang, Z. Yu, and Y. Chen, "Considering correlation between sensed and communication channels in gbsm for 6g isac applications," in *2022 IEEE Globecom Workshops (GC Wkshps)*. IEEE, 2022, pp. 1317–1322.

[222] Z. Zhang, R. He, B. Ai, M. Yang, C. Li, H. Mi, and Z. Zhang, "A general channel model for integrated sensing and communication scenarios," *IEEE Communications Magazine*, vol. 61, no. 5, pp. 68–74, 2023.

[223] Y. Liu, J. Zhang, Y. Zhang, Z. Yuan, and G. Liu, "A shared cluster-based stochastic channel model for joint communication and sensing systems," *arXiv preprint arXiv:2211.06615*, 2022.

[224] Z. Zhang, R. He, M. Yang *et al.*, "Millimeter wave channel measurements and analysis for integrated sensing and communication scenario," in *Proc. IEEE APS'23*, 2023, pp. 1–2.

[225] J. Salo, G. Del Galdo, J. Salmi, P. Kyösti, M. Milojevic, D. Laselva, and C. Schneider, "Matlab implementation of the 3gpp spatial channel model (3gpp tr 25.996)," *on-line, Jan*, 2005.

[226] J. Wang, C.-X. Wang, J. Huang, and Y. Chen, "6g thz propagation channel characteristics and modeling: Recent developments and future challenges," *IEEE Communications Magazine*, pp. 1–8, 2022.

[227] X. Wang, Z. Zhang, D. He, K. Guan, D. Liu, J. Dou, S. Mumtaz, and S. Al-Rubaye, "A multi - task learning model for super resolution of wireless channel characteristics," in *GLOBECOM 2022 - 2022 IEEE Global Communications Conference*, 2022, pp. 952–957.

[228] C. Huang, R. He, B. Ai, A. F. Molisch, B. K. Lau, K. Haneda, B. Liu, C.-X. Wang, M. Yang, C. Oestges, and Z. Zhong, "Artificial intelligence enabled radio propagation for communications—part i: Channel characterization and antenna-channel optimization," *IEEE Transactions on Antennas and Propagation*, vol. 70, no. 6, pp. 3939–3954, 2022.

[229] C. Huang, A. F. Molisch, R. He, R. Wang, P. Tang, and Z. Zhong, "Machine-learning-based data processing techniques for vehicle-to-vehicle channel modeling," *IEEE Comm. Mag.*, pp. 109–115, 2019.

[230] S. Mohammadjafari, S. Roginsky, E. Kavurmacioglu, M. Cevik, J. Ethier, and A. B. Bener, "Machine learning-based radio coverage prediction in urban environments," *IEEE Transactions on Network and Service Management*, vol. 17, no. 4, pp. 2117–2130, 2020.

[231] R. Levie, C. Yapar, G. Kutyniok, and G. Caire, "Radiounet: Fast radio map estimation with convolutional neural networks," *IEEE Transactions on Wireless Communications*, vol. 20, no. 6, pp. 4001–4015, 2021.

[232] Y. Yu, W.-J. Lu, Y. Liu, and H.-B. Zhu, "Neural-network-based root mean delay spread model for ubiquitous indoor internet-of-things scenarios," *IEEE Internet of Things Journal*, vol. 7, no. 6, pp. 5580–5589, 2020.

[233] A. Bharti, R. Adeogun, X. Cai, W. Fan, F.-X. Briol, L. Clavier, and T. Pedersen, "Joint modeling of received power, mean delay, and delay spread for wideband radio channels," *IEEE Transactions on Antennas and Propagation*, vol. 69, no. 8, pp. 4871–4882, 2021.

[234] Y. Miao, "Interpreting frequency shift in translational-rotational mobility using source-generic mode channel," in *2020 IEEE Globecom Workshops (GC Wkshps*, 2020, pp. 1–6.

[235] R. Hersyandika, Y. Miao, and S. Pollin, "Guard beam: Protecting mmwave communication through in-band early blockage prediction," in *GLOBECOM 2022 - 2022 IEEE Global Communications Conference*, 2022, pp. 4093–4098.

[236] K. Mao, Q. Zhu, F. Duan, Y. Qiu, M. Song, W. Fan, and Y. Miao, "A2g channel measurement and characterization via tnn for uav multi-scenario communications," in *GLOBECOM 2022 - 2022 IEEE Global Communications Conference*, 2022, pp. 4461–4466.

[237] R. He, B. K. Lau, C. Oestges, K. Haneda, and B. Liu, "Guest editorial artificial intelligence in radio propagation for communications," *IEEE Transactions on Antennas and Propagation*, vol. 70, no. 6, pp. 3934–3938, 2022.

[238] H. Mi, B. Ai, R. He, R. Caromi, J. Wang, A. Bodi, C. Gentile, A. Chiumento, and Y. Miao, "Cluster association for 3D environment based on 60 GHz indoor channel measurements," in *Proc. EuCAP'23*, 2023, pp. 1–4.

[239] Y. Miao, W. Fan, J. Takada, R. He, X. Yin, M. Yang, J. Rodríguez-Piñeiro, A. A. Glazunov, W. Wang, and Y. Gong, "Comparing channel emulation algorithms by using plane waves and spherical vector waves in multiprobe anechoic chamber setups," *IEEE Transactions on Antennas and Propagation*, vol. 67, no. 6, pp. 4091–4103, 2019.

[240] K. Shen, S. Safapourhajari, T. De Pessemier, L. Martens, W. Joseph, and Y. Miao, "Optimizing the focusing performance of non-ideal cell-free mmimo using genetic algorithm for indoor scenario," *IEEE Transactions on Wireless Communications*, vol. 21, no. 10, pp. 8832–8845, 2022.

[241] K. Shen, T. De Pessemier, L. Martens, W. Joseph, and Y. Miao, "Genetic algorithm combined with ray tracer for optimizing cell-free mmimo topology in a confined environment," in *2021 15th European Conference on Antennas and Propagation (EuCAP)*, 2021, pp. 1–5.

[242] H. Alidoustaghdam, Y. Miao, and A. Kokkeler, "Integrating tdd communication and radar sensing in co-located planar array: A genetic algorithm enabled aperture design," in *2022 2nd IEEE International Symposium on Joint Communications Sensing (JCS)*, 2022, pp. 1–6.

[243] B. van Berlo, Y. Miao, R. Hersyandika, N. Meratnia, T. Ozcelebi, A. Kokkeler, and S. Pollin, "Intelligent blockage recognition using cellular mmwave beamforming data: Feasibility study," in *GLOBECOM 2022 - 2022 IEEE Global Communications Conference*, 2022, pp. 4576–4582.

[244] B. van Berlo, Y. Miao, R. Hersyandika, B. Willetts, K. Mao, A. Zare, S. Pollin, and N. Meratnia, "26 ghz ofdm and 77 ghz fmcw radar dataset for domain shift invariant blockage prediction," 2023-01-10.

[245] H. Eslami, S. V. Tran, and A. M. Eltawil, "Design and implementation of a scalable channel emulator for wideband MIMO systems," *IEEE transactions on vehicular technology*, vol. 58, no. 9, pp. 4698–4709, 2009.

[246] W. Fan, P. Kyösti, L. Hentilä, and G. F. Pedersen, "A flexible millimeter-wave radio channel emulator design with experimental validations," *IEEE Transactions on Antennas and Propagation*, vol. 66, no. 11, pp. 6446–6451, 2018.

[247] D. Fei, B. Zhang, R. He, and L. Xiong, "Development of 4x4 parallel MIMO channel sounder for high-speed scenarios," in *Communications and Networking: 11th EAI International Conference, ChinaCom 2016, Chongqing, China, September 24–26, 2016, Proceedings, Part I.* Springer, 2017, pp. 463–471.

[248] J. Ding, D. Fei, R. He, Z. Zhong, and B. Ai, "Research on wideband channel measurement system based on software defined radio," *International Journal of Future Generation Communication and Networking*, vol. 8, no. 6, pp. 23–34, 2015.

[249] D. Fei, L. Xiong, H. Yan, and S. Huang, "Hardware-in-the-loop simulation of LTE system in high-speed environment," in *2013 8th International Conference on Communications and Networking in China (CHINACOM)*. IEEE, 2013, pp. 323–327.

[250] J. Ding, "Measurement, modeling and emulation of time-frequency dispersion characteristics for high-speed railway channels," Ph.D. dissertation, Ph. D. dissertation, Beijing Jiaotong University, Beijing, China, 2018.

[251] B. Zhang, Z. Zhong, R. He, G. Dahman, J. Ding, S. Lin, B. Ai, and M. Yang, "Measurement-based markov modeling for multi-link channels in railway communication systems," *IEEE Transactions on Intelligent Transportation Systems*, vol. 20, no. 3, pp. 985–999, 2018.

[252] S. Priebe, M. Kannicht, M. Jacob, and T. Kürner, "Ultra broadband indoor channel measurements and calibrated ray tracing propagation modeling at thz frequencies," *Journal of Communications and Networks*, vol. 15, no. 6, pp. 547–558, 2013.

[253] R. Takahashi, K. Shibata, and M. Kim, "Development and verification of double-directional channel sounder at 300 ghz," in *2022 International Symposium on Antennas and Propagation (ISAP)*, 2022, pp. 523–524.

[254] N. A. Abbasi, A. Hariharan, A. M. Nair, A. S. Almaiman, F. B. Rottenberg, A. E. Willner, and A. F. Molisch, "Double directional channel measurements for thz communications in an urban environment," in *ICC 2020 - 2020 IEEE International Conference on Communications (ICC)*, 2020, pp. 1–6.

[255] M. F. De Guzman, P. Koivumäki, and K. Haneda, "Double-directional multipath data at 140 ghz derived from measurement-based ray-launcher," in *2022 IEEE 95th Vehicular Technology Conference: (VTC2022-Spring)*, 2022, pp. 1–6.

[256] C. U. Bas, R. Wang, S. Sangodoyin, D. Psychoudakis, T. Henige, R. Monroe, J. Park, C. J. Zhang, and A. F. Molisch, "Real-time millimeter-wave mimo channel sounder for dynamic directional measurements," *IEEE Transactions on Vehicular Technology*, vol. 68, no. 9, pp. 8775–8789, 2019.

[257] R. Wang, O. Renaudin, C. U. Bas, S. Sangodoyin, and A. F. Molisch, "On channel sounding with switched arrays in fast time-varying channels," *IEEE Transactions on Wireless Communications*, vol. 18, no. 8, pp. 3843–3855, 2019.

[258] A. Sayeed and J. Brady, "Beamspace mimo channel modeling and measurement: Methodology and results at 28ghz," in *2016 IEEE Globecom Workshops (GC Wkshps)*, 2016, pp. 1–6.

[259] M. Abbasi, V. Fusco, O. Yurduseven, and T. Fromenteze, "Frequency-diverse multimode millimetre-wave constant-r lens-loaded cavity," *Scientific Reports*, vol. 10, 12 2020.

[260] O. Yurduseven, M. Abbasi, T. Fromenteze, and V. Fusco, "Frequency-diverse computational direction of arrival estimation technique," *Scientific Reports*, vol. 9, 11 2019.

[261] J. Sarrazin and G. Valerio, "Multibeam leaky-wave antenna for mm-wave wide-angular-range aoa estimation," in *2022 16th European Conference on Antennas and Propagation (EuCAP)*, 2022, pp. 1–5.

[262] ——, "H-plane-scanning multibeam leaky-wave antenna for wide-angular-range aoa estimation at mm-wave," in *2023 17th European Conference on Antennas and Propagation (EuCAP)*, 2023, pp. 1–5.

[263] A. A. Oliner and D. R. Jackson, "Chapter 15 - surface-waves and leaky-wave antennas," in *Antenna Engineering Handbook. 5th ed.*, J. L. Volakis, Ed. New York: McGraw-Hill Education, ed. 2019.

[264] M. Poveda-García, D. Cañete-Rebenaque, and J. L. Gómez-Tornero, "Frequency-scanned monopulse pattern synthesis using leaky-wave antennas for enhanced power-based direction-of-arrival estimation," *IEEE Transactions on Antennas and Propagation*, vol. 67, no. 11, pp. 7071–7086, 2019.

[265] J. Sarrazin, "Music-based angle-of-arrival estimation using multi-beam leaky-wave antennas," in *2021 XXXIVth General Assembly and Scientific Symposium of the International Union of Radio Science (URSI GASS)*, 2021, pp. 1–4.

[266] Q. Zhang, J. Sarrazin, M. Casaletti, G. Valerio, P. D. Doncker, and A. Benlarbi-Delai, "Enhanced scanning range design for leaky-wave antenna (lwa) at 60 ghz," in *2019 13th European Conference on Antennas and Propagation (EuCAP)*, 2019, pp. 1–5.

[267] X. Zeng, Q. Chen, O. Zetterstrom, and O. Quevedo-Teruel, "Fully metallic glide-symmetric leaky-wave antenna at k-band with lens-augmented scanning," *IEEE Transactions on Antennas and Propagation*, vol. 70, no. 8, pp. 7158–7163, 2022.

[268] M. K. Emara, D. J. King, H. V. Nguyen, S. Abielmona, and S. Gupta, "Millimeter-wave slot array antenna front-end for amplitude-only direction finding," *IEEE Transactions on Antennas and Propagation*, vol. 68, no. 7, pp. 5365–5374, 2020.

[269] M. Poveda-García, A. Gómez-Alcaraz, D. Cañete-Rebenaque, A. S. Martinez-Sala, and J. L. Gómez-Tornero, "Rssi-based direction-of-departure estimation in bluetooth low energy using an array of frequency-steered leaky-wave antennas," *IEEE Access*, vol. 8, pp. 9380–9394, 2020.

[270] H. Paaso, A. Mämmelä, D. Patron, and K. R. Dandekar, "Doa estimation through modified unitary music algorithm for crlh leaky-wave antennas," in *2013 IEEE 24th Annual International Symposium on Personal, Indoor, and Mobile Radio Communications (PIMRC)*, 2013, pp. 311–315.